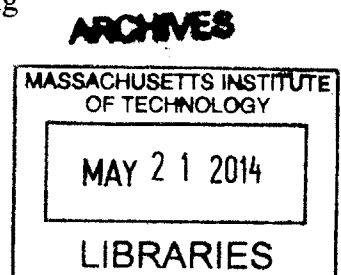


Simulation of Hydrology and Population Dynamics of  
*Anopheles* Mosquitoes Around the Koka Reservoir in Ethiopia

by  
Noriko Endo  
B.E. Civil Engineering  
The University of Tokyo, 2011

Submitted to the Department of Civil and Environmental Engineering  
in partial fulfillment of the requirements for the degree of  
Master of Science in Civil and Environmental Engineering  
at the  
Massachusetts Institute of Technology  
February 2014



© 2014 Massachusetts Institute of Technology. All rights reserved.

Signature of Author: \_\_\_\_\_  
Department of Civil and Environmental Engineering  
January 17, 2014

Certified by: \_\_\_\_\_  
Elfatih A. B. Eltahir  
Professor of Civil and Environmental Engineering  
Thesis Supervisor

Accepted by: \_\_\_\_\_  
Heidi M. Nepf  
Chairman, Departmental Committee for Graduate Students



# Simulation of Hydrology and Population Dynamics of *Anopheles* Mosquitoes Around the Koka Reservoir in Ethiopia

by  
Noriko Endo

Submitted to the Department of Civil and Environmental Engineering  
on January 17th, 2014 in partial fulfillment of the requirements for the degree of  
Master of Science in Civil and Environmental Engineering

## Abstract

This thesis applies the HYDRology, Entomology and MAlaria Transmission Simulator (HYDREMATS) to the environment around a water resources reservoir in Ethiopia. HYDREMATS was modified to simulate the local hydrology and the mosquito population dynamics influenced by the reservoir system. The hydrology component of HYDREMATS including a representation of the groundwater was coupled with a reservoir model to describe the spatiotemporal variability of the groundwater table, and the variability in shoreline locations. The entomology component was modified to match the relatively humid environment.

HYDREMATS was applied to two villages around the Koka Reservoir in Ethiopia, one adjacent to the reservoir, Ejersa, and the other located 12 km away from it, Gudedo. Meteorological data were collected from July 2011 to February 2013. Entomological data collection started in July 2012 and continued until February 2013. Adult mosquitoes were sampled from the two field sites and classified at the genus level, i.e., *Anopheles* or *Culex*. Because of their geographical proximity, the climatology in Ejersa and the climatology in Gudedo were comparable; however, entomological conditions in the two villages were distinct. Ejersa experienced an enhanced and prolonged mosquito season.

HYDREMATS was able to simulate the hydrology and the population dynamics of *Anopheles* mosquitoes at both sites for the period, from January 2012 to February 2013. The model applied to Ejersa simulated a large mosquito population and a prolonged mosquito breeding season because of the existence of the reservoir, in agreement with observations. Especially, a large mosquito population in the post-rainy season was sustained in the simulation due to a large shoreline breeding area. The model applied to Gudedo simulated smaller mosquito population,

but it failed to reproduce observed adult mosquito population dynamics correctly. However, the simulated adult mosquito population dynamics in Gudedo resembled those of the observed larvae samples. Further model calibration and validation will be conducted as more data become available. This study demonstrates that HYDREMATS can serve as an effective tool to simulate local hydrology and mosquito population dynamics at a reservoir environment, given hydrological and entomological parameters specified for the given field site.

Thesis Supervisor: Elfatih A. B. Eltahir

Title: Professor of Civil and Environmental Engineering



## Acknowledgements

This work was supported by the MIT and Masdar Institute Cooperative Program, the US National Science Foundation, as well as fellowships from Japan Student Service Organization and MIT Energy Initiative.

I am indebted to my advisor, Elfatih A. B. Eltahir, who not only provided me with academic knowledge in various fields but also guided me in every aspect in conducting this study. I am grateful for his providing me with significant time to consult research ideas and difficulties, and some hints for starting up a new life at MIT.

I am also thankful for having unusual opportunities to conduct field surveys in Ethiopia, to work at the interdisciplinary field, and to meet great friends involved in my study and my graduate life. Teresa K. Yamana and Osama M. Seidahmed, as well as William Jobin, Richard Pollack and Tony Kiszewski shared with me their knowledge about entomology and malaria. I would like to thank Mariam M. Allam, Alison Hoyt and many other friends at Parsons for supporting my life.

I would also like to give my special thanks to Ashenafi Adugna, who helped me in conducting field surveys in Ethiopia. He was the person who I could fully trust, understood my research motivation and technical works, and made my stay in Ethiopia enjoyable.

Finally, I would like to acknowledge my family for their constant support and encouragement throughout my life.

## Table of Contents

Abstract .....	3
Acknowledgements .....	5
Table of Contents .....	6
List of figures .....	8
List of tables .....	11
Chapter 1: Introduction .....	12
1.1 Background .....	12
1.2 Research Objectives .....	13
Chapter 2: Field Observations .....	15
2.1 Field Sites Description: Ejersa and Gudedo .....	15
2.2 Climate and Hydrological Data .....	18
2.2.1 Meteorological Data .....	18
2.2.2 Soil Moisture Data .....	24
2.2.3 Reservoir Water Level Data .....	25
2.2.4 Groundwater Table Data .....	27
2.3 Entomological Data .....	28
2.3.1 Mosquito Species Present around the Koka Reservoir .....	28
2.3.2 Adult Mosquito Data Collection .....	29
2.3.3 Larvae Data Collection .....	33
2.4 Clinical Data .....	38
Chapter 3: HYDREMATS: Model Description .....	40
3.1 Original Model Description .....	40
3.2 Model Development .....	42
3.2.1 Large Water Body Representation in the Hydrology Model .....	42
3.2.2 Model Adjustments for a Wet Environment in the Entomology Model .....	44
3.2.3 Utilization of Different Breeding Sites in the Entomology Model .....	47
3.3 Model Input and Output .....	48
3.3.1 Hydrology Model Input .....	49

3.3.2 Hydrology Model Output.....	52
3.3.3 Entomology Model Input.....	53
3.3.4 Entomology Model Output.....	53
Chapter 4: Model Application to Two Villages around the Koka Reservoir .....	55
4.1 Model Application to Ejersa.....	55
4.1.1 Ejersa Field Setting and Model Parameters.....	55
4.1.2 Data Preparation .....	58
4.1.3 Hydrology Model Output .....	60
4.1.4 Entomology Model Output.....	68
4.2 Model Application to Gudedo.....	69
4.2.1 Gudedo Field Setting and Model Parameters .....	71
4.2.2 Hydrology Model Output .....	73
4.2.3 Entomology Model Output.....	76
4.3 Discussion .....	79
4.3.1 Comparison between Ejersa and Gudedo.....	79
4.3.2 Discussion of Mosquito Dynamics in Ejersa.....	81
4.3.3 Discussion of Mosquito Dynamics in Gudedo .....	84
Chapter 5: Conclusion and Future Work.....	87
References.....	89

## List of figures

Figure 2-1 Location of the field site .....	15
Figure 2-2 Meteorology around the Koka Reservoir. ....	16
Figure 2-3 Ejersa field setting.....	19
Figure 2-4 Gudedo field setting .....	20
Figure 2-5 Meteorological station deployed in Gudedo .....	21
Figure 2-6 Gudedo met data .....	22
Figure 2-7 Ejersa met data .....	23
Figure 2-8 The Koka Reservoir water level (meter above sea level).....	25
Figure 2-9 Contour lines at the shoreline of the Koka Reservoir .....	26
Figure 2-10 Well locations and observed GWT.....	27
Figure 2-11 Indoor light trap set in Gudedo .....	30
Figure 2-12 Number of Anopheles captured by light traps.....	32
Figure 2-13 Pool in Ejersa sustained by rainfall and leak from a pipe .....	34
Figure 2-14 Shoreline at the beginning of the rainy season, when the water level is low.....	34
Figure 2-15 Shoreline in the middle of the rainy season, when the water level is relatively high .....	35
Figure 2-16 Manmade pool in Gudedo .....	35
Figure 2-17 Manmade pool created during a construction period.....	36
Figure 2-18 Number of larvae and pupae collected from Ejersa pools .....	37
Figure 2-19 Number of larvae and pupae collected from Gudedo pools.....	37
Figure 2-20 Monthly incidence of malaria in Ejersa .....	39
Figure 3-1 Corrected aquatic stage development rate.....	46
Figure 3-2 Utility probability functions for oviposition .....	48
Figure 3-3 Crusting of the soil surface observed around the Koka Reservoir.....	50

Figure 3-4 Flags depending on the type of pools simulated in HYDREMATS .....	52
Figure 3-5 Location of human settlements in Ethiopia.....	54
Figure 4-1 Ejersa topography.....	56
Figure 4-2 Gudedo-Ejersa daily meteorological data comparison for the maximum overlap (Jun. 2012 – Feb. 2013) .....	59
Figure 4-3 Gudedo-Ejersa daily meteorological data comparison for the rainy season overlap (Aug. 2012 – Feb. 2013).....	59
Figure 4-4 Water depth output at hour 1 on day 102 .....	62
Figure 4-5 Water depth output at hour 1 on day 272 .....	63
Figure 4-6 Comparison of soil moisture at Ejersa Met Station .....	65
Figure 4-7 Comparison of soil moisture at Ejersa Soil Moisture Station .....	65
Figure 4-8 Simulated soil moisture profiles at Met Station and Soil Moisture Station in Ejersa .....	66
Figure 4-9 Simulated and observed GWT .....	67
Figure 4-10 Spatial distribution of GWT simulated at the top of the simulation domain .....	68
Figure 4-11 Ejersa mosquito simulation and observation.....	70
Figure 4-12 Analysis of aquatic stage mosquitoes: numbers of breeding sites and larvae.....	70
Figure 4-13 Gudedo topography.....	72
Figure 4-14 Trench found in Gudedo.....	74
Figure 4-15 Gudedo simulation pool output.....	75
Figure 4-16 Volumetric water content at Gudedo MS .....	76
Figure 4-17 Gudedo mosquito simulation and observation. ....	77
Figure 4-18 Gudedo mosquito simulation and rainfall .....	78
Figure 4-19 Comparison of simulated mosquito population and observed larvae in Gudedo.....	78
Figure 4-20 Climate in Ejersa and Gudedo.....	80
Figure 4-21 Observed adult <i>anopheline</i> population in Ejersa and Gudedo .....	80

Figure 4-22 Simulated adult *anopheline* population in Ejersa and Gudedo .....81

Figure 4-23 Shoreline vegetation at middle reservoir level .....83

Figure 4-24 Shoreline vegetation at high reservoir level .....84

## List of tables

Table 2-1 Characteristics of the Koka Reservoir .....	17
Table 2-2 Characteristics of Anopheles mosquitoes present around the Koka Reservoir .....	29
Table 2-3 Ejersa light trap house features.....	31
Table 2-4 Gudedo light trap house features .....	31
Table 2-5 Description of pools for larvae dipping .....	34
Table 3-1 Hydrology model input and resolution originally obtained.....	45
Table 3-2 Aquatic stage development rate parameters .....	48
Table 3-3 Utilization parameters for oviposition .....	51
Table 4-1 Ejersa hydraulic parameters.....	57
Table 4-2 Coefficients for 1st-order linear regression models for the maximum overlap .....	60
Table 4-3 Coefficients for 1st-order linear regression models for the rainy season overlap ...	60
Table 4-4 Hydrology model parameters for Gudedo .....	73

## Chapter 1: Introduction

### 1.1 Background

Malaria is a major public-health challenge affecting more than one hundred countries, most of which are in Africa. WHO (2012) estimated that 3.3 billion people are at risk of contracting malaria and that 219 million malaria cases and 660,000 deaths occurred in 2010 worldwide. In addition to its health impact, malaria affects countries economically. The loss of human life and the loss of working days due to illness in highly malarious countries reduces household income and countries' GDP; income levels of countries with intense malaria in 1995 were only 33% of the corresponding income levels of malaria-free countries. (Gallup and Sachs, 2001; Sachs and Malaney, 2002).

Malaria has attracted global attention and has been targeted for control and elimination. The Millennium Development Goals (MDGs) set one of its goals in Target 6C to “have halted by 2015 and begun to reverse the incidence of malaria” in a 2007 resolution. The Roll Back Malaria (RBM) partnership aims to “reduce global malaria cases by 75% by end-2015” from 2000 levels (WHO, 2011).

Malaria is a complex parasitic diseases transmitted by female *Anopheles* mosquitoes. The main parasites responsible for malaria are *plasmodium falciparum* (*P.f.*) and *plasmodium vivax* (*P.v.*). *P.f.* is the parasite responsible for the most deaths due to malaria, while *P.v.* is the parasite commonly found worldwide. Because malaria is transmitted by mosquitoes and because mosquitoes lay eggs in water bodies, local hydrology, as well as local climate, is highly linked to malaria.

Dams and reservoirs are associated with elevated risks of malaria risk as well as other water-related tropical diseases such as schistosomiasis and filarias. They provide favorable breeding sites for vectors (TVA, 1947; Jobin, 1999; Sow *et al.*, 2002; Erlanger *et al.*, 2005; Keiser *et al.*, 2005; Steinmann *et al.*, 2006; Kibret *et al.*, 2009; Yewhalawet *et al.*, 2009). More and more dams have been constructed in both developed and developing countries for various purposes: flood control, irrigation and hydropower. Dam construction accelerated after the Second World War due to the relatively fast economic growth. By 2000, there were over 45,000 large dams in over 140 countries (WCD, 2000). Some 160 to 320 new large dams are estimated to be constructed annually around the world, a high percentage of which are now in African countries (WCD, 2000). However, little attention has been paid to the control of water-related tropical diseases.

In the past two decades, numerical simulation models of malaria have been developed with variable complexities (Martens *et al.*, 1995; Martens *et al.*, 1999; Depinay *et al.*, 2004; Patz *et al.*, 2005; Clennon *et al.*, 2010; Ermert *et al.*, 2011; Parham *et al.*, 2012). These models are



developed for the purposes of understanding malaria transmission dynamics, predicting future malaria risks, and evaluating the effectiveness of interventions.

The HYDRology, Entomology and MAlaria Transmission Simulator (HYDREMATS) is a malaria simulation tool developed by Bomblies *et al.* (2008). HYDREMATS is a mechanistic model that provides explicit representation of the spatial determinants of malaria transmission. The model has been applied to villages in West Africa with multiple objectives. Bomblies and Eltahir (2009) and Yamana and Eltahir (2013) applied HYDREMATS to analyze the impact of climate change on malaria in West Africa. Gianotti *et al.* (2009) studied the potential of environmental management techniques as a vector control strategy, such as leveling of topographic depressions, soil surface plowing, using HYDREMATS. The model, however, has yet to be applied to an environment with the presence of a reservoir. HYDREMATS is the only model to date that can simulate the formation of surface water bodies and their interaction with mosquitoes explicitly at a village scale. This unique characteristic of HYDREMATS will facilitate simulation of the local hydrology and nearby mosquito population dynamics influenced by a reservoir. This will in turn allow analysis of the effectiveness of potential interventions to control malaria.

This study focuses on two villages around the Koka Reservoir in Ethiopia. Like many Sub-Saharan African countries, Ethiopia has been challenged by endemic malaria. In Ethiopia, about 50 million people, or 68% of the population, are estimated to live at risk of malaria (Ethiopia MoH, 2006). Due to its large hydropower potential, Ethiopia has been intent on dam construction. The country's estimated hydropower potential is about 45,000 MW, yet only 1,500 MW of energy has been exploited from the existing 15 dams (EEPCo, 2013). In 2012, the Ethiopian Electric Power Corporation (EEPCo), the state-owned sole electric company, revised a 25-year master plan and announced a target power generation capacity of 37,000 MW by 2037 (Alternet, 2013). Expected adverse health impacts due to dam construction highlights the importance of studying the hydrology and mosquito population dynamics in this region. A model such as HYDREMATS will also help assess the effectiveness of interventions around reservoirs once the model is adapted for an environment with a reservoir.

## **1.2 Research Objectives**

The primary objectives of this study are to further develop HYDREMATS so that it represents the hydrological and entomological systems affected by a reservoir, and to test the updated HYDREMATS against field observations. To do this, we (1) set up field instruments and collected data, (2) modified HYDREMATS to represent a reservoir environment, and (3) applied HYDREMATS to the study sites.

These three activities are addressed in Chapters 2, 3 and 4, respectively. Chapter 2 describes two field sites, Ejersa and Gudedo, and the data collection conducted there. Meteorological data and entomological data were collected from the two field sites. The data collection method and the observed data are described. The modified HYDREMATS is presented in Chapter 3, as well as a short description of the original model. The two main components of HYDREMATS, the hydrology model and the entomology model, were modified to represent the reservoir environment. HYDREMATS was applied to each field site in Chapter 4. The updated HYDREMATS was applied to Ejersa because of its proximity to a reservoir. The original HYDREMATS was applied to Gudedo, due to the limited impact of the reservoir at that site. Finally, conclusions and suggestions for future study are made in Chapter 5.

## Chapter 2: Field Observations

Two field sites were selected near the Koka Reservoir in Ethiopia. Climatological and entomological data were collected from the two sites. Those data were used as model inputs and for model calibration. In this chapter, the two field sites are described in 2.1 and data collection methods are explained from 2.2 to 2.4. Sections 2.2 to 2.4 also show the observational data collected for this study.

### 2.1 Field Sites Description: Ejersa and Gudedo

The study was undertaken near the Koka Reservoir (N8°25'; E39°05'), Ethiopia. Two villages were selected; one adjacent to the reservoir, Ejersa, and the other approximately 12 km away from the reservoir, Gudedo (Fig. 2-1). This area was previously studied by the International Water Management Institution (IWMI) with a focus on entomological processes (Kibret *et al.*, 2009). The study by IWMI has provided useful background for this research.

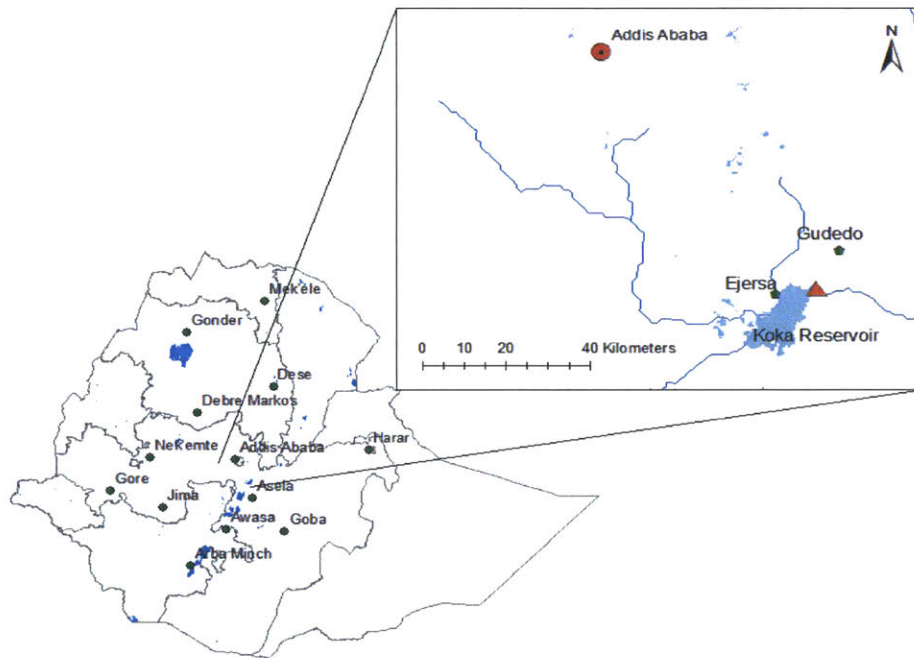
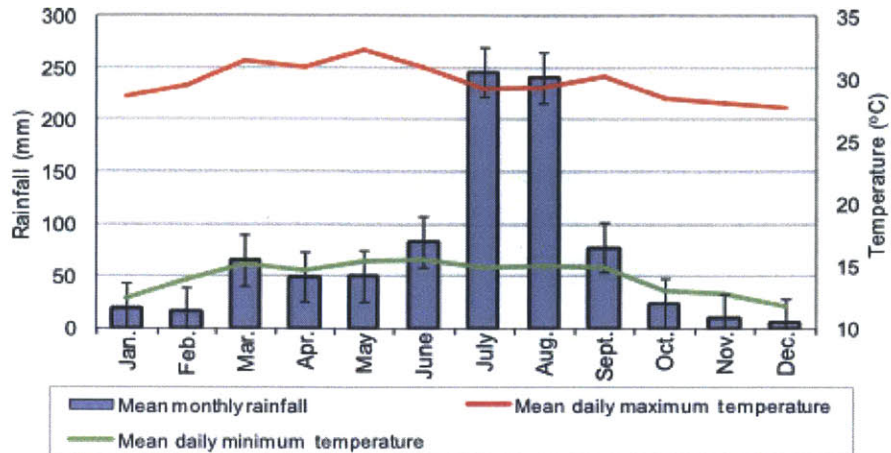


Figure 2-1 Location of the field site

The Koka Reservoir is located at the center of Ethiopia, approximately 80km southeast of Addis Ababa. The water bodies crossing the country from northeast to southwest indicates the location of the Ethiopian Rift Valley. Ejersa is adjacent to the reservoir and located northwest of the reservoir. Gudedo is approximately 12km northeast of the reservoir. The Koka Dam is marked with an orange triangle at the northeast of the reservoir and is connected to the Awash River.



**Figure 2-2 Meteorology around the Koka Reservoir**

Monthly mean over 1994 to 2007 measured at the Koka Dam. Figure adapted from Kibret *et al.* (2009).

Other than the existence of the reservoir next to Ejersa, the local climates at both sites are similar. The study sites are located in the center of Ethiopia, embraced by the Ethiopian Rift Valley. The area has three seasons, the main rainy season from mid-June to mid-September, the secondary rainy season from March to May, and the dry season for the rest of the year. The annual rainfall is around 880 mm, but it shows a large inter-annual variability (Kibret *et al.*, 2009). The mean annual temperature is about 21°C with a slightly lower temperature in the rainy season and a slightly higher temperature in dry season. Typical temperature and precipitation patterns around the Koka Reservoir is shown in Fig. 2-2.

The Koka Reservoir is located in the south of Awash River Basin within the Ethiopian Rift Valley. The catchment area of the Koka Reservoir is 11,500 km<sup>2</sup>, and the annual runoff is 1,610 Mm<sup>3</sup>, which is equivalent to an average annual flow of 51 m<sup>3</sup>/s (Kibret *et al.*, 2009). The Koka Dam is located at the northeast edge of the reservoir. It was the first dam in Ethiopia, commissioned in 1960 primarily for hydropower generation. It now works as a multi-purpose dam operated by Ethiopian Electric Power Corporation (EEPCo). The reservoir currently supplies approximately 6% of the national grid power and agricultural water for the 6,000 ha Wonji sugarcane irrigation scheme (Kibret *et al.*, 2009). More details on the dam are described in Table 2-1 (Personal correspondence with EEPCo, 2012). The reservoir water level changes by approximately eight meters annually. It experiences a decline in water level of approximately 2 cm/day after the rainy season and an increase of 4 cm/day during the rainy season.

The geology of the area is characterized by fractured late tertiary volcanic plain (Ayenew *et al.*, 2008). Research around the Koka Reservoir suggests groundwater plays a significant role in

total water yield in the basin (Chekol *et al.*, 2007; Furi *et al.* 2011).

**Table 2-1 Characteristics of the Koka Reservoir**

\* Like many other reservoirs, sedimentation has been a big problem in the Koka Reservoir (Abebe, 2001). Kibret *et al.* (2009) reported that the initial design capacity of 1,850Mm<sup>3</sup> was reduced to 1,188 Mm<sup>3</sup> by 1999, while continuous work to remove sediment has been implemented.

Dam	
Dam location	8°28'N 39°9'E
Dam type	arch gravity dam
Reservoir	
Maximum water level (meter above sill level)	110.1
Minimum water level (meter above sill level)	102
Storage capacity of the reservoir	1500 Mm <sup>3</sup> *
Surface area	200 km <sup>2</sup>
Hydropower	
Installed capacity	42 MW
Average production capacity	110 GWH
Regulated flow	42.3 m <sup>3</sup> /s

Ejersa (N8°27'; E39°04') is a set of three small communities called *kebele*, located adjacent to the Koka Reservoir. Field equipment was placed at Dungugi-Bekele *kebele*, whose population was 2851 with 589 households in 2012 (Personal correspondence with local administrator, 2012). Dungugi-Bekele *kebele* is located at about 1600 meters above sea level (masl). The main crops grown are onions, tomatoes, soybean, tef and wheat. People cultivate crops using water pumped from wells at topographically low areas near shoreline before the rainy season. Reservoir high waters submerge these low areas in the rainy season, and these floodwaters bring fertile soil every year. Some people fish at the reservoir. The topography in Ejersa is gentle and the shoreline slope is 1.3 degrees (Kibret *et al.*, 2009).

Gudedo (N8°33'; E39°12') was selected as a control village. Jogo-Gudedo *kebele*, which had 3162 residents and 650 households in 2012 (Personal correspondence with local administrator, 2012) was equipped with mosquito light traps. The elevation of Gudedo is about 200m higher than that of Ejersa. Gudedo has a diverse landscape and the elevation around Jogo-Gudedo *kebele* ranges between 1740 and 1865 masl. This farming kabele stands 12km away from the

reservoir. While there is little agreement on the maximum mosquito flight distance, it is generally agreed that mosquitoes cannot fly more than 5km (Gillies, 1961). Thus, mosquito population dynamics in Gudedo are considered to have little influence from the Koka Reservoir. The predominant crops grown in the area are soybeans, tef and wheat. The two villages are somewhat representative of central Ethiopia in terms of climate and economic activity. The similarity of the villages will allow comparison of the effects of a large water body, i.e., Koka Reservoir, on mosquito population dynamics.

Each field site was equipped with a meteorological station (MS), a soil moisture station (SMS) and CDC mosquito light traps, which are explained in detail in the next section. The locations of these instruments in Ejersa and Gudedo are shown in Fig. 2-3 and Fig. 2-4, respectively. The daily water level of the Koka Reservoir was obtained from EEPCo, the operator of the Koka Dam. Our preliminary research and data collection was carried out in summer 2011, and continuous data collection has been conducted since July 2012. Adult mosquitoes were collected on a weekly basis in both Ejersa and Gudedo in the rainy season, from July 2012 to November 2012. In the dry season, from December 2012 to February 2013, the frequency was reduced to biweekly and monthly in Ejersa and Gudedo respectively. Mosquitoes collected in the light traps are classified at the genus level.

## **2.2 Climate and Hydrological Data**

### **2.2.1 Meteorological Data**

Meteorological stations (MSs) were equipped in Ejersa and Gudedo in summer 2011, while the practical data collection started in July 2012 in Ejersa. The MSs measured temperature, relative humidity, precipitation, wind speed and wind direction, incoming short wave radiation, and soil moisture at three depths. All instruments except rain gages and soil moisture probes were mounted on 6-foot steel tripods (Fig. 2-5). Temperature and relative humidity (RH) were measured using Campbell HMP45C-L11 temperature/RH probes enclosed in solar shields. Precipitation was measured with Campbell TE525-L50 rain gauges mounted on separate poles from the main tripods. Campbell 03002-L11 wind sentries measured wind speed and wind direction. Incoming solar radiation was measured with Campbell LI200-L11 pyranometers. All the data from the instruments were recorded with Campbell CR1000-ST-SW-NC data loggers. The data loggers were sealed in locked enclosures mounted on the tripods. Each system was powered by a Campbell SP20 solar panel supported by a 12 Amp - 7 volt sealed gel battery and a charge controller. All the data were automatically collected every 30 minutes and stored in the loggers.



## Ejersa Field Setting



0 0.25 0.5 1 Kilometers

### Legend

- ★ Met Station
- ★ Soil Moisture Station
- ◆ GW Monitoring Well
- Dipping Pool
- ▲ Light Trap House



Figure 2-3 Ejersa field setting

Red rectangle shows the 3km x 3km simulation domain. The elevation in the domain varies between 1590 and 1642 masl excluding the elevation of the reservoir bed.

## Gudedo Field Setting

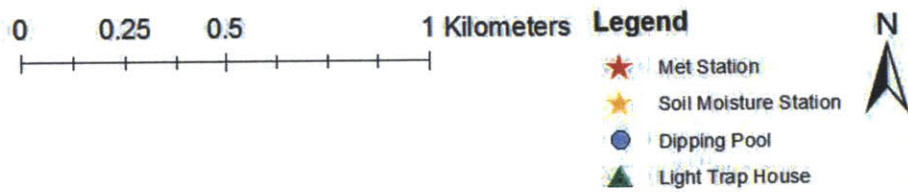
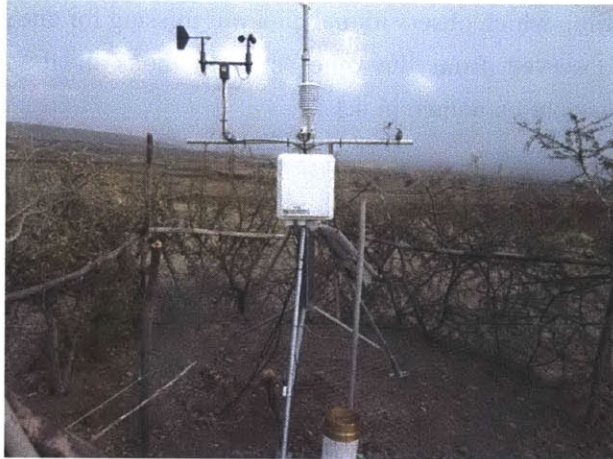


Figure 2-4 Gudedo field setting

Red rectangle shows the 2km x 2km simulation domain. The elevation in the domain varies between 1740 and 1865 masl.





**Figure 2-5 Meteorological station deployed in Gudedo**

Temperature and relative humidity were measured inside a solar shield apparatus at the center of the crossarm. A wind vane and a pyranometer were set at the left and the right of the crossarm in this picture, respectively. The rain gauge is a white bucket with a gold-colored top mounted separately from the tripod. Soil moisture was also measured at the MSs from three depths. A data logger in a white enclosure was powered by a solar panel.

In Gudedo, meteorological data have been collected since the middle of July 2011. The temperature (Fig. 2-6 (a)) in 2012 varied from 15.5 °C to 24.5 °C with the annual mean being 19.8 °C. Relative humidity was high in the rainy season, and low in the dry season with daily minimum of 11.4 % in May (Fig. 2-6 (b)). The annual rainfall in 2012 was 806 mm, 90% of which fell between mid-June and September. Incoming short radiation shown in Fig. 2-6 (d) had little seasonal variability. It was slightly higher than that observed in Ejersa because the elevation in Gudedo is about 200m higher. The wind speed observed in Gudedo had a mean of 3.4 m/s (Fig. 2-6 (e)). The wind speed was, in general, higher in the dry season and lower in the rainy season. The wind direction data are shown in Fig. 2-6 (f) only from July 2012 because the wind vane alignment was corrected at that time. The wind direction was measured with respect to the north increasing clockwise. The wind mainly blew from the southwest in the rainy season and from southeast in the dry season.

In Ejersa, meteorological data collection started in June 2012, and the data are shown in Fig. 2-7. Overall, the data collected in Ejersa were similar to the data collected in Gudedo. The annual average temperature of 21.2 was slightly higher than that of Gudedo because of the difference in elevation. The wind blew towards the reservoir in the rainy season, and from the reservoir in the dry season. For about two weeks in January 2013, a technical fault led to a cessation of data collection.

The meteorological data were used as simulation model inputs. Model inputs are explained in

3.1.3. For the period during which observational data was missing for one site, input data were prepared using data observed from the other site. Methods of the preparation of the complementary input data are explained in 4.1.2.

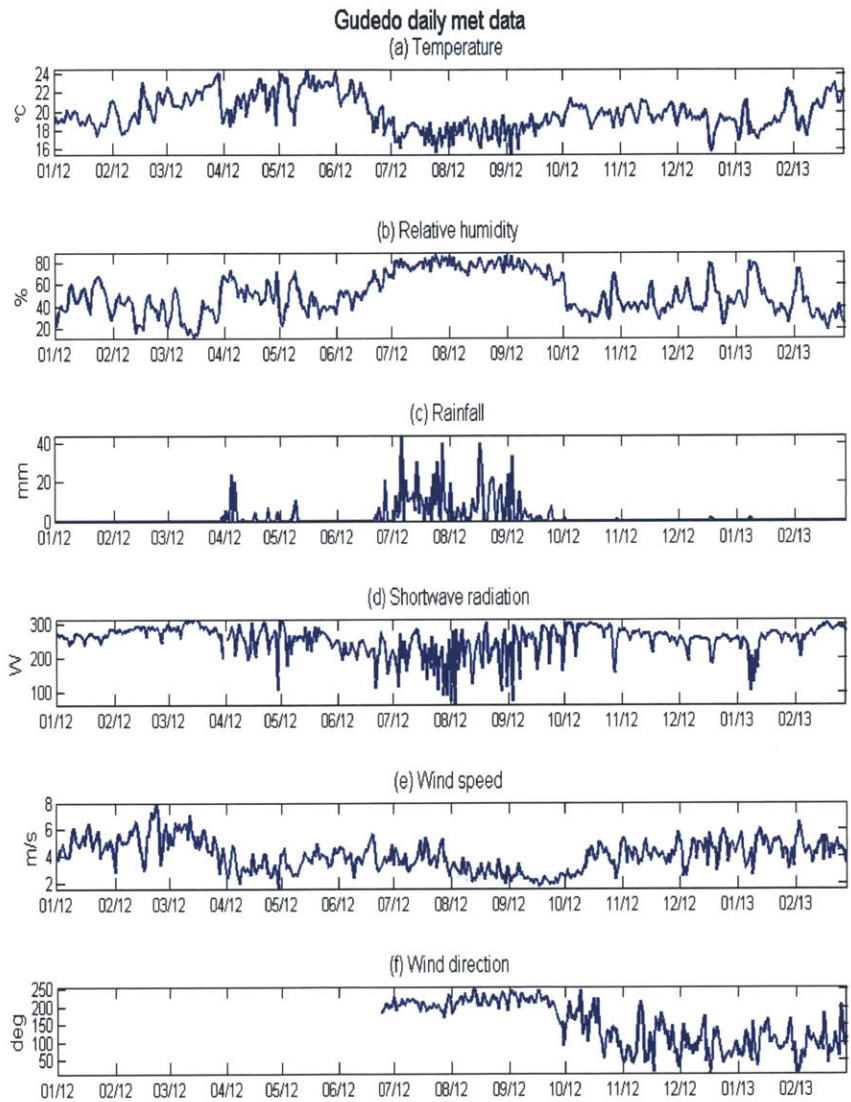


**Figure 2-6 Gudedo met data**

**Observational data from July 2011 to February 2013 were shown.**

**(a)temperature [°C], (b)relative humidity [%], (c)rainfall [mm/h], (d)shortwave radiation [W], (e)wind speed [m/s], (f)wind direction [deg]**

**The alignment of the wind sentry was not accurate before July 2012, hence the data are not shown.**

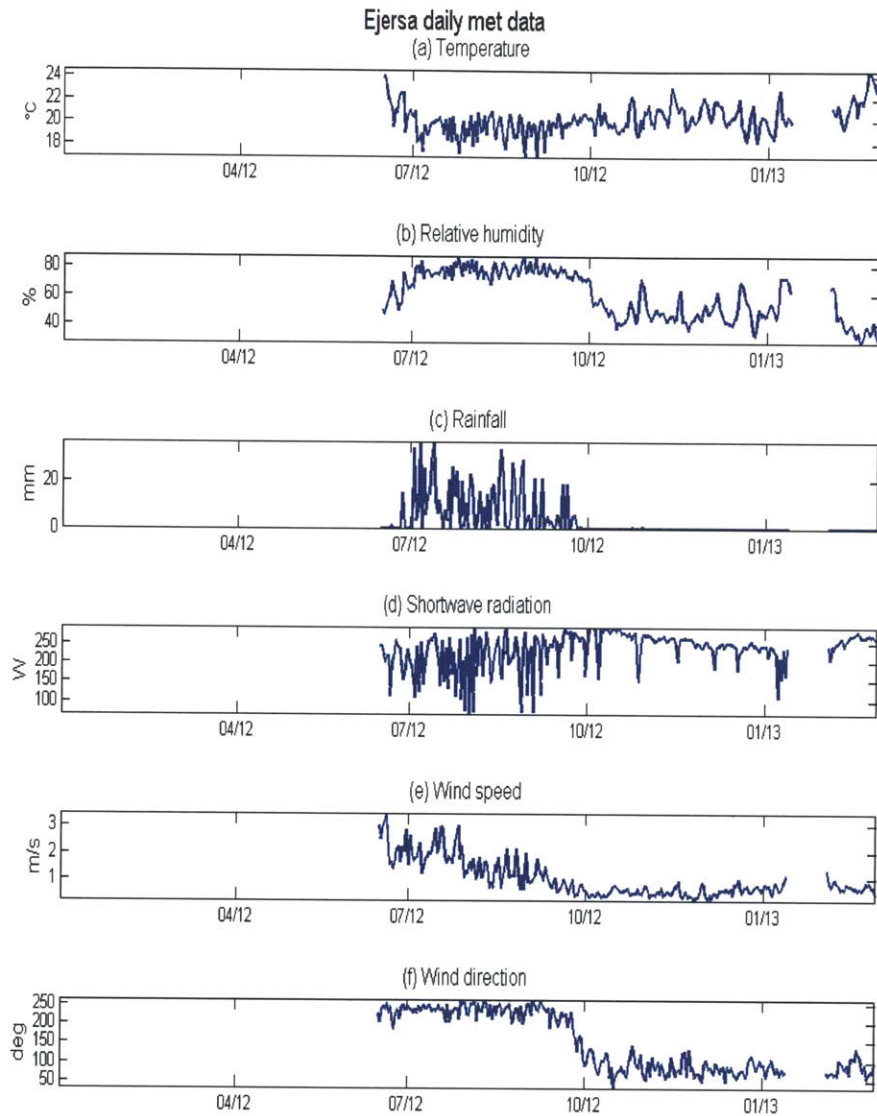


**Figure 2-7 Ejersa met data**

Observational data from June 2012 to February 2013 were shown.

(a)temperature [ $^{\circ}\text{C}$ ], (b)relative humidity [%], (c)rainfall [mm/h], (d)shortwave radiation [W], (e)wind speed [m/s], (f)wind direction [deg]

A technical fault occurred in late January in 2013.

### 2.2.2 Soil Moisture Data

Soil moisture data were collected from both the MSs and SMSs. The MSs were equipped with Campbell CS616-L11 soil moisture probes and the SMSs with Campbell CS625 soil moisture probes. The volumetric water content (VWC) was measured at 15, 30 and 100cm below surface. The SMSs were set in both study sites in summer 2011 followed by actual data collection beginning in July 2012. The data were recorded at 30-minute intervals with Campbell CR200 Data Loggers. Each logger was sealed in a locked enclosure and was powered by a Campbell SP10 solar panel supported by a 12 Amp - 7 volt sealed gel battery and a charge controller.

Soil moisture probes indirectly measure the VWC. They send electric signals in the soil and measure the travel time of the signals. The travel time of the signals is a function of water in the soil as water is the only soil constituent that has a high dielectric permittivity. The observed travel time of the signal can be transferred to the VWC using empirical forms. In this study, standard calibration coefficients for a quadratic form were employed to obtain the VWC estimates ( $VWC_{est}$ ) following Campbell Scientific (2012). The quadratic form reads,

$$VWC_{est} = -0.0663 - 0.0063 \times t + 0.0007 \times t^2, \quad (2-1)$$

where  $t$  is the travel time of the pulse in Campbell CS616-L11 soil moisture. Readers should note that this form does not necessarily fit all soil types. The coefficients were derived for loam soil. For other types of soil texture, different coefficients are expected to fit observations better. The amount of soil organic matter and soil temperature also affect the model fit. In this study, the standard calibration coefficients by Campbell Scientific were employed. The calibration of the VWC readings were conducted using weighting factors ( $f$ ), that is:

$$VWC_{cal} = VWC_{est} \times f. \quad (2-2)$$

The maximum  $VWC_{est}$  observed in the field sites during the rainy season was as high as  $0.7 \text{ m}^3 \text{ m}^{-3}$ . The highest possible value of  $VWC_{est}$  is the porosity of the soil, but the value of 0.7 exceeded the porosity typically observed for any type of soil. In addition, the observed  $VWC_{est}$  at the 30cm depth remained high, around 0.6, for the entire rainy season even for days without rainfall events. This observational data suggests that the recorded value around 0.6 was not even the saturated value, i.e., porosity. This erroneously high reading of VWC is most likely caused by improper calibration coefficients, which may be attributed to the soil type in the field sites, existence of micro-pores created by vegetation roots and detritus, and/or disruption of soil structure caused when the probes were inserted. In this study, the weighting factors were found using the porosity assigned and the soil moisture simulated in IBIS. The weighting factor  $f$  was set at 0.19 for Ejersa and 0.36 for Gudedo.

The SMS in Ejersa was located approximately 0.2km from the MS. The SMS and the MS in



Gudedo were approximately 1.5km apart from each other. A soil moisture probe placed at a depth of 15cm under the soil surface at the Gudedo MS was not working from the beginning, so no data were retrieved from it. In addition, the SMS in Gudedo faced a technical fault, leading to a long break in data collection for most of the study period.

### 2.2.3 Reservoir Water Level Data

The daily water level of the Koka Reservoir was obtained from EEPCo. They provided the water level data relative to a sill level, whose elevation was not obtained. In order to obtain the elevation of the reservoir water level in meter above sea level, the elevation of the water surface in DTM from Apollo Mapping satellite data were compared with the reservoir water level data from EEPCo on the same date when the satellite image was taken. The elevation-corrected reservoir water levels are shown in Fig. 2-8 for the study period of January 2012 to February 2013. The annual fluctuation for the period was seven meters with its highest peak in September and lowest value in July. During the rainy season, the reservoir water level increased at a rate of approximately four cm per day. During the dry season, the recession rate was about two cm per day.

The area submerged under the reservoir was analyzed using the reservoir water level data and topography data. Fig. 2-9 illustrates the contour lines at the shore of the Koka Reservoir. The areas to the right of the contours shows the submerged area depending on reservoir water levels. The figure suggests that a large area becomes inundated when the water level is above 1594 masl, which likely occurs from September to December.

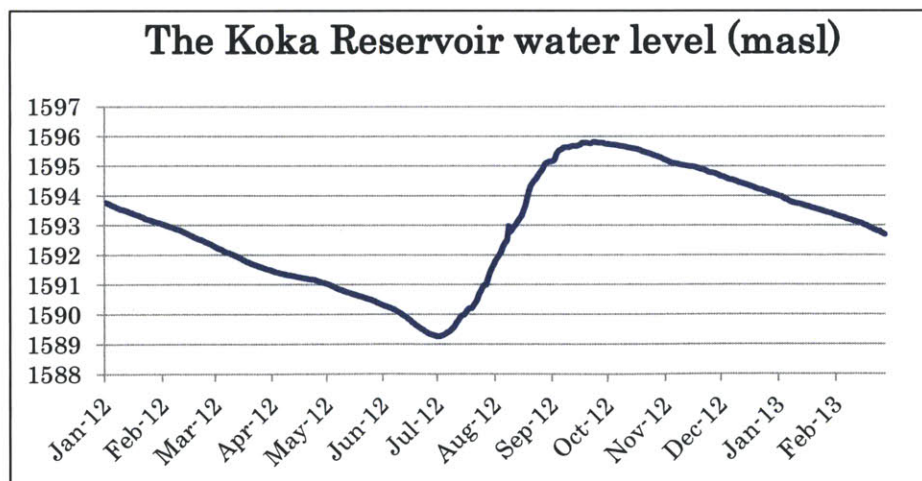
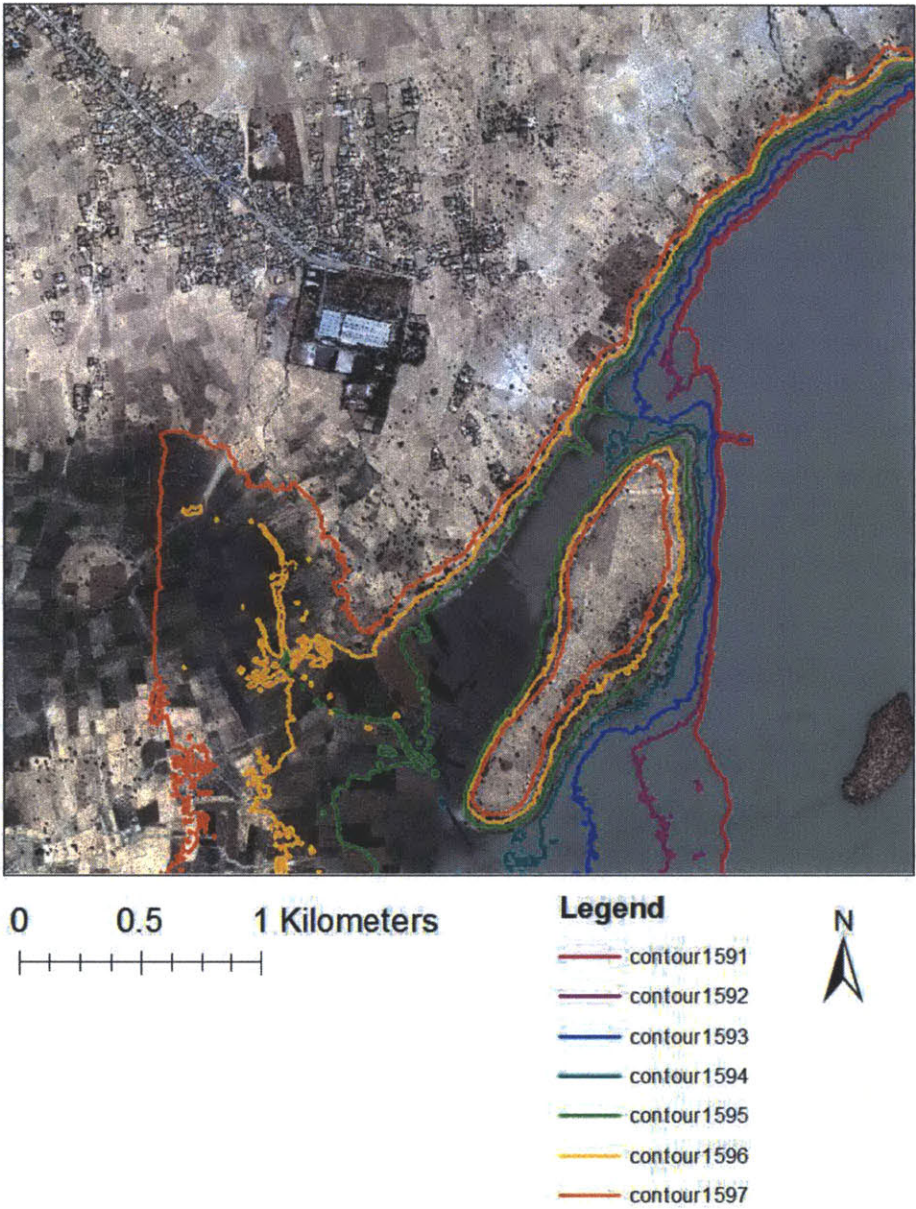


Figure 2-8 The Koka Reservoir water level (meter above sea level)

The reservoir water level changes by about eight meters annually. It experiences a decline in water level of approximately 2 cm/day after the rainy season and an increase of 4 cm/day during the rainy season.

Shoreline contours



**Figure 2-9 Contour lines at the shoreline of the Koka Reservoir**  
The areas to the right of the contour lines show the areas submerged in the reservoir depending to reservoir water levels.



### 2.2.4 Groundwater Table Data

To measure the variation in groundwater levels in Ejersa, pressure transducers were placed in three wells in Ejersa. HOBO U20 Water Level Loggers were employed for this purpose. In Ejersa, the GWT is shallow because of its proximity to the reservoir, and it is expected to fluctuate responding to the change in the reservoir water level. The loggers were placed in wells aligned perpendicular to the reservoir shoreline as much as possible (Fig. 2-3, Fig. 2-10). Gudedo was not equipped with loggers because it is too far away from the Koka Reservoir to have a shallow GWT. Evidence of a deep GWT was obtained from local residents, who reported that no groundwater was observed when digging a hole 25 meters deep at a construction site near Gudedo (Personal correspondence with local person, 2012). The GWT data were compared with simulation outputs and used to calibrate hydraulic parameters. However, unfortunately, the data collection was interrupted by local people many times, so the data were not obtained for the whole study period. In addition, a transducer in well 1 was stolen before any data was downloaded from it. Hence in this study, a limited amount of data was used for model calibration. All available GWT elevation data are shown in Fig. 2-10 up to Feb. 2013. More data will become available in the future.

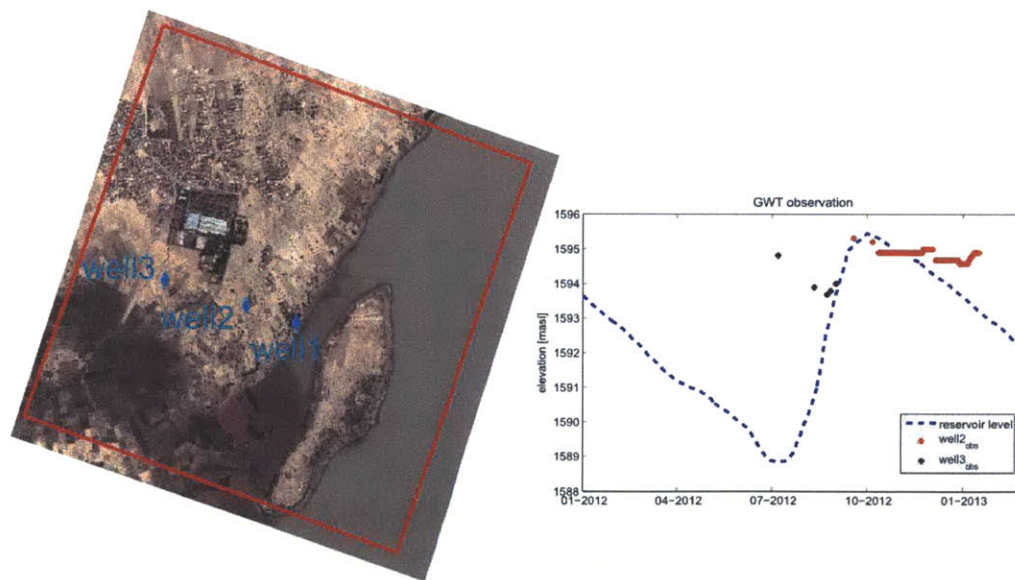


**Figure 2-10 Well locations and observed GWT**

Left figure shows the location of observational wells (well1, 2, 3). Right figure shows the observed GWT elevations at well 2 (red asterisks) and well 3 (black asterisks). No observational data were collected from well 1. Observed reservoir water levels are shown in blue dash line.

## 2.3 Entomological Data

Adult mosquitoes and aquatic stage mosquitoes were monitored in Ejersa and Gudedo on a weekly to monthly basis. The adult mosquito collection was conducted using CDC light traps. Adult mosquitoes were classified into genus using the naked eye. Larvae dipping was conducted at the same frequency as the adult mosquito collection using a dipper and classified at the genus level. The methods and the results of entomological data collection are shown in this section.

### 2.3.1 Mosquito Species Present around the Koka Reservoir

*Anopheles* species present around the Koka reservoir are *An. arabiensis*, *An. funestus*, *An. pharoensis*, and *An. coustani*. The major *Anopheles* species is *An. arabiensis* followed by *An. funestus*. *An. pharoensis*, and *An. coustani* are less commonly found (Endo, 2013; Kibret *et al.*, 2009). As *An. arabiensis* is a complex of *An. gambiae*, *An. arabiensis* and other *An. gambiae* complex are morphologically identical so are indistinguishable even with a microscope. However, *An. arabiensis* is considered to be the only complex of *An. gambiae* present in the region (Ye-Ebiyo *et al.*, 2003; Reis *et al.*, 2011; Animut *et al.*, 2013).

*Culex* is another genus of mosquitoes, which was found around the Koka Reservoir in addition to *Anopheles*. The proportion of *Culex* captures in Ejersa was slightly higher than that of *Anopheles*. Significantly higher proportion of *Culex* was found in Gudedo. In the dry season, only *Culex* mosquitoes were found in Gudedo. Because the only species that transmits malaria is *Anopheles*, only the population dynamics of *Anopheles* were studied here.

Different species have different breeding behaviors. The behavioral features of the main four *Anopheles* species in the field sites are described in Table 2-2 following Gilles and Meillon (1968). *An. arabiensis* utilizes a great variety of water bodies including ephemeral rain-fed puddles, small hoof-prints, and semi-permanent open puddles. On the other hand, *An. funestus* almost exclusively uses permanent pools such as reservoir shoreline. Both *An. arabiensis* and *An. funestus* are important malaria vectors due to their anthropophilic behavior and significant presence around the Koka Reservoir. Animut *et al.* (2013) found in a similar environment about 75 km to the southwest of Ejersa that the human blood index (HBI) and the bovine blood index (BBI) are about 32% and 39% respectively for *An. arabiensis* and 22% and 50% respectively for *An. pharoensis*. *An. funestus* was not commonly found in the study, likely because of the absence of a permanent water body such as a reservoir. *An. funestus* is sometimes found to have an even higher vectorial ability than *An. gambiae* (Fontenille *et al.* 1997; Manga *et al.* 1997). The high vectorial ability of *An. funestus* is partly attributed to its high longevity (Gilles and Meillon, 1968).



**Table 2-2 Characteristics of Anopheles mosquitoes present around the Koka Reservoir**

(\*1) *An. arabiensis* utilizes a variety of water bodies, so their breeding sites are not limited to the pool types listed here.

(\*2) *An. arabiensis* shows large behavioral plasticity.

(\*3) Breeding sites are limited to near the edges if deep.

(\*4) *An. pharoensis* shows some postporandial endophilic tendency.

<i>An. Species</i>	Breeding site	Feeding site	Resting site
<i>An. arabiensis</i>	Shallow open sunlit puddles such as rain-fed pools, borrow-pits, hoof-prints and irrigated field puddles (*1)	- Anthropophilic but also zoophilic - Endophagic - Early and late eating	Endophilic but partially exophilic (*2)
<i>An. funestus</i>	Clear, permanent and sunlit water bodies such as swamps (*3), weedy sides of streams and shorelines	- Highly anthropophilic - Endophagic - Late biting	Endophilic
<i>An. pharoensis</i>	Permanent and vegetated water bodies such as irrigated fields and vegetated shorelines	- Anthropophilic but also zoophilic - Exophagic	Exophilic (*4)
<i>An. coustani</i>	Clear water with aquatic and semi-aquatic vegetation		

### 2.3.2 Adult Mosquito Data Collection

Adult mosquito samplings were conducted from July 2012 to February 2013. Adult mosquitoes were collected using CDC miniature light traps from 6 pm to 6 am. Six traps were deployed in each site, three inside and three outside houses. The locations of the traps in Ejersa and Gudedo are shown in Fig. 2-3 and Fig. 2-4 respectively. An indoor light trap house and an outdoor light trap house were clustered together. The criteria for selecting light trap locations were no use of electricity, no smoking (as much as possible), and no light outside. The light traps were placed in the same houses over the study period. The light traps set indoors were placed next to people's beds as mosquitoes are attracted by human odor, heat and CO<sub>2</sub> from breathing (Fig. 2-11). The traps were located 1.5m to 2m above the ground. The traps were charged by 6V-6Amp spillable lead acid batteries. Mosquitoes and other bugs collected in the traps were removed one or two days after the trap deployment, leaving the trap itself at exactly the same

location. Collected mosquitoes were classified at the genus level (i.e., *Anopheles* or *Culex*), and the sampled populations were counted. A field survey conducted after this study period revealed that *An. arabiensis* is the dominant species both in Ejersa and Guedo, accounting for approximately 90% of *Anopheline mosquitoes* present in the sites. Samples were collected on a weekly basis in both Ejersa and Guedo in the rainy season, from July 2012 to November 2012. In the dry season, from December 2012 to February 2013, the frequency was reduced to biweekly and monthly in Ejersa and Guedo, respectively.

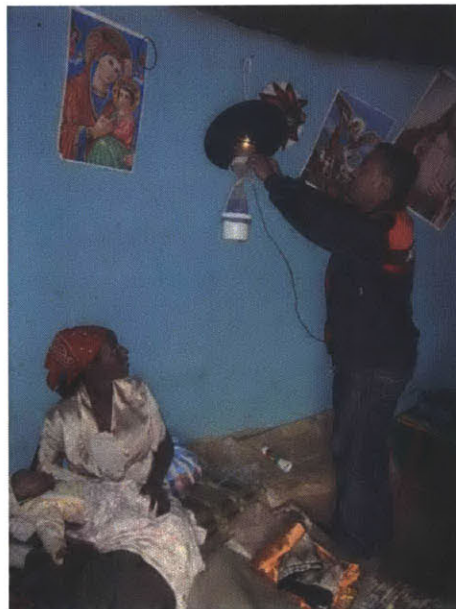


**Figure 2-11 Indoor light trap set in Guedo**

**Light traps were placed at about 1.5m to 2m above ground and near people’s sleeping place. The light traps were powered by 6V acid batteries and employed from 6pm to 6am.**

Table 2-3 and Table 2-4 below describe the features of light trap houses (LTHs) in Ejersa and Guedo, respectively. Houses typically seen in this area were round-shaped thatched huts, and square-shaped tin houses. The house walls are made of mud. The number of residents varied from three to ten with some exceptions. Houses used fire for cooking indoors. Although the fire and the resulting smoke were not meant to be used as repellent, they may have an impact on mosquito attraction. As is common around this area, every light trap house had livestock such as cows and chickens. The livestock were kept in the compounds.

The geographical proximity of the houses to mosquito breeding sites is another feature that needs to be mentioned. As is described in Table 2-5 in 2.3.3, the LTH 2E contained a rain-fed

pool in its compound, which was found to be a productive breeding site throughout the study period. As a result, the 2E light trap usually collected many mosquitoes. The LTH 1E is located closest to the shoreline. When the reservoir water level nears its peak, the shoreline can come to within a hundred meters of the house. The 1E light trap also collected many mosquitoes as compared to other houses. The LTH 1G in Gudedo had manmade pools both inside and outside the compound. The LTH 3G also had manmade pools outside its compound.

**Table 2-3 Ejersa light trap house features**

Light Trap Number	Indoor/Outdoor	House Type	Number of People	Smoke inside?	Light inside?	Livestock
1E	Indoor	Thatched, hut	3	Yes	No	Yes
2E	Outdoor	Tin, house	6	Yes	No	Yes
3E	Indoor	Thatched, hut	3	No	No	Yes
4E	Outdoor	Tin, house	10	No	No	Yes
5E	Indoor	Tin, house	1	No	No	Yes
6E	Outdoor	Thatched, hut	2	No	Yes	Yes

**Table 2-4 Gudedo light trap house features**

Light Trap Number	Indoor/Outdoor	House Type	Number of People	Smoke inside?	Light inside?	Livestock
1G	Indoor	Straw, hut	3	No	No	Yes
2G	Outdoor	Tin, house	7	No	Yes	Yes
3G	Indoor	Straw, hut	5	No	No	Yes
4G	Outdoor	Tin, house	5	No	No	Yes
5G	Indoor	Straw, house	4	No	No	Yes
6G	Outdoor	Straw, tin	7	No	No	Yes

Fig. 2-12 shows the total number of *Anopheles* mosquitoes collected in Ejersa and Gudedo. Sometimes (5 out of 162 collections in Ejersa and 3 out of 150 collections in Gudedo) light traps faced troubles such as wiring misconnections and battery shortages. Data collected from those mal-functioning light traps were replaced with the average of the values in the previous collection and the following collection from the same light trap house. In the third week of September, indoor residual spraying (IRS) was conducted in houses in Ejersa. As a result, the

number of mosquitoes collected in the light traps dropped sharply. The effect of IRS is generally expected to continue for months. However, the figure indicates that the effect likely lasted for only a couple of weeks, possibly due to drug resistance, the use of overly diluted solution, or inappropriate training in spraying. It is not easy to estimate how many mosquitoes would have been observed if it had not been for IRS. However, one may expect that the magnitude of the mosquito population would have increased while the timing of the population peak would remain unchanged.

Ejersa (red), as compared to Gudedo (blue), observed more *Anopheles* over the data collection period with a later peak, which reflects the impact of the reservoir. Over the period, approximately ten times more *Anopheles* mosquitoes were collected in Ejersa because the reservoir provides ample breeding sites for mosquitoes. In addition to the difference in total number, the timing of the peak in the mosquito population was different. The *Anopheles* population in Gudedo had a peak between mid-August and early-October, following the rainy season (July to September) with about a month of delay. This gap between the rainy season and mosquito season is commonly observed where no permanent water body such as a reservoir exists. Ejersa had a peak in *Anopheles* population in November, which is unlikely to be caused by rain-fed pools. This late peak and hence a prolonged mosquito season can be explained by the expansion of the reservoir area due to the increased inflow in the post-rainy season (September to November).

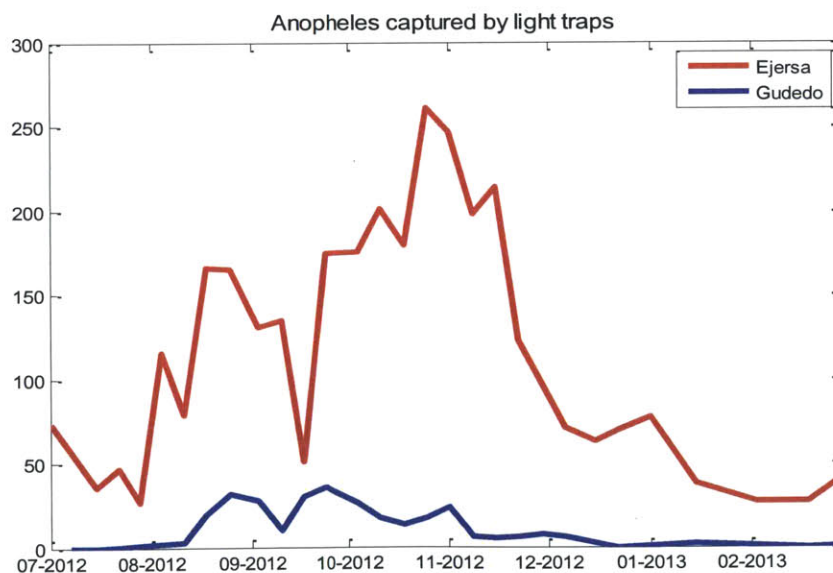


Figure 2-12 Number of Anopheles captured by light traps

### 2.3.3 Larvae Data Collection

At the same frequency as the adult mosquito collection, potential breeding sites were sampled for the existence of larvae from July 2012 to February 2013. Larvae found were classified at the genus level and the numbers of anopheles collected during the study period are reported in this section.

Field surveys to find potential mosquito breeding sites were conducted in July 2012, in the rainy season, within some 500 m<sup>2</sup> around the light trap houses. If the potential breeding sites were found, the location and the size of the pools were recorded. After several field visits, some locations were identified to be prone to the formation surface pools, and those locations were routinely surveyed for mosquito productivity. The features of the routinely observed pools are summarized in Table 2-5. The larvae dipping surveys were conducted using a dipper with a diameter of 12 cm at these pools. Six dips (a set of samples) were made for every square meter of pool surface area, unless otherwise noted. The samples were taken some 15 cm away from the pool periphery. Larvae were stored in glass vials, classified at the genus level with the naked eye, and the numbers of *Anopheles* and *Culex* were counted. The development stages of aquatic mosquitoes, i.e., first to forth instars and pupae, were not identified.



In Ejersa, only one rain-fed pool was routinely surveyed. Small pools were present. However, they often existed only for a short period after rainfall events, which were not suitable for routine surveys. The surveyed pool, however, was not completely fed by rainfall water. Leak from a pipe a tannery use provided a source of water. This is why this pool existed long enough to be a productive mosquito breeding site. This pool was found to contain many larvae.

Two sets of larvae samples were taken at reservoir shorelines, approximately 100m north and 100m south of a local road, which runs approximately along the line of latitude N8.452°, where a watch house stands. The location of shoreline changes according to the change in the reservoir water level. The exact locations of larvae dipping were not recorded because the shoreline location can be traced using water level data and elevation data.



In Gudedo, five pools were found to persist during the rainy season. Three pools were manmade pools located next to local houses. These three pools were often found to be positive mosquito breeding sites. The other two were created during the process of construction. Aquatic stage mosquitoes were rarely found in these two pools.

The results of larvae dipping for the survey period from July 2012 to February 2013 are shown in Fig. 2-18 and Fig. 2-19, for Ejersa and Gudedo, respectively. The results reflect the difference in mosquito breeding seasons between the two villages. In Ejersa, larvae were found almost throughout the survey period. The rain-fed pool in Ejersa, which is constantly fed by a

**Table 2-5 Description of pools for larvae dipping**

Ejersa	
Rain-fed pool	<p>A pool inside the LTH 1E compound.            Two set of samples were taken from this pool.            *Note that the pool is not completely rain-fed. Water leaking from a pipe that a tannery uses sustained this pool.</p>  <p style="text-align: center;"><b>Figure 2-13 Pool in Ejersa sustained by rainfall and leak from a pipe</b></p>
Shoreline	<p>Two sets of samples were taken at the north and at the south of a local road, which runs along a line of N8.452°. The location of sampling changed along with the change in shoreline locations.</p>  <p style="text-align: center;"><b>Figure 2-14 Shoreline at the beginning of the rainy season, when the water level is low</b></p>



	 <p data-bbox="461 638 1279 709"><b>Figure 2-15 Shoreline in the middle of the rainy season, when the water level is relatively high</b></p>
Gudedo	
Rain-fed pool 1	<p data-bbox="461 814 1024 886">A manmade pool inside the LTG 1G compound. A set of samples was taken from this pool.</p>  <p data-bbox="672 1339 1073 1367"><b>Figure 2-16 Manmade pool in Gudedo</b></p>
Rain-fed pool 2	<p data-bbox="461 1409 1036 1480">A manmade pool outside the LTG 1G compound. A set of samples was taken from this pool.</p>
Rain-fed pool 3	<p data-bbox="461 1497 1031 1568">A manmade pool next to the LTG 3G compound. A set of samples was taken from this pool.</p>
Rain-fed pool 4	<p data-bbox="461 1585 1289 1698">A pool supposedly made during construction of a new road. A set of samples was taken from this pool, although the size of the pool was large.</p>
Rain-fed pool 5	<p data-bbox="461 1717 1289 1873">A pool supposedly made during the construction of a new road. The pool is located besides the old main road. A set of samples was taken from this pool, although the size of the pool was large.</p>



**Figure 2-17 Manmade pool created during a construction period**

pipe leak, was especially productive because of its stability. The variability in the productivity of shoreline water was larger. This variability is due to the fact that the location of the shoreline keeps changing and so does the environment of the breeding site. Under heavy rainfall and wavy conditions, a small number of larvae were observed.

Larvae in Gudedo were observed only during the rainy season. This is primarily because the existence of the breeding sites depends solely on rainfall. After the rainy season, approximately after October, no larvae were observed in Gudedo. All potential breeding sites disappeared in November. Pool 1 in Gudedo was often found to be productive. This productivity could be attributed the limited number of breeding sites in Gudedo; limited choice of oviposition sites for mosquitoes may have increased the density of aquatic stage mosquitoes in the pool.

In addition to the limited number of samples, readers should note the limitation of the accuracy of the sampling method. Different microhabitats within a pool create heterogeneity in larval concentration. One dip would contain no larvae while another dip from the same breeding site may find many larvae. Human error in larvae dipping is another concern. Because of their small body size, younger instar larvae tend to be omitted from counting, and hence the number of larvae is underreported. One may disturb the water of breeding sites, leading larvae to swim away or dive into water. As a result, fewer larvae are found. In this study, care was taken to minimize these errors. Multiple dips were taken in a single sample to minimize the effect of heterogeneity of breeding sites.



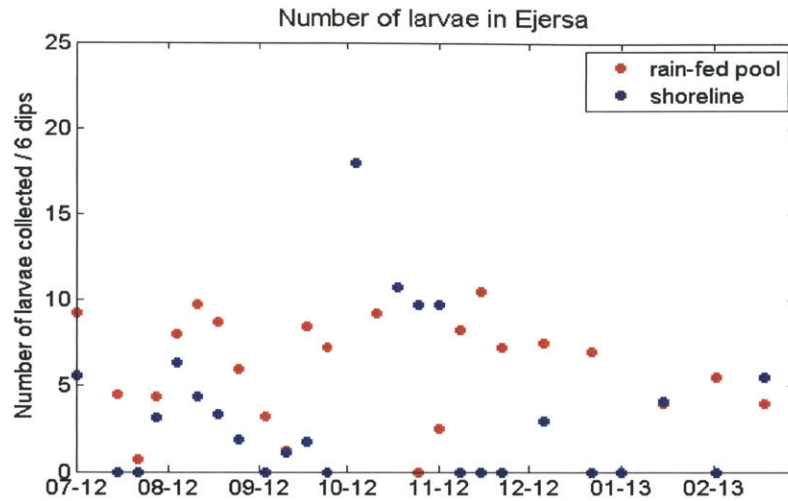


**Figure 2-18** Number of larvae and pupae collected from Ejersa pools

The plot shows the average of the total number of larvae and pupae collected from each set of samples (six dips). Shoreline points include both samples taken from the northern and southern shoreline locations. The rain-fed pool shown in blue is not completely sustained by rainfall. Hence it persisted even after the rainy season.

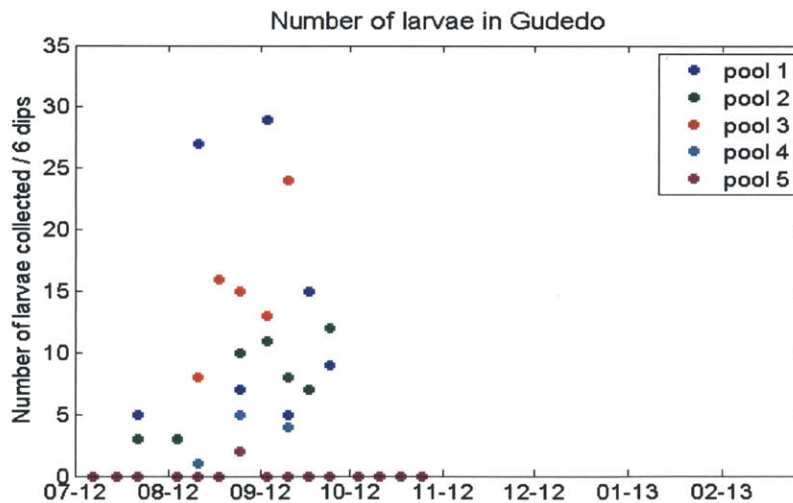


**Figure 2-19** Number of larvae and pupae collected from Gudedo pools

The plot shows the total number of larvae and pupae collected from a set of sample at each pool. One set of sample was taken from each type of pools in Gudedo. The zero values mean that samples were negative. The absence of the data points means that the pools dried out. After November, no pool was observed in Gudedo.

## 2.4 Clinical Data

Analyzing clinical malaria data is important because the population dynamics of *Anopheline* mosquitoes does not necessarily mirror that of malaria incidence. Although the simulation of malaria incidence is not the main focus of this study, malaria incidence data are shown in this section in order to provide general characteristics of malaria epidemics around the Koka Reservoir.

Data on malaria incidence in Ejersa were obtained from a local clinic in Ejersa. Fig. 2-20 contains malaria incidence in Ejersa over five years from July 2008 to June 2013 (the Ethiopian calendar year begins in July). Diagnoses were all made by rapid diagnosis test (RDT) kits, which were provided free of charge to local people by the government. No active survey was conducted during the five years and the reported cases are based on voluntarily visits to the clinic. The figure illustrates that the malaria incidence peaks around October, well after the main rainy season (July – Sep.). It is usually observed that malaria season follows mosquito breeding season, whose trend resembles that of rainfall with a few weeks of delay. In Ejersa, as shown in 2.3.2, the mosquito population dynamics is not fully explained by rainfall events. The prolonged mosquito breeding season results in the late arrival of the malaria peak in October. In addition, ambient temperature also accounts for the malaria transmission trend. After the main rainy season, the air temperature rises slightly increasing the longevity of mosquitoes and decreasing extrinsic incubation period of parasites. This is understood to be the mechanism of the high malaria incidence following the main rainy season. Similarly, malaria incidence has a second peak following the secondary rainy season (Apr. – May). Although the rainfall during the secondary rainy season is only 10% of the annual total rainfall, the significance of malaria incidence at that time is relatively high. This high malaria incidence around June is likely because the temperature in the secondary rainy season is higher than in the main rainy season.

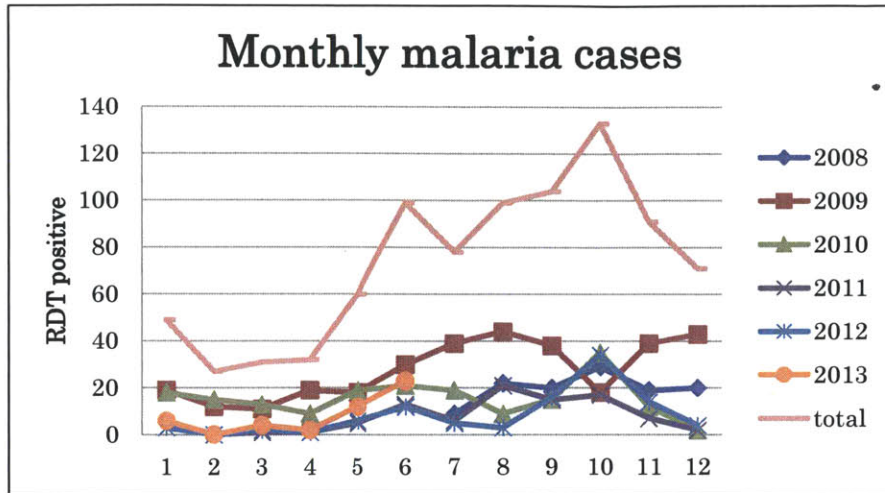


Figure 2-20 Monthly incidence of malaria in Ejersa

The data were obtained from July 2008 to June 2013. The total malaria incidence observed in Ejersa over the five years is shown in pink line.

### **Chapter 3: HYDREMATS: Model Description**

The HYDRology Entomology and Malaria Transmission Simulator (HYDREMATS) was originally developed by Bomblies *et al.* (2008) and has been applied to villages in West Africa (Bomblies *et al.*, 2008; Bomblies and Eltahir, 2009; Gianotti *et al.*, 2009; Yamana and Eltahir, 2010; Yamana, 2011). In this study, HYDREMATS was combined with a reservoir model, which has a direct representation of reservoir water and the groundwater table (GWT), to represent the environment in Ejersa. The model was also tailored for a relatively humid environment around the Koka Reservoir, Ethiopia.

A short description of the original HYDREMATS (Bomblies *et al.*, 2008) is presented in Section 3.1, followed by the model development in Section 3.2. Section 3.3 describes inputs to and outputs from HYDREMATS.

#### **3.1 Original Model Description**

HYDREMATS is composed of a hydrology model and an entomology model. The hydrology component, which was built upon the Integrated Biosphere Simulator (IBIS) (Foley *et al.*, 1996) uses climate and geological information to simulate spatially and temporally variable surface pools. The pool location, depth and temperature are used as inputs to the entomological model as well as other climate data. The entomological component simulates biological development, interaction with humans, and reproduction of mosquitoes, from which *Anopheles* population and malaria incidence are calculated. The close description of HYDREMATS is found in Bomblies *et al.* (2008).

##### **Hydrology Model**

The hydrology component of HYDREMATS couples the Integrated Biosphere Simulator (IBIS) (Foley *et al.*, 1996) and an overland flow model to simulate pool formation. In IBIS, water, energy and carbon fluxes are balanced within atmospheric layers, canopy layers, and soil layers representing a surrounding biosphere, of which the land surface module employs the land surface scheme (LSX) (Pollard and Thompson, 1995). The LSX simulates the water, energy, carbon dioxide and momentum balance at the surface. The overflow model coupled by Bomblies *et al.* (2008) is the distributed flow routing model, which uses the surface flow formulation by Lal (1998) in the alternate-direction implicit method (ADI). Using climatological inputs, i.e., precipitation, temperature, relative humidity, incoming solar radiation, and wind speed, the hydrology component of HYDREMATS simulates the formation

of pools, as a result of surface runoff routing, infiltration and evaporation. The simulation result of pool locations and pool depths is recorded in a file at an hourly time step. The persistence of the pools can be found by continuously reading the hourly output files.

The original HYDREMATS (Bomblies *et al.*, 2008) did not have a GWT representation. In a soil moisture solver, the bottom boundary of the soil layers was set to be partially permeable with a user-prescribed permeability ranging from zero (non-permeable) to one (fully-permeable). Bomblies (2008) added groundwater component to the model to represent an area with a shallow GWT. However, the GWT in this model responses only to vertical fluxes from infiltration and evaporation, and was spatially uniform, i.e. no consideration of lateral flux.

### **Entomology Model**

HYDREMATS employs an agent-based model in simulating mosquito population dynamics. Individual mosquitoes are modeled to behave probabilistically according to a set of decision rules. The decision rules respond to the ambient environment. Aquatic stage mosquitoes are modeled in six stages: eggs, first to fourth instar larvae, and pupae.

Adult mosquito agents are tracked individually in the model. They make probabilistic decisions in taking bloodmeals and laying eggs when they reach human houses and breeding pools, respectively. Mosquito survival rate and flight direction are function of the ambient environment. The survival rate depends on daily average temperature following Martens (1997). The death of each mosquito is simulated probabilistically using a uniform distribution function. The mosquito flight direction is calculated by a combination of random walk and CO<sub>2</sub> attraction; the weights of the two are user-defined. CO<sub>2</sub> attraction occurs when an individual mosquito senses CO<sub>2</sub> concentration of 0.01% above background, when it flies up the concentration gradient (Takken and Knols, 1999).

Mosquitoes interact with humans by taking bloodmeals in preparation for oviposition. They become infected by parasites if they take a bloodmeal from infectious people. Mosquitoes only become capable of transmitting malaria when they live longer than the temperature-dependent extrinsic incubation period after taking a bloodmeal from an infectious human. After taking a bloodmeal, mosquitoes find breeding sites and lay eggs with assigned probabilities.

Aquatic stage development is simulated in a compartmental structure for each grid cell. The representation of aquatic stage development borrows Depinay *et al.* (2004). Eggs advance from first to fourth stage larvae and to pupae, which can finally emerge into adult mosquitoes. The development rate at each stage is temperature dependent. Immature aquatic stage mosquitoes experience predation and cannibalism causing them to death. Their death rate also depends on

nutrient availability as well as natural mortality. When water at a pixel dries out, aquatic stage mosquitoes can move to surrounding cells if water exists; otherwise they die.

## **3.2 Model Development**

### **3.2.1 Large Water Body Representation in the Hydrology Model**

The representation of a large surface water body and the GWT are new additions to HYDREMATS. Reservoirs directly and indirectly impact the creation of mosquito breeding pools. Reservoirs have a direct impact through the creation of mosquito breeding sites at the shoreline. The reservoir also influences the creation of surface puddles through the existence of shallow water table.

#### **Direct Effect of the Reservoir: Shoreline**

Reservoirs provide mosquitoes with permanent breeding sites along the shoreline. Mosquitoes do not lay eggs in deep water to avoid waves. The wave effect becomes larger as the depth of water increases. Hence resolving the location and the area of shoreline where water depth is within a certain range, sometimes called the “illuminated shore zone” (Jobin, 2011), is critical in simulating mosquito breeding sites. In the updated HYDREMATS, using topography data and reservoir water levels, the area of inundation and the water depths were calculated. The impact of the level of the reservoir on mosquito population dynamics is non-linear. The shallow area suitable for mosquito oviposition is dictated by the reservoir water level and the shape of the surrounding topography. Also, when the location of shoreline shifts, the distance from mosquito breeding sites to human settlements changes. These topography-dependent mosquito breeding sites are explicitly represented in HYDREMATS. In addition to the absolute location and the area of illuminated shore zone, change in shoreline or water fluctuation may affect the mortality of larvae. In this study, the effect of water fluctuation on larvae was not included because the effect has not yet been quantified.

#### **Indirect Effect of the Reservoir: Groundwater Table**

Not only do reservoirs provide permanent mosquito breeding sites along their shorelines, but the existence of reservoirs also affects the creation of rain-fed pools through change in soil moisture. The GWT is generally shallow near a reservoir, and fluctuates as the reservoir water level changes. The location of the GWT affects the soil moisture profile, which determines the partition rate of rainfall into infiltration and surface runoff. When the GWT becomes shallow, local soil moisture increases, reducing the infiltration rate and increasing surface runoff. In this

situation, rain-fed pools are easily created and persist in the environment. On the other hand, when the GWT becomes deeper, more rainfall infiltrates into the soil, and fewer rain-fed pools are expected. In addition, if the GWT becomes higher than local topography, water starts to puddle on the ground. These pools are also used as breeding sites by mosquitoes.

The location of the GWT in the unsaturated zone is given by solving the following porous media equation:

$$S \frac{dh}{dt} = \nabla \cdot (Kh \nabla h) + r, \quad (3-1)$$

where  $h$  is depth of the groundwater or hydraulic head measured from the bedrock,  $S$  is storativity,  $K$  is hydraulic conductivity, and  $r$  is a recharge term.

When a large water body is located nearby, the groundwater flow can be approximated as a one-dimensional flow. Equation (3-1) then becomes

$$S \frac{dh}{dt} = \frac{d}{dx} \left( Kh \frac{dh}{dx} \right) + r. \quad (3-2)$$

Equation (3-2) is solved using a predictor-corrector method (Remson *et al.*, 1971). Recharge  $r$  is calculated from a soil moisture equation described by Bomblies *et al.* (2008) using Richards' equation and Campbell's equation.

The predictor-corrector method is a multi-stage method. For a time step of  $n$  and a grid point of  $i$ , the equation (3-2) is solved using a "predictor"

$$\Delta_x^2 h_i^{n+\frac{1}{2}} = \frac{S}{K} \frac{1}{h_i^n} \left( \frac{h_i^{n+\frac{1}{2}} - h_i^n}{\Delta t/2} \right) - \frac{1}{h_i^n} \left( \frac{h_{i+1}^n - h_{i-1}^n}{2\Delta x} \right)^2 - \frac{r}{2K} \quad (3-3)$$

and a "corrector"

$$\frac{1}{2} \Delta_x^2 (h_i^{n+1} + h_i^n) = \frac{S}{K} \frac{1}{h_i^{n+\frac{1}{2}}} \left( \frac{h_i^{n+1} - h_i^n}{\Delta t} \right) - \frac{1}{h_i^{n+\frac{1}{2}}} \left( \frac{h_{i+1}^{n+\frac{1}{2}} - h_{i-1}^{n+\frac{1}{2}}}{2\Delta x} \right)^2 - \frac{r}{2K}, \quad (3-4)$$

where

$$\Delta_x^2 h_i^n = \frac{h_{i+1}^n - 2h_i^n + h_{i-1}^n}{\Delta x^2}. \quad (3-5)$$

Assuming that the GWT is connected to the reservoir, the reservoir water level is used as a

boundary condition. The location of the boundary condition changes depending on the shoreline location. The shoreline location is resolved in a different algorithm based on the topography and the reservoir water level.

The Dirichlet boundary condition is applied to the other boundary away from the reservoir. Studies (Furi *et al.*, 2011; Chekol *et al.*, 2007) indicate that the groundwater flow component is significant in this region; however, the correct range and the seasonality of the baseflow are difficult to estimate. Thus, a constant head was used for the boundary condition in this study. In order to reflect the expected dominant flow direction towards the reservoir (Furi *et al.*, 2011), the constant head at the boundary was set higher than the annual maximum reservoir water level. This does not mean that the flow direction is toward the reservoir at any location throughout the year. Due to change in reservoir water levels, the flow direction near the reservoir switches signs. Although the boundary height was calibrated using observed GWT levels, the correct boundary condition remained unjustified. In order to minimize the impact of the boundary condition, the boundary was set far away (~10000m) from the simulation domain (~3000m). Around the simulation domain, the impact of the regional baseflow variation might be relatively small as compared to the impact of the reservoir fluctuation. The annual fluctuation of the reservoir water level is as high as seven meters.

The information of the GWT location is further utilized in solving the soil moisture equation. The number of unsaturated layers is calculated for each grid cell based on its elevation and the GWT location. A Dirichlet boundary condition is applied to the lowest unsaturated soil layer. The soil moisture equation is applied only to the unsaturated columns to maximize the computational efficiency.

### **3.2.2 Model Adjustments for a Wet Environment in the Entomology Model**

As HYDREMATS was originally developed for Niger, to represent dry Western Sub-Saharan Africa, some parts of the model required modifications in order to be applicable to the rather humid environment in Ethiopia. In addition, some minor modifications were made to better represent the ecosystem of *Anopheles* around the Koka Reservoir. The major modifications made in this study were related to aquatic stage development rates, adult mosquito survival rate, restriction of activities under rain, and pool persistence.

Aquatic stage development rates follows Depinay *et al.* (2004) in the original HYDREMATS (Bombliès *et al.*, 2008). The development rate per hour ( $r$ ) is given by the following equation:



$$r(T) = \frac{\rho_{25\text{ }^{\circ}\text{C}} \cdot \frac{T}{298} \cdot \exp\left[\frac{\Delta H_A^{\ddagger}}{R} \cdot \left(\frac{1}{298} - \frac{1}{T}\right)\right]}{1 + \exp\left[\frac{\Delta H_L}{R} \cdot \left(\frac{1}{T_{\frac{1}{2}L}} - \frac{1}{T}\right)\right] + \exp\left[\frac{\Delta H_H}{R} \cdot \left(\frac{1}{T_{\frac{1}{2}H}} - \frac{1}{T}\right)\right]}, \quad (3-6)$$

where  $T$  is the ambient temperature (K),  $\rho_{25\text{ }^{\circ}\text{C}}$  is the development rate per hour at 25  $^{\circ}\text{C}$ ,  $\Delta H_A^{\ddagger}$  is the enthalpy of activation of the reaction catalyzed by the enzyme ( $\text{cal} \cdot \text{mol}^{-1}$ ),  $\Delta H_L$  and  $\Delta H_H$  is the enthalpy change associated with low and high temperature inactivation of the enzyme respectively ( $\text{cal} \cdot \text{mol}^{-1}$ ),  $T_{\frac{1}{2}L}$  and  $T_{\frac{1}{2}H}$  is the temperature (K) where 50% of the enzyme is inactivated by low and high temperature respectively.  $R$  is the universal gas constant ( $1.987 \text{ cal} \cdot \text{mol}^{-1}$ ). Although this equation provides a powerful tool to evaluate the temperature-dependent development rates of eggs, larvae and pupae, the parameters reported by Depinay (2004: Table 3) failed to reproduce the published or estimated aquatic stage development times in the paper (Depinay, 2004: Table 1). Thus, new parameters were fitted using equation (3-6) and the reported aquatic stage development times. The newly fitted parameters are shown in Table 3-1. The parameters modified were  $\rho_{25\text{ }^{\circ}\text{C}}$  for larvae development rate and  $T_{\frac{1}{2}L}$  for pupae development rate. No parameter was modified for egg development rate. The functions of larvae development rate and pupae development rate are illustrated in Fig. 3-1.

**Table 3-1 Aquatic stage development rate parameters**

If a new parameter was applied, the parameter reported by Depinay (2004) is listed in parentheses.

	$\rho_{25\text{ }^{\circ}\text{C}}$	$\Delta H_A^{\ddagger}$	$\Delta H_L$	$T_{\frac{1}{2}L}$	$\Delta H_H$	$T_{\frac{1}{2}H}$
Eggs	0.0413	1	-170644	288.8	1000000	313.3
Larvae	0.0037 (0.037)	15684	-229902	286.4	822285	310.3
Pupae	0.034	1	-154394	288.0 (313.8)	554707	313.8

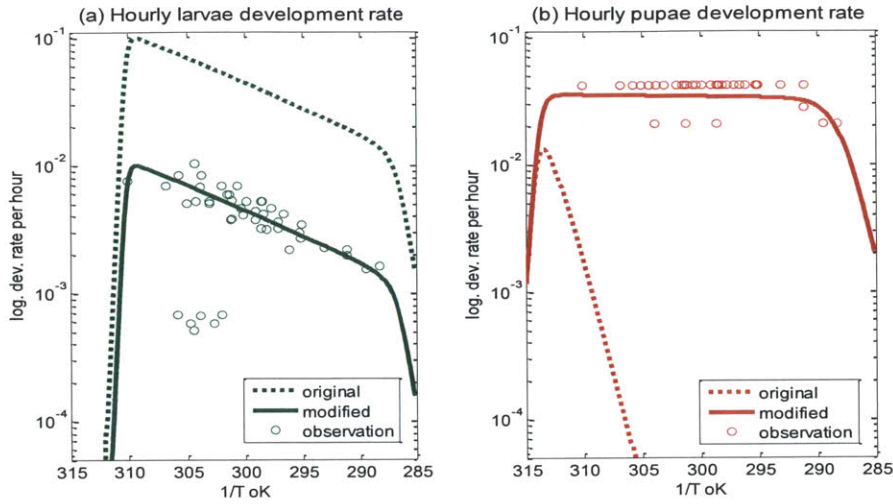


**Figure 3-1 Corrected aquatic stage development rate**

The solid line shows the function with newly modified parameters. The dotted line shows the function with original parameters.

Adult mosquito survival rate was modified to reflect the effect of humidity. HYDREMATS originally applied temperature-dependent survival using Martens' equation (Martens, 1998). Unlike Niger, where HYDREMATS was originally developed, Ethiopia has relatively high humidity throughout year. A new equation was applied following Parham *et al.* (2012), where survival rate at high relative humidity more closely represents observed data. Being a function of temperature  $T$  and relative humidity  $RH$ , the equation reads:

$$p(T, RH) = \exp\left(-\frac{1}{(\beta_2 T^2 + \beta_1 T + \beta_0)}\right), \quad (3-7)$$

where

$$\begin{bmatrix} \beta_2 \\ \beta_1 \\ \beta_0 \end{bmatrix} = \begin{bmatrix} 4.00 \times 10^{-6} \\ -2.32 \times 10^{-4} \\ 1.13 \times 10^{-3} \end{bmatrix} RH^2 + \begin{bmatrix} -1.09 \times 10^{-3} \\ 5.15 \times 10^{-2} \\ -1.58 \times 10^{-1} \end{bmatrix} RH + \begin{bmatrix} -2.25 \times 10^{-2} \\ 1.06 \\ -6.61 \end{bmatrix}. \quad (3-8)$$

In general, the Parham's equation (3-7) gives higher survival than Martens' equation.

Mosquito activities such as host seeking and oviposition are restricted under heavy rainfall. In the previous model, no consideration was made for mosquito activities during rainfall events. The result was a large number of ovipositions because shallow surface runoff is easily found by mosquitoes during heavy rainfall events in the simulation model. Some areas are, however, just temporary flow paths, and thus dry out quickly. In the simulation, mosquitoes

cannot distinguish those flow paths from ephemeral pools. Since those temporary flow paths appear under heavy rainfall, restricting mosquito activities under rainfall above a certain intensity helped to solve this problem. The threshold was set at 0.1 mm/h. This model restriction reflects field observations. Under rainfall events, mosquito activities are found to be suppressed (Charlwood and Braganca, 2012).

Although the creation of surface pools is explicitly simulated in the hydrology model, it cannot simulate the existence of microhabitats at the sub-grid scale. In the previous model, aquatic stage mosquitoes were forced to die soon after the pools dried out. However, a microhabitat remaining in a part of a pool may sustain immature mosquitoes for a certain period. In addition, the environment around the Koka Reservoir has high relative humidity during the rainy season, allowing immature mosquitoes to survive on a damp soil for several days (Koenraadt *et al.*, 2003). In this study, aquatic stage mosquitoes were allowed to develop for three days even after water at their living grid cells dried out, representing the existence of microhabitats and survival on a damp soil.

### 3.2.3 Utilization of Different Breeding Sites in the Entomology Model

Different types of pools provide different conditions for mosquito breeding. Pools are used as oviposition sites with different probabilities reflecting the preferences of mosquitoes. They also exhibit variable productivity. From the hydrology model outputs described in 3.1.4, water bodies can be identified as rain-fed pools, groundwater pools and shoreline water. These three types of breeding sites are assigned with different utilization functions, whose values also depend on their water depth.

The utilization function provides the probability that gravid mosquitoes lay eggs at a pool when they encounter one, i.e., when they are on a grid cell with water. The values of utilization function vary with pool depth within the range between minimum and maximum thresholds (*breedmin* and *breedmax*, respectively); only the water depth between them is suitable for oviposition. A constant maximum utilization probability (*utilprob*) is assigned for a certain range (from *breedmin* to *breedcom*). The utilization probability linearly decreases from *breedcom* to *breedmax*; the probability becomes zero at *breedmax*. Different types of pool may have different *breedmin*, *breedcom*, *breedmax* and *utilprob*.

Carrying capacity (*lmax*) is also set for each type of breeding sites. In this study, a uniform value of 200 mg m<sup>-2</sup> is set for *lmax* in each pool.

For example, *breedmax* for shoreline was set lower than that for rain-fed pools because shoreline water is more susceptible to wave action than rain-fed pools as water depth becomes

deeper. When the waves on the water surface becomes too large, mosquitoes choose not to lay eggs. 0.8 meters and 0.2 meters were chosen for *breedmax* for rain-fed pool and shoreline respectively. This means mosquitoes cannot lay eggs at rain-fed pools deeper than 0.8 meters and at shoreline water deeper than 0.2 meters. *Utilprob* was set higher for shoreline as a result of model calibration; parameters of 0.6 and 0.8 were chosen for rain-fed pool and shoreline, respectively. The parameters used in this study are summarized in Table 3-2 and the utilization functions are shown in Fig. 3-2.

**Table 3-2 Utilization parameters for oviposition**

	<i>breedmin</i> [m]	<i>breedcom</i> [m]	<i>Breedmax</i> [m]	<i>utilprob</i> [-]	<i>lmax</i> [mg m <sup>-2</sup> ]
Rain-fed pool	0.01	0.5	0.8	0.6	200
Groundwater pool	0.01	0.5	0.8	0.6	200
Shoreline	0.01	0.15	0.2	0.8	200

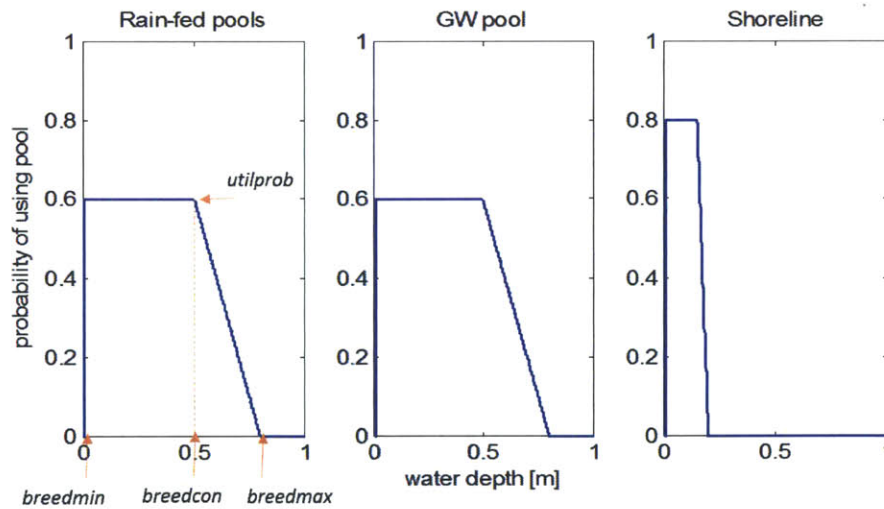


**Figure 3-2 Utility probability functions for oviposition**

### 3.3 Model Input and Output

### 3.3.1 Hydrology Model Input

Hydrology model inputs come from field data collection and global data sets. All the inputs used for the hydrology model are summarized in Table 3-3.

The model is sensitive to topography, hence a high resolution digital elevation model (DEM) is desired for HYDREMATS. Topography maps are becoming widely available, but high resolution products are not yet available free of charge for most Africa. HYDREMATS, whose main output from the hydrology model is the location and the duration of surface water, requires a high resolution DEM. The finest resolution we could obtain for this region free of charge was 30 meters, from Advanced Spaceborn Thermal Emission and Reflection Radiometer (ASTER). The ASTER DEM was used in the Gudedo model. For Ejersa, an 8-meter fine resolution digital terrain model (DTM) collected by WorldView-1 was purchased from Apollo Mapping. The accuracy of the product is 8-meter LE90%. The finer resolution DTM was obtained for Ejersa to closely resolve the shoreline breeding habitat. The smaller variability of topography in Ejersa necessitates using a finer resolution model because sub-regional depressions are prone to the creation of surface pools. The DTM does not give the elevation of a submerged surface. To obtain the maximum topographical information, the DTM was collected when the reservoir water level was near its minimum around the end of June. For the submerged area at that time, the soil surface elevation was estimated using the nearby shoreline slope. A lower resolution DEM may suffice in other regions depending on their environment and topography. Clennon *et al.* (2010) found in Zambia that a 90-meter-resolution Shuttle Rader Topography Mission (SRTM) DEM functioned better than a 30-meter-resolution ASTER DEM in their simulations. Micro-topographies such as tire ruts and hoof-prints have a scale of less than a meter and thus are not captured by the DEM. However, these depressions are shown to disappear too rapidly to allow completion of the development cycle for larvae. Thus, they play a negligible role in mosquito population dynamics (Bomblies *et al.*, 2008).

Soil type is specified by the percentage of soil, silt and clay for each layer. These values were obtained from Harmonized World Soil Database (HWSD) v 1.2. The soil type data assign hydraulic conductivity for each pixel and layer. The hydraulic conductivity can be further calibrated.

A vegetation map is used in IBIS to simulate canopy phenology, and Manning's roughness coefficient is assigned according to the vegetation type. Land coverage data were obtained from the University of Maryland (UMD) with 1-km resolution. Manning's coefficient was obtained from the land cover type. The surface runoff model is sensitive to Manning's coefficient, so the value can also be modified for model calibration.

Climate forcings in HYDREMATS have a resolution of one hour. The data required are

precipitation, temperature humidity, wind speed and incoming shortwave radiation. All of the data were collected from *in situ* MSs, which were coded to collect 30-minute data.

Daily reservoir water level data were obtained from EEPCo. Linearly interpolated data were used to create an hourly input to resolve the location of the reservoir shoreline and the GWT.

Additional parameters necessary to run the groundwater flow model, which was a newly added component to represent the Ejersa ecosystem, are horizontal hydraulic conductivity, storativity, location of the bedrock and boundary conditions. These parameters were assigned based on literature values as well as the HWSO dataset.

The grid resolution and time step are user-specified. The grid size can be a combination of 10m, 20m, 40m and 80m in x- and y-direction. The default time step is ten minutes. For the surface runoff model, a smaller time step is assigned automatically in HYDREMATS when a flow occurs. This is because the time scale of flow through a grid cell is usually less than ten minutes, especially when the flow depth is high. When the maximum depth of the surface flow exceeds one millimeter, the overland flow model runs with a temporal resolution of one second.

The hydraulic conductivity of the top layer was modified to be more impermeable as crusting of the soil was observed in the field survey (Fig. 3-3) and other studies (Welderufael *et al.*, 2008).

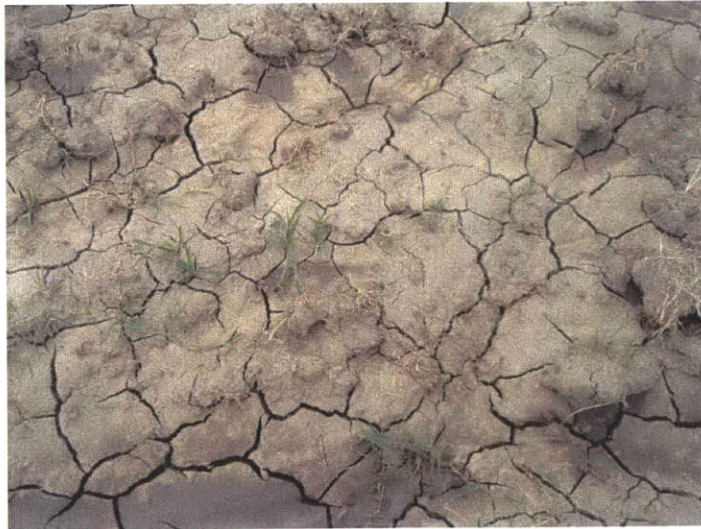


**Figure 3-3 Crusting of the soil surface observed around the Koka Reservoir**



**Table 3-3 Hydrology model input and resolution**

Variable	Type	Spatial resolution	Temporal resolution	Source
Topography	distributed	30m	n/a	ASTER
		8m	n/a	Apollo Mapping DTM
Soil type	distributed	30 arc-second	n/a	Harmonized World Soil Database
(Hydraulic conductivity)	distributed			Assigned based on soil type
Vegetation	distributed	1 km	n/a	UMD Global Land Cover Classification
(roughness)	distributed			Assigned based on vegetation
Precipitation	lumped	n/a	30 minutes	MS
Temperature	lumped	n/a	30 minutes	MS
Humidity	lumped	n/a	30 minutes	MS
Wind speed	lumped	n/a	30 minutes	MS
Solar radiation	lumped	n/a	30 minutes	MS
Reservoir head	single measurement	n/a	daily	Ethiopian Electric Power Corporation
Grid resolution		User-defined (combination of 10m, 20m, 40m, 80m)		
Time step			User-defined (default is 10 minutes)	

### 3.3.2 Hydrology Model Output

Water depth and water temperature raster data are generated at an hourly time step and served as the entomology model input. In running the hydrology model, different types of surface water are flagged with different numbers (Fig. 3-4). Rain-fed puddles have flag one, and they are usually short lived. If the GWT becomes higher than the local topography, surface pools are simulated with flag two, which are semi-permanent pools. Reservoir water close to the shoreline is flagged three, while the deep water at the offshore has a flag of five. Soil without ponding is flagged zero. Water bodies with flags one to three (rain-fed pool, groundwater pool and shoreline illuminated shore zone) are used by *Anopheles* mosquitoes with different probabilities reflecting their preferences of the breeding site. The probability of using a pool is a function of pool depth and pool type.

Explicit representation of surface water bodies is the main output of the hydrology component of HYDREMATS, which serves as an entomology model input. The depth of the surface water at each grid cell over the domain is written into hourly output files. In order to differentiate different types of breeding sites, values of the additive inverse of water depths are recorded for groundwater pools. In addition, the location of a shoreline is saved at the same hourly time step. Because saving high spatial resolution data at an hourly time step requires substantial computer memory, this approach is more efficient than outputting the aforementioned flag at every time step. If the source of the surface water is groundwater, negative values of the same magnitude are stored.

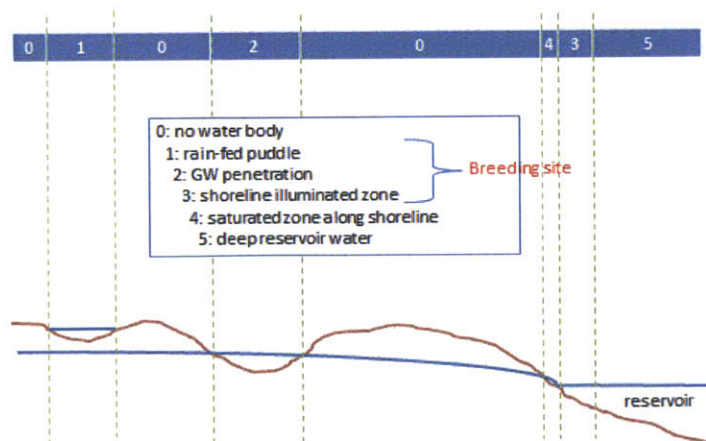


Figure 3-4 Flags depending on the type of pools simulated in HYDREMATS

Water temperature is simulated and saved as raster data at an hourly time step. This output also serves as an input to the entomology model, affecting the development rate of aquatic stage mosquitoes. Because IBIS was not originally developed for areas with large water bodies, the simulation of water temperature over the reservoir was erroneous. For this study, the water temperature at the reservoir was set equal to air temperature. This is not always a valid assumption especially for deep water. However, the fact that shallow water along the shoreline is the only area where mosquitoes can lay eggs and that the shoreline area around the Koka Reservoir is not covered by large canopy makes this assumption reasonable in this context.

For the purpose of model calibration and validation, soil moisture at specific points was monitored. Soil moisture for each layer was longitudinally followed for the location of the MSs and SMSs in HYDREMATS, and was compared with field observation data at three depths.

### **3.3.3 Entomology Model Input**

Simulation in the entomology model requires water depth and water temperature outputs from the hydrology model as well as local meteorology and environmental data. The hydrology model outputs are prepared at the same time interval as the time step in the entomology model (nominally one hour). In addition to the water depth output, the location of shoreline is also used in order to distinguish reservoir water from other surface pools. Water temperature data are used to calculate the development rates of aquatic mosquitoes. Meteorological data are used for simulation of adult mosquito behaviors and their biology. Daily temperature and humidity dictate the mosquito longevity. Wind speed and wind direction influence mosquito flight direction. Location of human habitats is another input data required to run HYDREMATS. The distribution of human settlements also impacts the mosquito flight direction and chances of taking bloodmeals. Mosquitoes take bloodmeals when they arrive at human settlement grid cells with a user-defined probability. The input of the location of human settlements was prepared from a satellite picture using ArcGIS. Human houses were sampled on the picture and were converted into a raster data. Fig. 3-5 is an example showing how human settlement input data were prepared.

### **3.3.4 Entomology Model Output**

The main output from the entomology model is mosquito population. However, as



**Figure 3-5 Location of human settlements in Egersa**

The location of houses (orange) is superimposed on an Egersa satellite picture. A fishnet function with 10m by 10m grids was placed over the picture, and the pixels overlaying houses were selected.

HYDREMATS explicitly simulates the location of pools and mosquito life events, it has the advantage of being able to obtain all other information simulated in the model. Outputs of number of pools, number of aquatic stage mosquitoes in each pool, and dried-out larvae are of importance in analyzing mosquito dynamics. Although it is not the primary focus of this study, HYDREMATS also simulates malaria incidence.

## **Chapter 4: Model Application to Two Villages around the Koka Reservoir**

In this chapter, the updated HYDREMATS is applied to two villages around the Koka Reservoir, Ethiopia. Meteorological data collected from January 2012 to February 2013 were used as a forcing to the model. Entomological data collection and meteorological data collection in Ejersa started in July 2012. The simulation was run from January 2012 to February 2013, but the model calibration was conducted using the data obtained from July 2012 to February 2013. Although the data collection period was rather short and the model needs to be tested for multiple years in the future, the model was able to capture adequately the local hydrological system and mosquito population dynamics for the study period. Further data collection expected in the future will provide more data for rigorous calibration of HYDREMATS.

### **4.1 Model Application to Ejersa**

HYDREMATS was applied to Ejersa, and the results are shown in this section. First, the topography data and other input parameters for the Ejersa model are provided in 4.1.1. Subsection 4.1.2 describes the preparation of forcing data. The hydrology and the entomology model outputs were shown in 4.1.3 and 4.1.4 respectively. Finally, implications for malaria incidence are made in 4.1.5.

#### **4.1.1 Ejersa Field Setting and Model Parameters**

Ejersa is located in the Awash Basin in the Ethiopian Great Rift Valley. Ejersa is a set of three *kebeles* located to the northwest of the Koka Reservoir. HYDREMATS was applied to a three kilometers by three kilometers region indicated by a red square in Fig. 2-3, which mostly covers Dungugi-Bekele *kebele*, the *kebele* closest to the reservoir.

Topography data are one of the most important inputs in the model. An 8-meter-resolution DTM was obtained from Apollo Mapping and converted into a 10-meter-resolution raster to serve as a model input (Fig. 4-1). Although the DTM data were collected when the reservoir water level was close to its annual minimum, some part of the simulation domain was still submerged in the reservoir, and thus the ground elevation data were not available for that part of the area. The missing ground elevation data were supplemented using the information of adjacent shoreline slope obtained from the DTM.



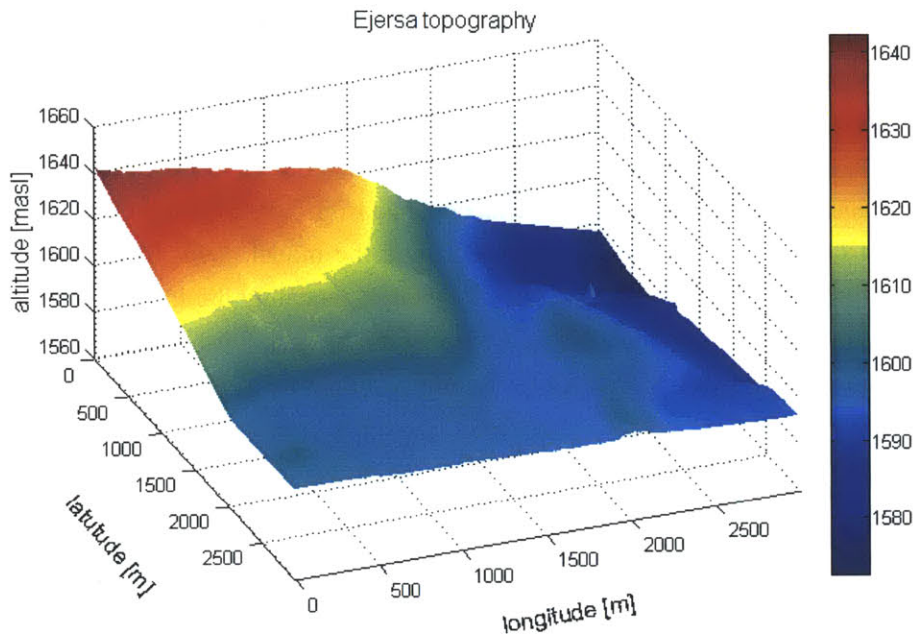


**Figure 4-1 Ejersa topography**

The topography map was created based on a 8-meter-resolution DEM from Apollo Mapping. X (longitude) axis shows the distance in meter from the west edge of the domain, y (latitude) from the north edge of the domain. Z (altitude) axis shows elevation in meter above sea level (mas). The area below 1590m at the east is submerged under the reservoir throughout the year. The area at the southwest is relatively low and the reservoir water approaches the area when the reservoir water level becomes high. While other area is cultivated only during the rainy season, this area is utilized as a crop land during the dry season using groundwater.

The hydraulic parameters assigned for the Ejersa model are shown in Table 4-1. During model calibration these parameters were tuned within the range reported in the literature and available global data sets.

The HWSD soil dataset was used to estimate parameters for porosity, hydraulic conductivity and storativity; then parameters were modified to calibrate the model. Based on the soil components obtained from HWSD, IBIS assigned a porosity of 0.35 and a hydraulic conductivity of 0.14 m/d. The vertical hydraulic conductivity was calibrated using an observed soil moisture profile, and the horizontal conductivity was calibrated in the groundwater flow model by comparison with the observed GWT data. The parameters were changed by small increments, and the soil moisture results and the GWT results were manually compared with



observational data. Parameters which resulted in the most similar observational data sets were selected. More rigorous calibration method will be required in the future study. As a result of calibration, the vertical and horizontal hydraulic conductivities were set at 1.1 m/d and 3.5 m/d, respectively. The vertical hydraulic conductivity at the top layer was ten times lower than the lower layers reflecting the crusting effect (Fig. 3-3). Ayenew *et al.* (2008) estimated that the hydraulic conductivity in the basin ranges from 0.1 to 138 m/d, which is consistent with the calibrated parameters. The horizontal hydraulic conductivity was set higher than the vertical hydraulic conductivity. This is in agreement with field observations in the literature. Storativity was also calibrated within the range reported by Johnson (1967).

The location of bedrock was set as zero meters above sea level. This parameter was not calibrated because of the scant observational data of the GWT and because other parameters such as the hydraulic conductivity and storativity also needed to be calibrated in the model. The tune-up of the parameter will be conducted as more observational data become available.

The Manning’s roughness coefficient was assigned using land cover data from UMD. The vegetation type in Ejersa was classified as grassland or cropland, and Manning’s roughness coefficient was assigned as 0.036.

The number of soil layers and the soil layer thicknesses are user-defined variables. While the default number of soil layers in IBIS is six, the new model with groundwater representation needs more layers to resolve the location of the GWT. A larger number of soil layers allow more accurate computation, sacrificing computational efficiency. In this study, 35 layers were used with a thickness of 0.5 meters except the top five layers. Smaller thicknesses were assigned to the top five layers.

**Table 4-1 Ejersa hydraulic parameters**

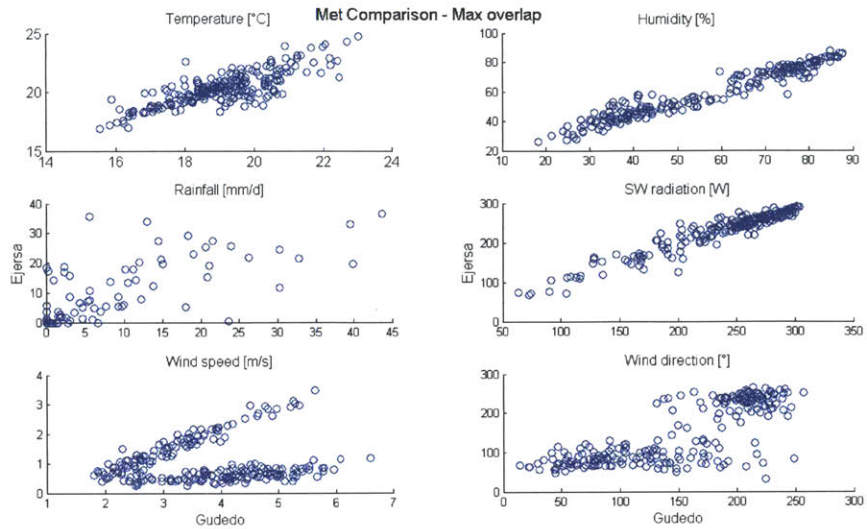
<b>Parameters</b>	
<b>Porosity</b>	0.35
<b>Hydraulic conductivity (vertical, without crusting)</b>	1.1 m/d
<b>Hydraulic conductivity (horizontal)</b>	3.5 m/d
<b>Storativity</b>	0.04
<b>Location of bedrock</b>	0 masl
<b>Manning coefficient</b>	0.035

#### 4.1.2 Data Preparation

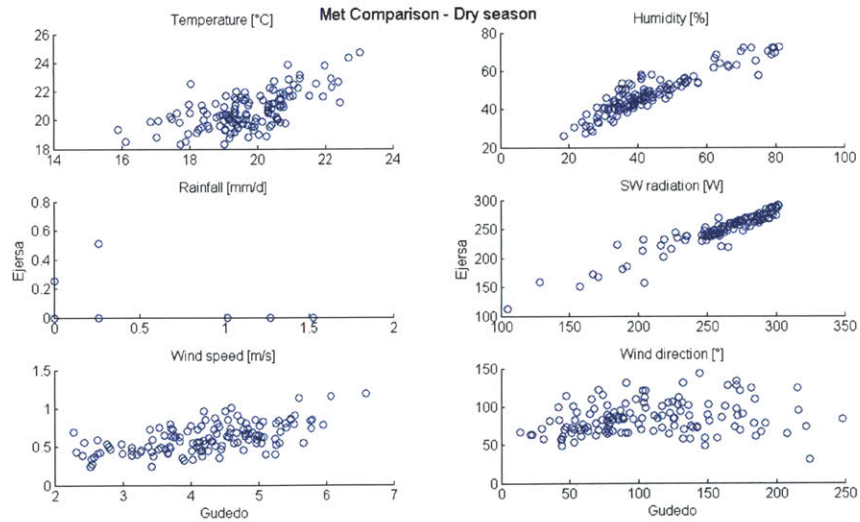
The simulation was run from January 2012 to February 2013, during which meteorological data in Ejersa were partially not available. A complete set of forcing data became available from the MS in Ejersa from July 15<sup>th</sup>, 2012. The MS experienced a data recording problem for about 20 days from the mid-January to the mid-February in 2013 (from 11 am Jan. 14<sup>th</sup> to 10 am Feb. 2<sup>nd</sup>). To prepare the forcing data for the period that the data were missing, first the data collected from the Ejersa and Gudedo MS were compared in regression analyses, and then the missing data were prepared applying the regression models.

Fig. 4-2 demonstrates the comparison of the field-collected meteorological data from Ejersa and Gudedo for the maximum overlap period, i.e., from June 15<sup>th</sup>, 2012 to January 14<sup>th</sup>, 2013 and from February 2<sup>nd</sup>, 2013 to February 28<sup>th</sup>, 2013. Note that this period contains both the rainy season and the dry season. Fig. 4-2 and Table 4-2 show that temperature, humidity and shortwave radiation data from both sites correlate well, which is reasonable given the physical proximity of the sites. Hence, these missing forcing data for the Ejersa model were prepared using the Gudedo observational data in the regression model shown in Table 4-2. In order to maintain zero radiation at night time, the regression model was applied only when the observed radiation in Gudedo was non-zero; incoming shortwave radiation in Ejersa was set to be zero when the Gudedo data showed no incoming radiation. Wind speed and wind direction show two distinct patterns for the rain season and the dry season (Fig. 4-2). Because the data missing period was in the dry season, data for the dry season were extracted and analyzed to realize better correlations. Fig. 4-3 shows the result of the metrological data comparison of the two sites for the dry season. Table 4-3 presents the result of regression analyses for the corresponding period. Although the correlation coefficient for wind direction decreased, the one for wind speed increased significantly from 0.13 to 0.60. The regression models for the dry season were applied to estimate wind speed and wind direction in Ejersa. Due to the low correlation coefficient for the wind direction regression model, the estimate was less reliable. However, the wind direction is an input only for the entomology model, and the influence of the wind direction on mosquito population dynamics is supposed to be minimal in the dry season because the mosquito population is small.

Overall, the input meteorological data prepared for the missing data period in Ejersa were accurate due to geographical proximity. In addition, the main focus in this study was the hydrology and mosquito population dynamics during and after the rainy season in 2012, and the most of the filled data were used only until the arrival of the rainy season. We can also consider the pre-rainy season as a spin-up period for the model simulation.



**Figure 4-2 Gudedo-Ejersa daily meteorological data comparison for the maximum overlap (Jun. 2012 – Feb. 2013)**  
**Gudedo on the x-axis, and Ejersa on the y-axis. Units are temperature [°C], humidity [%], rain [mm/d], shortwave radiation [W], wind speed [m/s] and wind direction [deg].**



**Figure 4-3 Gudedo-Ejersa daily meteorological data comparison for the rainy season overlap (Aug. 2012 – Feb. 2013)**  
**Gudedo on the x-axis, and Ejersa on the y-axis. Units are temperature [°C], humidity [%], rain [mm/d], shortwave radiation [W], wind speed [m/s] and wind direction [deg].**

**Table 4-2 Coefficients for 1st-order linear regression models for the maximum overlap**

$y=ax+b+e$ , where  $y$ =Ejersa data,  $x$ =Gudedo data,  $e$ =error

The first and the second row show the coefficients  $a$  and  $b$ , and the third row shows the correlation coefficient for each regression model. Regression models were applied to temperature, relative humidity, daily rainfall, short wave radiation, wind speed and wind direction.

<b>Max overlap</b>	<b>temp</b>	<b>humidity</b>	<b>rain</b>	<b>SWrad</b>	<b>Wspd</b>	<b>Wdir</b>
<b>a</b>	<b>0.75</b>	<b>0.81</b>	<b>0.83</b>	<b>0.89</b>	<b>0.082</b>	<b>0.92</b>
<b>b</b>	<b>5.8</b>	<b>13</b>	<b>0.92</b>	<b>18</b>	<b>0.72</b>	<b>11</b>
<b>corrcoef</b>	<b>0.81</b>	<b>0.97</b>	<b>0.80</b>	<b>0.96</b>	<b>0.13</b>	<b>0.78</b>

**Table 4-3 Coefficients for 1st-order linear regression models for the rainy season overlap**

$y=ax+b+e$ , where  $y$ =Ejersa data,  $x$ =Gudedo data,  $e$ =error

The first and the second row show the coefficients  $a$  and  $b$ , and the third row show the correlation coefficient for each regression model. Regression models were applied to temperature, relative humidity, daily rainfall, short wave radiation, wind speed and wind direction.

<b>Dry season</b>	<b>temp</b>	<b>humidity</b>	<b>rain</b>	<b>SWrad</b>	<b>Wspd</b>	<b>Wdir</b>
<b>a</b>	<b>0.62</b>	<b>0.69</b>	<b>0.020</b>	<b>0.86</b>	<b>0.12</b>	<b>0.087</b>
<b>b</b>	<b>8.4</b>	<b>18</b>	<b>0.0051</b>	<b>39</b>	<b>0.098</b>	<b>76</b>
<b>corrcoef</b>	<b>0.64</b>	<b>0.92</b>	<b>0.081</b>	<b>0.94</b>	<b>0.60</b>	<b>0.21</b>

### 4.1.3 Hydrology Model Output

The main outputs from the hydrology model are the explicit representations of surface water depth and water temperature. These outputs are written in ascii files at an hourly interval, and used as entomology model inputs. In addition, simulated soil moisture profiles and the GWT elevations are compared here to validate the model.

The location and the depth of surface water is one of the main outputs and is also used as an

entomology model input. Fig. 4-4 and Fig. 4-5 are snapshots of the water depth output from HYDREMATS. Fig. 4-4 demonstrates the surface water simulated in the secondary rainy season in April. During this period, the reservoir water level was relatively low, so the shoreline was located further from the village. A comparison of Fig. 4-4 and Fig. 4-5 shows that the shoreline slope was sharper during the secondary rainy season, which also reduced the area of shoreline available as a breeding site. Rain-fed pools were found at topographically low areas in the south. An example of the surface water profile during the main rainy season is found in Fig. 4-5. The snapshot was taken at the end of September. Around this time, the reservoir water level became high bringing the shoreline closer to the village. The shoreline slope around this time was small, so a relatively large area became a mosquito breeding site. A comparison between Fig. 4-4 and Fig. 4-5 also reveals that the shoreline changed by as much as one kilometer in horizontal direction in a year in the south of the simulation domain. No groundwater pools were simulated to occur during the study period.

Although the depth of pools indicates how long the pools stay there, the persistence of the pools is only calculated by reading the hourly output files continuously. Rain-fed pools were found to be more persistent in the main rainy season than in the secondary rainy season mainly because of the high intensity and high frequency of precipitation during that time.

Because it was difficult to obtain field observation data on pool locations and pool depths over the domain, the model validation was conducted using soil moisture values. Soil moisture values were recorded automatically at two *in-situ* stations in the simulation domain. In HYDREMATS, soil moisture is measured as a form of water saturation. On the other hand, field observation of soil moisture uses a form of volumetric water content (VWC). For comparison, the simulated water saturation values were converted into VWC by multiplying the porosity used in the model. Readers should be reminded that the observational soil moisture data were calibrated using Equation (2-2) and a weighting factor 0.19, making the absolute value of VWC less reliable. A large gap between the porosity set in HYDREMATS and the porosity inferred from observation was recognized, so obtaining an accurate porosity for this field site and a proper weighting factor will be future tasks.

The comparison of observed and simulated soil moisture is presented in Fig. 4-6 for the Ejersa MS and Fig. 4-7 for the Ejersa SMS. At both stations, *in-situ* data collection started in mid-July, so only available observational data are shown here. Both observational data (Fig. 4-6 (a) and Fig. 4-7 (a)) and simulation output (Fig. 4-6 (b) and Fig. 4-7 (b)) show that the soil layers at depths of 15cm and 30cm did not become saturated throughout the main rainy season, maintaining VWC around  $0.1 \text{ m}^3 \text{ m}^{-3}$ , about 30% of saturation. Although small spikes of VWC values due to increased soil moisture were observed after rainfall events, the values did not reach porosity. Soil at 15 cm below the surface is likely not close enough to experience

### Ejersa hydrology model output: d102h1

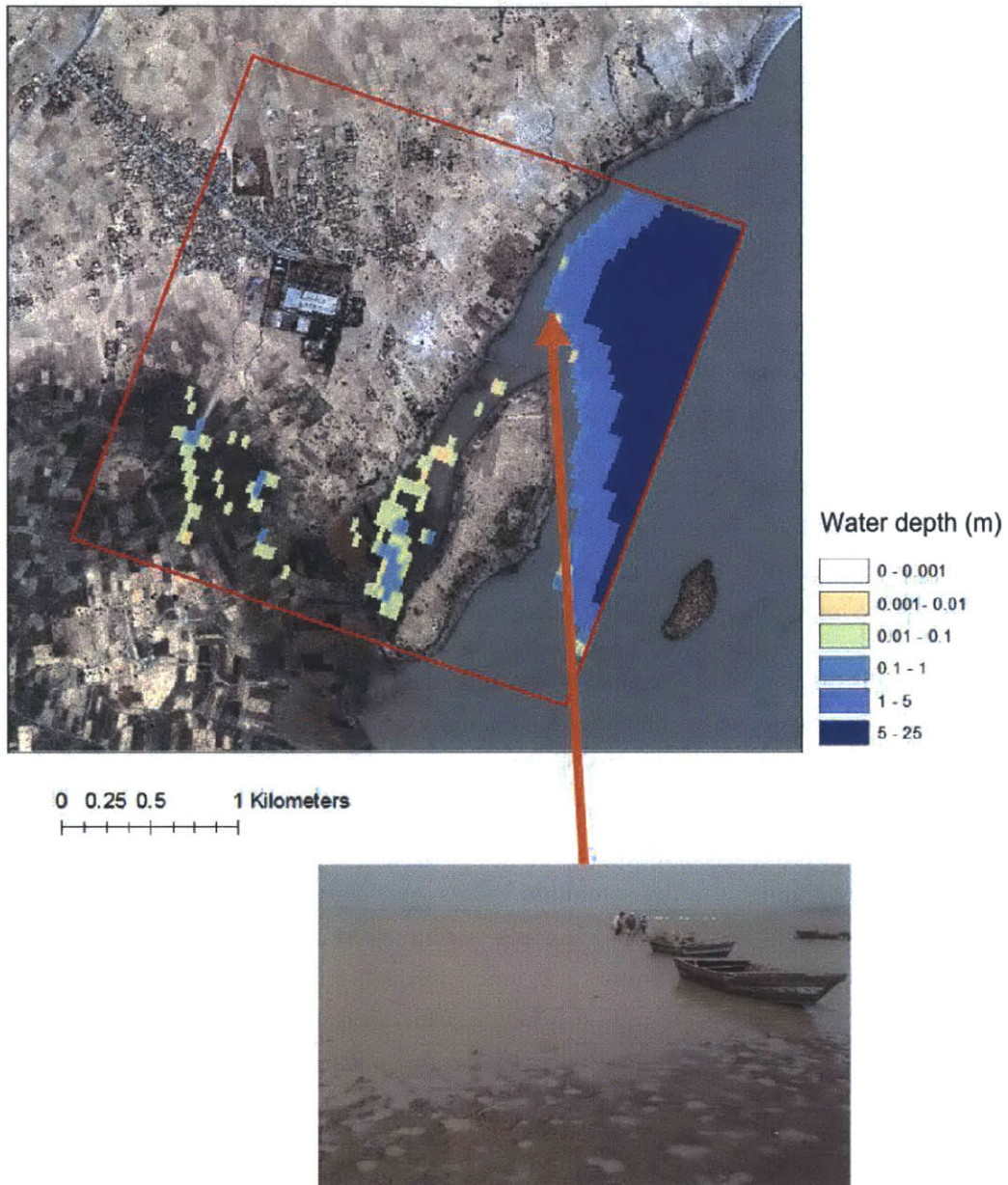


**Figure 4-4 Water depth output at hour 1 on day 102**

A snapshot of water depth output at 1 am on Julian day 102, during the secondary rainy season in April. Colors indicate the depth of water in each grid cell. A red square shows the 3km by 3km simulation domain. Because the reservoir water level is relatively low, the shoreline is far from the village. Rain-fed pools are found at the topographically low areas in the south. A photo of the real pool corresponding to a simulated pool location is presented (bottom). The date that the picture was taken does not necessarily correspond to the date of the simulation output shown here.



Ejersa hydrology model output: d272h1

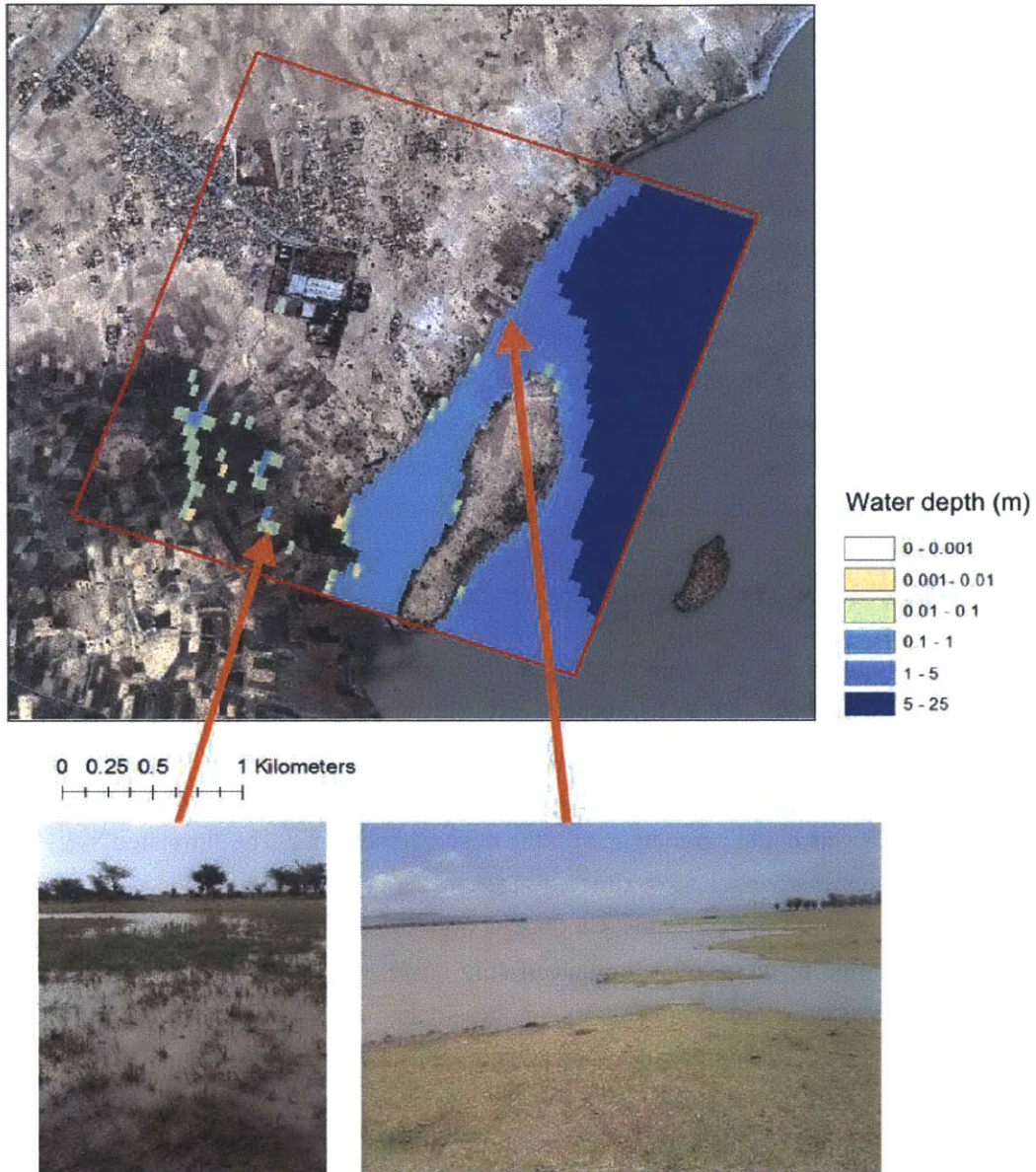


Figure 4-5 Water depth output at hour 1 on day 272

A snapshot of water depth output at 1 am on Julian day 272, during the main rainy season at the end of September is shown (top). Colors indicate the depth of water in each grid cell. A red square shows the 3km by 3km simulation domain. Because the reservoir water level is relatively high, the shoreline is close to the village. The shallow area of the reservoir is used as a mosquito breeding site, as are rain-fed pools found in the topographically low areas in the southwest. Photos of the real pools corresponding to simulated pool locations are presented (bottom). The dates that the pictures were taken do not necessarily correspond to the date of the simulation output shown here.

saturation. At a depth of 100cm, the observational data suggest that relatively high soil moisture was sustained at the SMS until the end of the rainy season, which was not observed at the MS.

At the MS, the 100cm soil moisture probe showed increase in soil moisture in the middle of July, approximately two weeks after the start of the main rainy season. Then the soil moisture gradually decreased. This soil moisture behavior at a deep layer at the MS suggests that the high intensity of rainfall at the beginning of the rainy season reached a depth of 100cm in two weeks. The following low intensity of rainfall resulted in a lower percolation rate reaching the 100cm depth, so the soil moisture in the mid- to late-period of the main rainy season decreased. In contrast to the observed soil moisture at the MS, the observed water content at the 100cm depth at the SMS held water until the end of the rainy season. One of the possible reasons is that the SMS received more surface runoff, which resulted in higher amount of infiltration. Another possible reason is that the soil water was sustained from below due to the shallow GWT. The location of the SMS was closer to the shoreline than that of the MS, and the GWT at the MS was observed to become as shallow as two to three meters below ground surface. The heterogeneity of soil type and vegetation type, or the existence of macro-pores may also have contributed to the difference in the observations.

Fig. 4-6 and Fig. 4-7 show that the simulated VWC in the top two layers behaved similarly to that observed in the MS and SMS, respectively. However, the quicker decrease in simulated VWC than observed suggests that larger evaporation was simulated or higher hydraulic conductivities were applied in HYDREMATS. The behavior of the simulated VWC at 100cm depth at the MS was not in agreement with the observed behavior. The simulated VWC in Fig. 4-6 (b) indicates that water took time to reach a depth of 100cm at the MS. The VWC simulation for the SMS behaved closer to observation. The simulated VWC at a depth of 100cm at the SMS started to increase at the end of July, about two weeks later than observed and maintained the relatively high VWC until October. In the simulation, the earlier increase in soil moisture at the SMS was expected to be caused mainly by high infiltration, but also partially due to the existence of the shallow GWT. Fig. 4-8 shows the longitudinal profile and the vertical profile of the simulated soil moisture as a form of water saturation. The soil layers with water saturation of one are below the GWT. It shows that the depth to the groundwater was smaller at SMS than at MS. Although the GWT at the SMS was not shallow enough to significantly impact the soil moisture at 100cm depth in the simulation, this difference in the location of the GWT may have had a small impact in the simulated soil moisture values.

Finally, model validation was conducted using observed and simulated GWT data. Simulated and observed GWT elevations were shown in Fig. 4-9. Although no observational data were obtained from well 1 and the data collection period was limited, the figure shows that the newly added component of the groundwater flow model simulated the spatiotemporal dynamics of

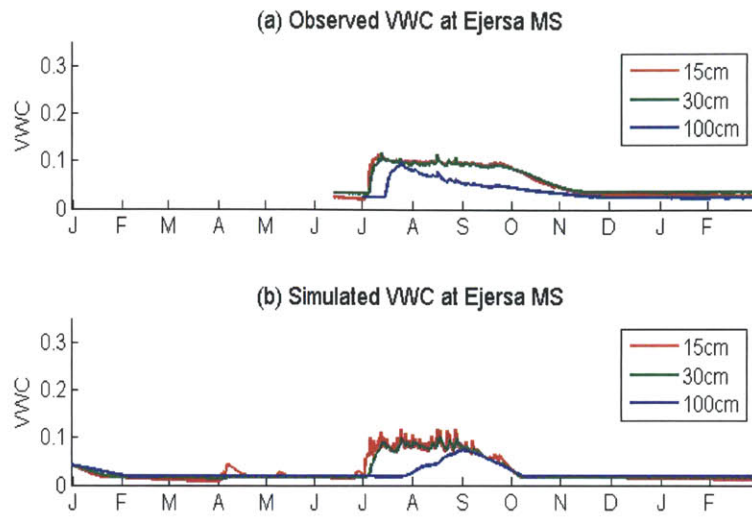


**Figure 4-6 Comparison of soil moisture at Ejersa Met Station**

The observed VWC (a) and simulated VWC (b) at depth of 15cm, 30cm and 100cm at the Ejersa MS. The *in-situ* observation station started its operation in the middle of June.

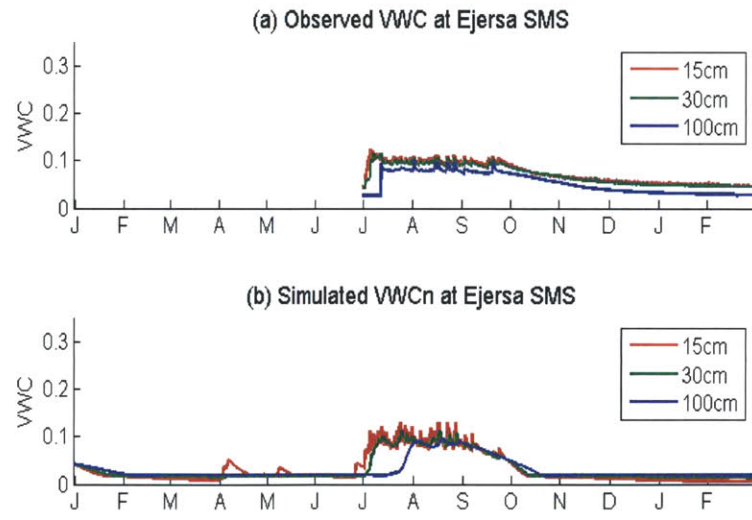


**Figure 4-7 Comparison of soil moisture at Ejersa Soil Moisture Station**

The observed VWC (a) and simulated VWC (b) at depth of 15cm, 30cm and 100cm at the Ejersa SMS. The *in-situ* observation station started its operation in the middle of June.

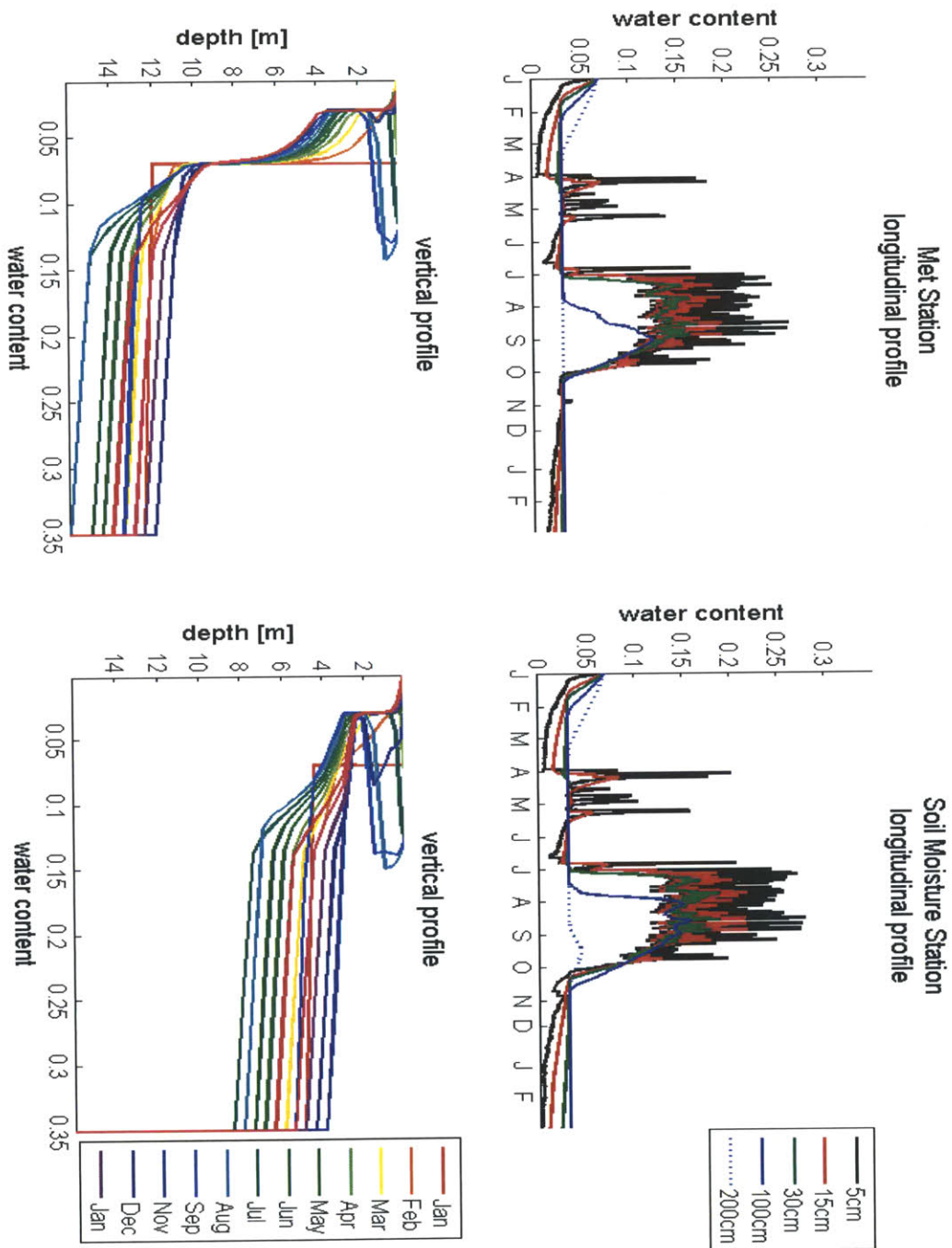


**Figure 4-8 Simulated soil moisture profiles at Met Station and Soil Moisture Station in Ejersa**  
 Left and right figures show simulated water saturation at the Ejersa MS and the Ejersa SMS, respectively. The top two figures are longitudinal profiles and the bottom two figures are vertical profiles of the simulated soil moisture.



the groundwater fluctuation. However, the first two observational data from well 3 were in disagreement with simulation. The well 3 locates furthest from the reservoir, and thus the simulation result was the least sensitive to the fluctuation of the reservoir water level. Observation at well 2 shows a good agreement with simulation. In the one-dimensional groundwater flow model, the boundary condition applied to the side of the reservoir was the observed reservoir water head. The boundary condition at the other side was user-defined prescribed constant head. This boundary value itself was not validated with field observations, but it was chosen so that the simulated GWT elevations matches observed GWT elevations at the two wells (Fig. 4-9). The inaccuracy of the boundary condition away from the reservoir was likely led to the discrepancy between the simulation and the observation at well 3. The use of a larger value for the user-defined constant head or the use of a prescribed flow boundary condition, if the data were available, would increase the accuracy of the groundwater simulation. However, in Ejersa, the depth to the groundwater is shallow enough to affect the formation of surface pools only close to the reservoir. Although the elevation of the GWT increases outward from the reservoir, a larger increase in surface elevation increases the depth of the unsaturated zone (Fig. 4-1 and Fig. 4-10). Thus, the importance of the GWT simulation far from the reservoir and the choice of the boundary condition are insignificant for this study area. Simulated spatial distribution of the GWT is shown in Fig. 4-10.

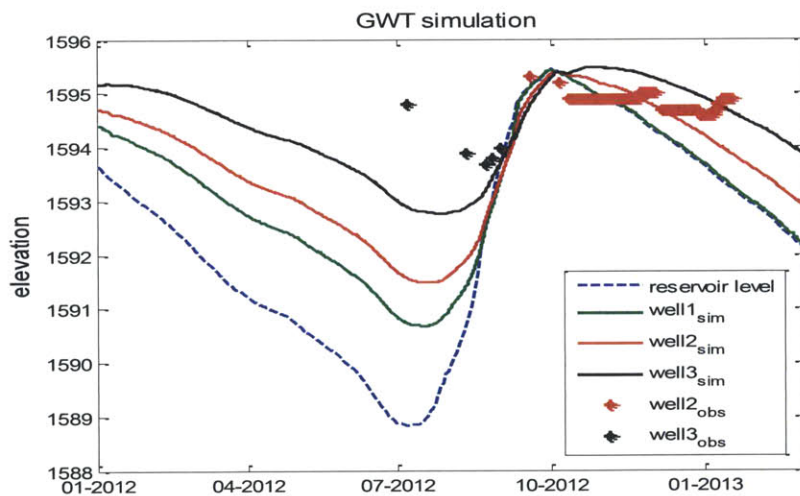


**Figure 4-9 Simulated and observed GWT**

Solid lines are simulated GWT elevations. Asterisks are observed GWT elevations. Green, red and black colors correspond to well 1, well 2 and well 3, locations of which are described Fig. 2-10. No observational data were obtained from well 1 because the instrument was stolen. The blue dotted line is the observed reservoir water head, which was used as a boundary condition. From September to December, the reservoir levels and the simulated GWT at well 1 coincide, meaning the well 1 was covered by the reservoir water. This is in agreement with observation.

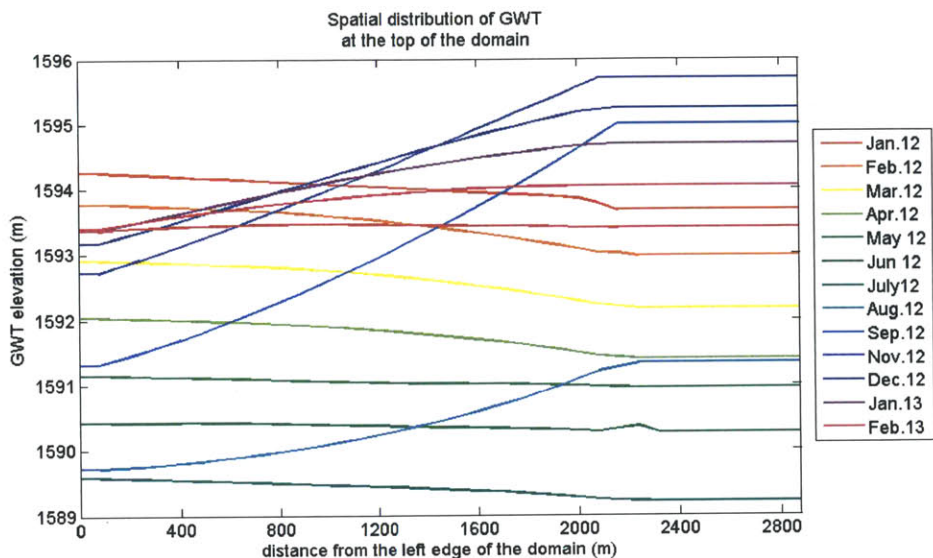


**Figure 4-10 Spatial distribution of GWT simulated at the top of the simulation domain**

Simulated GWT elevations are present for the top row of the simulation domain. Different lines indicate different months. At the north part of the simulation domain, annual change in shoreline location is not significant, compared to the south part of the simulation domain. Before the main rainy season, when reservoir water levels are low, groundwater flows towards the reservoir. After August, the flow direction changes in the simulation domain, responding to increased reservoir levels. Note that the left boundary condition was applied not to the left edge of the simulation domain, but to far away from the reservoir.

In this section, outputs of surface water locations and depths were illustrated. The surface water locations and depths are the main outputs from the hydrology model and also important inputs for the entomology model. The soil moisture data and the GWT data demonstrated the accuracy of the hydrology model, which validates the use of the hydrology model outputs for the entomology model. Further model calibration will be conducted as more data become available. The following section follows to show the results from the entomological model in HYDREMATS.

#### 4.1.4 Entomology Model Output

The dynamics of the mosquito population were simulated in HYDREMATS using meteorological data and the outputs from the hydrology model described in the previous section as model inputs. The comparison of the simulated and observed population of *Anopheles* mosquitoes is shown in Fig. 4-11. The simulation was run with an initial population of 1000,



which also served as a minimum number of mosquitoes that should exist in the model to allow population growth in the next mosquito growing season. Smaller values of initial population and minimum population lead to chaotic model results; mosquito population grows in one simulation but the population crushes in another simulation. This is because the model is highly non-linear and is based on multiple probabilistic formulae. The simulated mosquito population (Fig. 4-11, blue solid line) had two peaks, one in the late rainy season and the other after the rainy season. Only a small increase in mosquito population was simulated during the secondary rainy season around April. The observed mosquito population (Fig. 4-11, green asterisks) is the number of mosquito collected in the six light traps in Ejersa. The observational data are shown from July 2012, when the adult mosquito survey started. In the middle of September, IRS was conducted in Ejersa. As a result, the number of mosquito captured by light traps dropped significantly (Fig. 4-11, red asterisk). The effect of IRS made the comparison between simulation and observation difficult because the magnitude and the duration of the effectiveness of IRS are not known. However, it is likely that the effect of IRS did not last long. In 2012, a local malaria laboratory reported that mosquitoes developed resistance against a chemical used in IRS, and so another type of chemical (propoxur) had to be adopted in 2013, after the study period (Personal correspondence with regional clinic, 2013). In HYDREMATS, the effect of IRS was not simulated. Assuming the effect of IRS was short-lived, Fig. 4-11 reveals that HYDREMATS simulated the dynamics of mosquito population relatively accurately. The timing of the increase in mosquito population and the magnitude of the population increase were simulated well. However, HYDREMATS simulated the decrease in mosquito population about three weeks later than observed.

This dynamics of the mosquito population can be explained by examining simulated breeding sites shown in Fig. 4-12. The figure shows the number of pool grid cells and the number of aquatic stage mosquitoes simulated. The first peak in adult mosquito population was created by mosquitoes emerging from rain-fed pools (Fig. 4-12, red solid line and red asterisks) from July to September. The second peak was brought by shoreline water. From September to November, the increased reservoir water inundated a large area in the simulation domain, creating favorable mosquito breeding sites (Fig. 4-12, blue solid line). Following the expansion in shoreline breeding sites, a large number of aquatic stage mosquitoes were simulated at the shoreline (Fig. 4-12, blue asterisks). Few groundwater pools and aquatic stage mosquitoes were simulated there.

## **4.2 Model Application to Gudedo**

In this section, the results of the HYDREMATS applied to Gudedo are shown. Gudedo is a

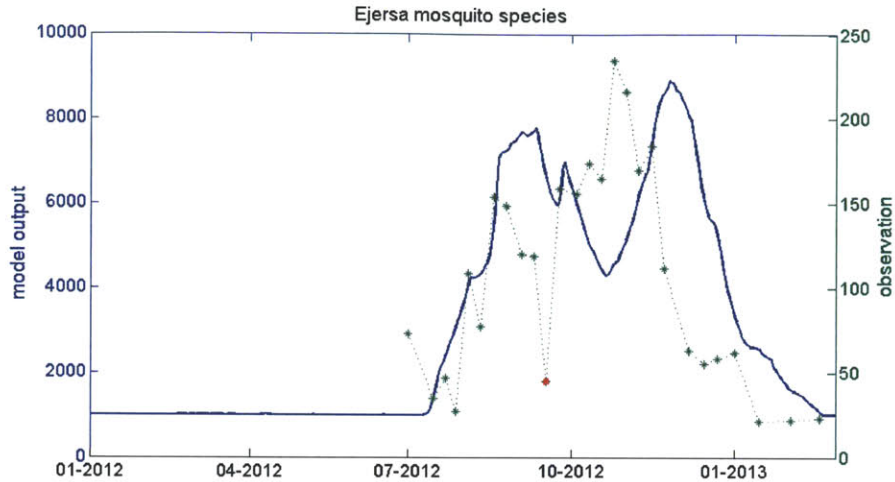


**Figure 4-11 Ejersa mosquito simulation and observation**

The blue solid line shows the simulated mosquito population and the green asterisks show the number of mosquitoes captured by the six light traps. The initial and the minimum number of mosquito population were set at 1000 in the simulation. The observed mosquito population marked as red indicates the number of mosquitoes captured soon after IRS.

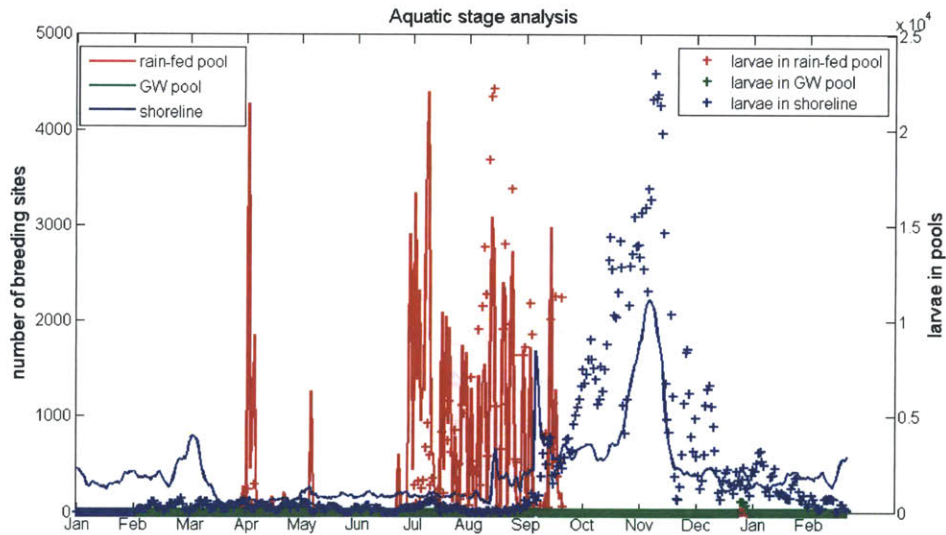


**Figure 4-12 Analysis of aquatic stage mosquitoes: numbers of breeding sites and larvae**

The solid lines show the number of pools simulated in HYDREMATS. The asterisks are the simulated aquatic stage mosquitoes in each pool. Red, green and blue colors indicate rain-fed pool, groundwater pool and shoreline water, respectively.

village about twelve kilometers away from the Koka Reservoir serving as a control site in this study. The original HYDREMATS (Bomblies *et al.*, 2008) was applied to Gudedo as the village does not require reservoir representation. First, a topography map and input parameters for the Gudedo model are provided in 4.2.1. Hydrology and entomology model results are shown in 4.2.2 and 4.2.3, respectively.

#### **4.2.1 Gudedo Field Setting and Model Parameters**

Gudedo serves as the control site in this study, due to the absence of a large water body nearby. The climate in Gudedo and Ejersa is similar, although the 200m higher elevation in Gudedo results in 1.4 °C lower temperature on average throughout the year. Another difference between the two sites is the topography. Gudedo is topographically more variable including steep dry rivers, which typically has a width of 2-5m and a depth of 3-10m. In addition, construction of a highway to the capital started in mid- 2012 in Gudedo. The construction has changed the geography around Gudedo and left some man-made pools. The pools are usually 5m in diameter with turbid water. During the field survey, no larvae were found in these pools. However, there is a possibility that those pools are used as mosquito breeding sites. The locations of these pools were not represented in the model in this study because the ASTER DEM was produced before the construction started and because it was not easy to detect the location of all the pools, whose existence is contingent on the construction. HYDREMATS was applied to a two kilometers by two kilometers region indicated by a red square frame in Fig. 2-4.

Model inputs for the hydrology model were prepared according to 3.1.3. The elevation data came from ASTER DEM, which is the finest resolution DEM available for this area free of charge. The Gudedo topography is shown in Fig. 4-13. The major hydraulic parameters assigned for the Gudedo model are summarized in Table 4-4. These parameters were derived from input data, i.e. soil type and vegetation type. Different hydraulic conductivity and Manning coefficient modified within the range found in literature affected soil moisture simulation and overland flow simulation little. Thus, model calibration resulted in the employment of the original hydraulic values.

The porosity and hydraulic conductivities were assigned in IBIS relying on the HWSD soil dataset. The HWSD provides the proportions of sand, clay and silt in soil at different depths. For Gudedo, the soil profile was obtained for the upper (0-30cm) and lower (30-100cm) soil columns. Although the porosity changed little over the soil columns, a subtle difference in the soil components in the two columns assigned different hydraulic conductivities in IBIS. The hydraulic conductivities in the upper and lower column were set at 0.31 m/d and 0.055 m/d,

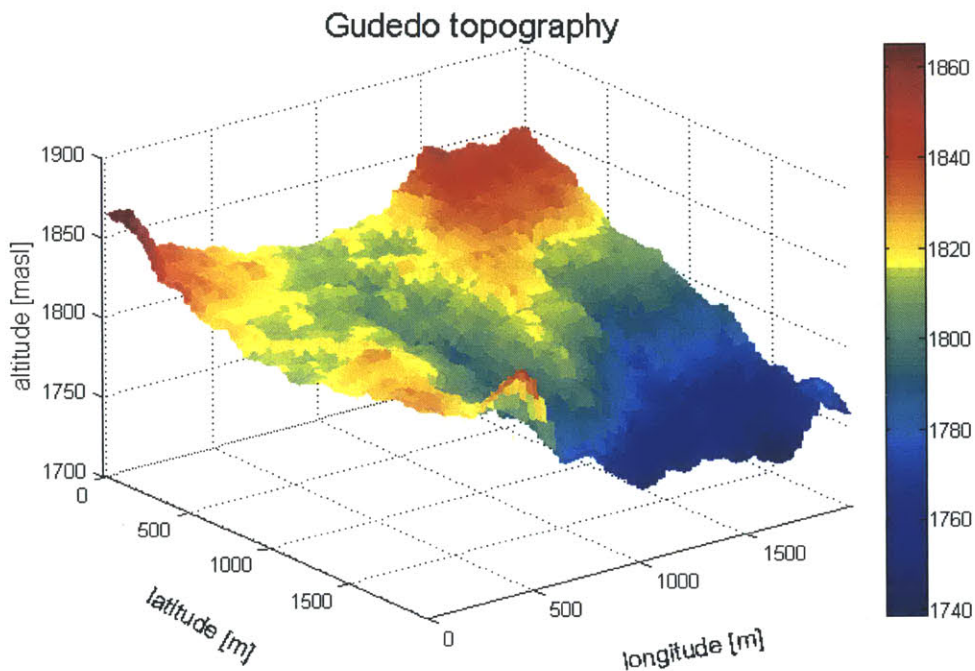


**Figure 4-13 Gudedo topography**

The topography map was created based on a 30-meter-resolution DEM from ASTER for the simulation domain. X (longitude) axis shows the distance in meter from the west edge of the domain, y (latitude) axis from the north edge of the domain. Z (altitude) axis shows elevation in meter above sea level (masl). A road runs from east to west in the south of the simulation domain. The elevation generally decreases from north to south. The elevation varies by more than 100m within the 2km by 2km simulation domain.

respectively. In order to reflect the crusting effect observed at the site, the hydraulic conductivity at the topmost layer was lowered tenfold.

The Manning’s roughness coefficient was assigned using land cover data from UMD. The vegetation type in Gudedo was mainly classified as wooded grassland, and a Manning’s roughness coefficient of 0.050 was assigned.

Following the default setting of IBIS, the number of soil layer was set at six. The thicknesses of the soil layers were set at 5cm, 10cm, 10cm, 50cm, 50cm and 100cm from top to bottom. The small thickness at the top layer also reflected thin crusting layer observed in Gudedo. The lower boundary condition in soil moisture solver was set to be fully permeable. The permeability at the lower boundary condition was set to one.

**Table 4-4 Hydrology model parameters for Guedo**

<b>Parameters</b>	
<b>Porosity</b>	0.463
<b>Hydraulic conductivity (1<sup>st</sup> layer)</b>	0.031 m/d
<b>Hydraulic conductivity (2<sup>nd</sup>-4<sup>th</sup> layer)</b>	0.31 m/d
<b>Hydraulic conductivity (5<sup>th</sup>-6<sup>th</sup> layer)</b>	0.055 m/d
<b>Manning coefficient</b>	0.050
<b>Permeability at lower B.C.</b>	1.

### **4.2.2 Hydrology Model Output**

The hydrology model outputs are the depths and the locations of surface pools and the pool temperature. The outputs are written in ascii files at an hourly time step with a spatial resolution of 10m.

A snapshot of the water depth output is shown in Fig. 4-15. The output of simulated water pools was superimposed on a satellite picture of Guedo. In the satellite picture, water can be recognized in a trench at the center running from north to south. However, the model output failed to represent the existence of the narrow water path. This is due to the low resolution (~30m) of the DEM used as a model input. The trench is usually 2-5m wide and 3-10m deep (Fig. 4-14). The 30m-resolution DEM cannot represent this sub-grid scale topography. It is one of the model limitations that HYDREMATS is highly reliant on DEM inputs and that accurate high resolution DEMs are rarely available for the African continent if not purchased. This is especially true for locations like Guedo where topography shows a large variability at the sub-grid scale. In Guedo, however, water in trenches only appears during and soon after rain events, and water runs downstream quickly. Because this short-lived and fast-flowing water is not suitable as a mosquito oviposition site, the water in the trenches is less likely to be used by mosquitoes. In addition, water in the trenches runs without inundating the surrounding area because the channels are deep. Hence the water in the channels is not expected to create surface pools around it.

HYDREMATS does not include inflow to channels from outside the domain. A larger catchment area than the simulation domain could be another reason why HYDREMATS failed to simulate water in ditches. However, as discussed, simulating water in ditches is likely of negligible importance in the simulation of mosquito population.





**Figure 4-14 Trench found in Gudedo**

**The picture shows a relatively large trench. It is about 4m wide and 3m deep. From this picture taken about one day after a rainfall event, no remaining water is found in the trench.**

HYDREMATS is thus seen to simulate only rain-fed surface puddles attributed to small scale depressions. Those pools are expected to be of much greater importance to the mosquito ecosystem as compared to fast-flowing and short-lived water in channels. Readers should note that this interpretation is not necessarily applicable to every field site.

One way to validate the hydrology model is to compare soil moisture observation values and simulated values. However, although two *in-situ* soil moisture measuring stations (MS and SMS) were employed in Gudedo, the one in the SMS faced a technical fault, leading to a long break in data collection. Unfortunately, soil moisture data were not obtained for a long enough period to be used for model calibration from the SMS. Thus, the hydrology model calibration was conducted using the data obtained from the MS. The MS was located in the northeast of the simulation domain (Fig. 2-4). The elevation of the MS is about 1830 masl, and the soil type was observed as silty sand.

The comparison of the observed and simulated soil moisture is presented in Fig. 4-16. Fig. 4-16 (a) shows the observed VWC at depth of 30cm and 100cm below surface at Gudedo MS. The observational data show the 30cm-depth probe responded to the main rainy season (July-Sep.) and also slightly to the secondary rainy season (Apr.-Mar.). The 100cm-depth probe only responded to the rain during the main rainy season with a smaller magnitude. The simulated VWC in Fig. 4-16 (b) was obtained from the grid cell that contains the MS. Because the default values of soil layer depths in IBIS were applied, the observed depths and the simulated depths did not coincide. The simulated VWC at 25cm depth resembled the behavior of the observed VWC at 30cm depth. The figure suggests that the behavior of soil at the depth of 100cm was



Gudedo hydrology model output: d270h17

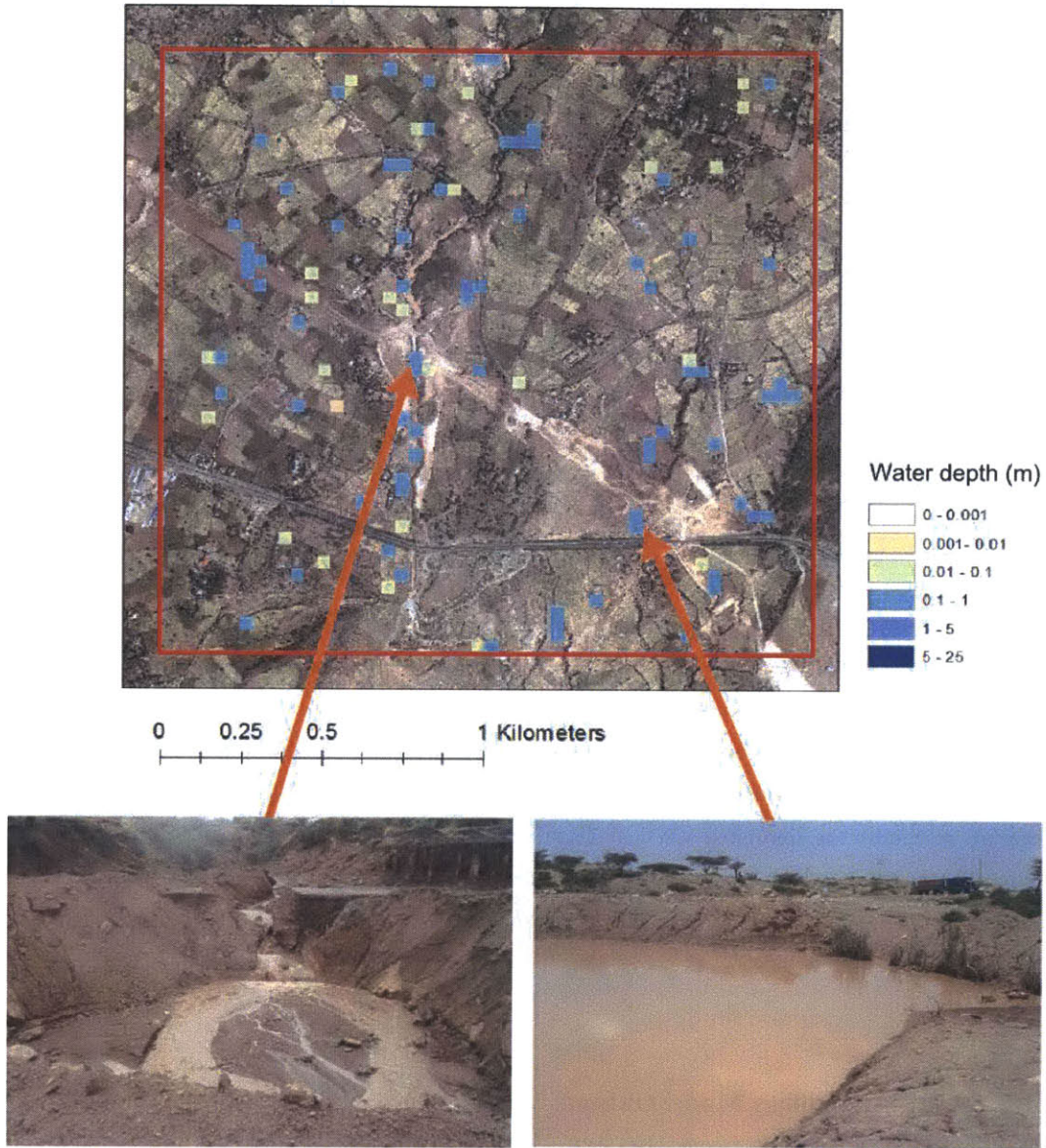


**Figure 4-15 Gudedo simulation pool output**

The simulation output of surface pools are superimposed on the satellite picture (top). The simulation output of 270th Julian day (Sep. 26th) 5pm was chosen. The color indicate the depth of the simulated pools. The majority of the pools have a depth between 0.07 and 0.29m. Photos of the real pools corresponding to simulated pool locations are presented (bottom). The dates that the pictures were taken do not necessarily correspond to the date of the simulation output shown here.

simulated around 75cm depth in HYDREMATS. At 75cm depth in the simulation, soil moisture did not start to increase until mid-July, as was observed at 100cm depth at the MS.

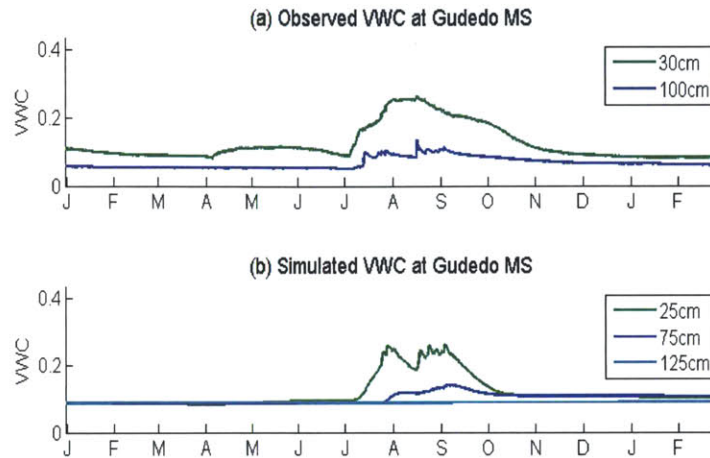


**Figure 4-16 Volumetric water content at Gudedo MS**

The figure (a) shows the observed VWC and the figure (b) shows the simulated VWC at the Gudedo MS. Observational data from the top probe (15cm below the surface) is not shown because it was highly erroneous. Because the default values of soil layer depths in IBIS were applied, the observed depths and simulated depths did not coincide. The behavior of the observed VWC at 30cm below surface (green in figure (a)) resembles the simulated VWC at 25cm below surface. The soil moisture profile observed at 100cm below surface is close to the soil moisture profile simulated 75cm below the surface, while percolated water during the main rainy season arrives later in the simulation than in the observation.

### 4.2.3 Entomology Model Output

The population dynamics of *Anopheles* mosquito in Gudedo were simulated. As well as meteorological data, the hourly outputs of pool depth and pool temperature from the hydrology model were used as model inputs in the entomology model. The parameters for the Gudedo entomology model were set identical to the ones for the Ejersa model.

The simulation results are shown below. Fig. 4-17 compares the adult mosquito population in the simulation and in the observations. In this simulation, the initial number of *Anopheles* mosquitoes was set as 1000, which also serves as the minimum number of the population maintained in the simulation. Fig. 4-18 shows that simulated mosquito increased in number during the secondary rainy season (Apr.) and the main rainy season (July-Sep.). The population



increase in the secondary rainy season was about 60% of the initial number, and it was about 140% in the main rainy season. The magnitude of the population growth was about five times smaller than the one simulated in the Ejersa model. This result is consistent with observational data, where the observed maximum population in Gudedo was about seven times smaller than that in Ejersa. However, Fig.4-17 shows that HYDREMATS failed to correctly simulate the period when the mosquito population increased. In the simulation, mosquitoes increased in number from the beginning of July to the end of September in the main rainy season, whereas a small number of mosquitoes were observed until the end of December in the field site.

Fig. 4-18 shows that the simulated mosquito population in Gudedo was highly correlated with rainfall. Mosquito population dynamics followed the rainfall trend with a delay, which is usually found in the literature (Bomblies *et al.*, 2008; Kibret *et al.*, 2009; Parham *et al.*, 2012). The delay reflects the time that aquatic stage mosquitoes require to mature.

Although the simulated and observed adult mosquito populations were not similar, the simulated adult mosquito population dynamics resembled those of the observed larvae samples (Fig. 4-19). The number of larvae shown in Fig. 4-19 is the sum of the larvae sampled from the five larvae dipping pools, whose individual data are shown in Fig. 2-19. This result suggests that the mosquitoes observed after October emerged from pools which were not sampled in our field survey or from water bodies which existed outside the simulation domain.

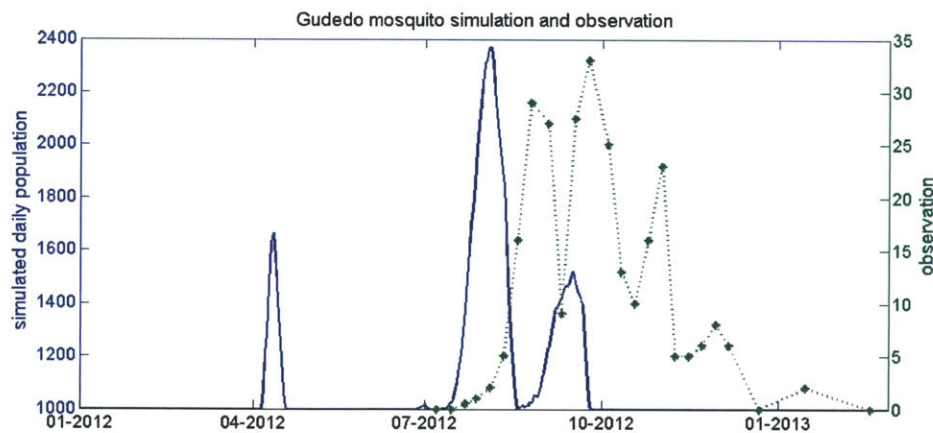


**Figure 4-17 Gudedo mosquito simulation and observation**

The blue solid line indicates the daily average of simulated mosquito population. The green asterisks are the observational data of total number of *Anopheles* mosquitoes captured at six light trap houses. The observation started in July, so no data exists before that. The observation frequency was weekly during- and after the rainy season (July-Nov.) and monthly during the dry season (Dec.-Feb.).

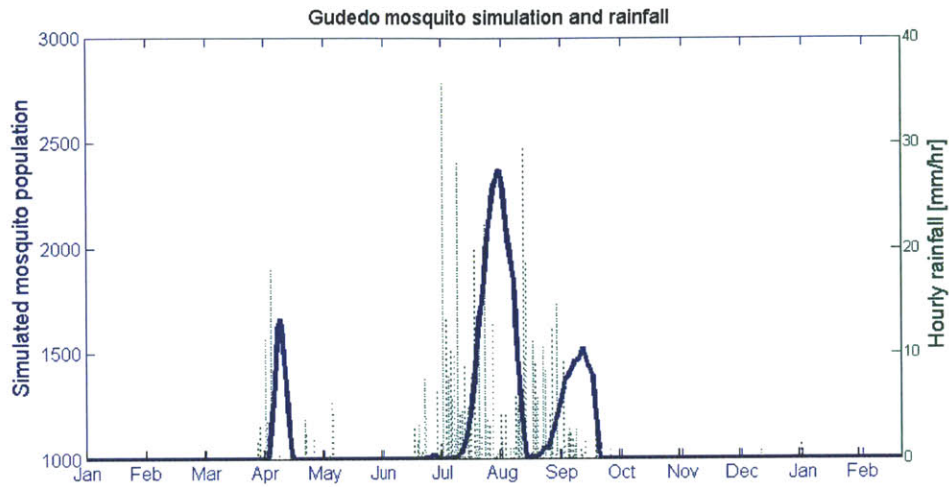


**Figure 4-18 Gudedo mosquito simulation and rainfall**

The blue solid line shows the mosquito population simulated with the initial and the minimum population of 1000. The simulated mosquito population peaked at the end of July. The green dotted line shows the hourly precipitation observed.

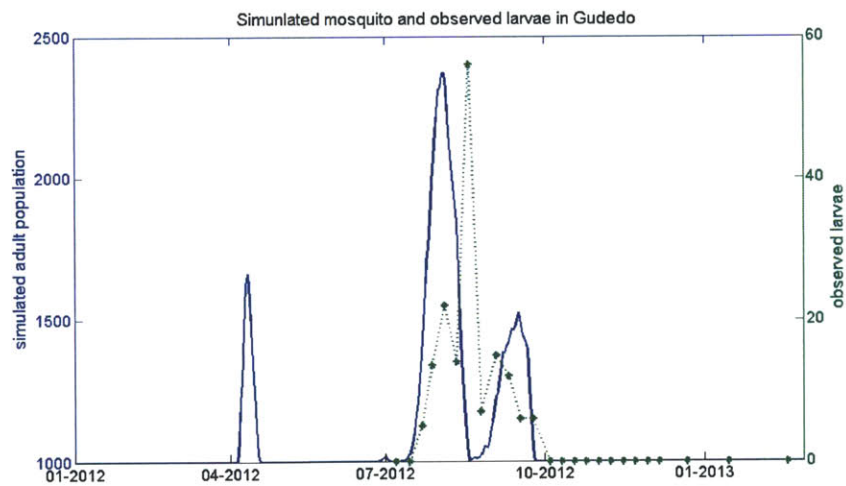


**Figure 4-19 Comparison of simulated mosquito population and observed larvae in Gudedo**

The simulated adult mosquito population is shown in the blue solid line. The green asterisks show the number of larvae sampled from five pools in Gudedo.

## 4.3 Discussion

### 4.3.1 Comparison between Ejersa and Gudedo

Ejersa and Gudedo are located around the Koka Reservoir, at the center of Ethiopia. They are approximately 15 km away from each other. Because of their geographical proximity, climate in Ejersa and Gudedo is comparable (Fig. 4-20). Annual temperature in Ejersa and Gudedo is 21.2 °C and 19.8 °C, respectively. Annual temperature in Gudedo is slightly lower than that in Ejersa because the elevation in Gudedo is about 200 m higher. The two villages experience similar precipitation pattern. They have two rainy seasons; the main rainy season from mid-June to mid-September, the secondary rainy season from March to May. Total precipitation during the main rainy season in 2012 was 816 mm and 718 mm in Ejersa and Gudedo, respectively.

However, observed mosquito dynamics are distinct. As shown in Fig. 4-21, Ejersa experiences enhanced and prolonged mosquito season. Over the study period, approximately ten times more *Anopheles* mosquitoes were collected in Ejersa than in Gudedo, even though IRS was conducted in September in Ejersa. In addition, Ejersa maintains a relatively large mosquito population even after the rainy season, which was not observed clearly in Gudedo. Mosquito dynamics partially depend on climatological factors. The fact that the two villages have similar climatology but different entomology suggests that the difference in environment plays an important role in governing mosquito population dynamics around the area.

The major difference in Ejersa and Gudedo environment is the existence of a reservoir. Ejersa is located adjacent to the Koka Reservoir, whereas Gudedo is about 12 km away from it. Because the mosquito flight distance is only a few kilometers, it is unlikely that the mosquito population in Gudedo is supported by the reservoir. The reservoir system also affects GWT. GWT table was observed to be shallow in Ejersa especially close to the reservoir. On the other hand, Gudedo expects deep GWT.

Other environmental factors such as topographical roughness, soil type and vegetation type may have certain impacts on mosquito population dynamics. Despite the geographical proximity, topographic characteristics were different in Ejersa and in Gudedo. Topography in Ejersa was mild, whereas that in Gudedo was significantly rough.

Incorporating major climatological and environmental factors, HYDREMATS was able to capture the difference in *Anopheles* mosquito population dynamics between Ejersa and Gudedo (Fig. 4-22). Although no observational data on mosquito population exist before July 2012, population dynamics simulated for the main rainy season in 2012 in the two field sites were comparable to the observation. Discussions on the simulated mosquito population dynamics are presented in the following sections.

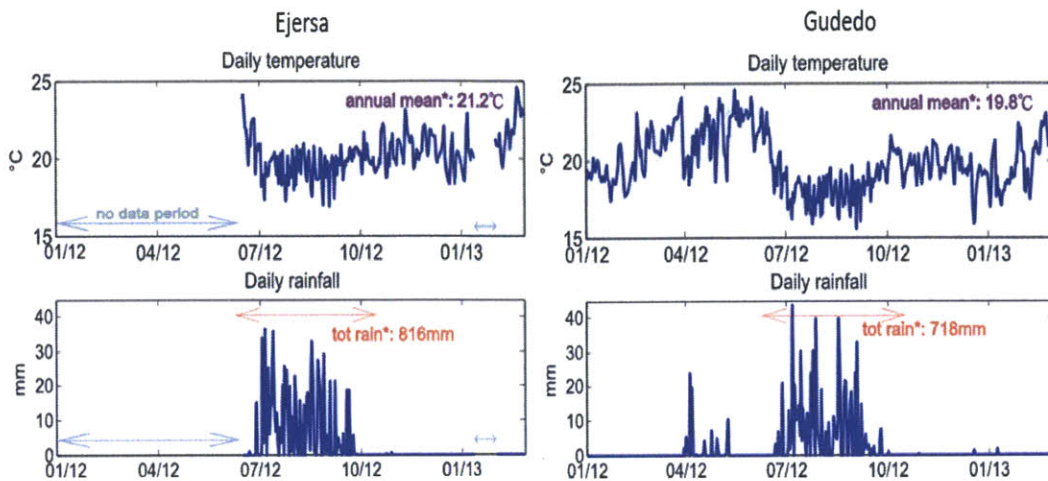


**Figure 4-20 Climate in Ejersa and Guedo**

Top figures show daily temperature and bottom figures show daily rainfall available for the study period from Jan. 2012 to Feb. 2013. Left figures are for Ejersa and right figures are for Guedo. Mean annual temperature is 21.2 °C in Ejersa and 19.8 °C in Guedo. The mean temperatures were calculated using data from July 2012 to July 2013. Total precipitation for the main rainy season in 2012 was 816 mm and 718 mm in Ejersa and in Guedo, respectively.

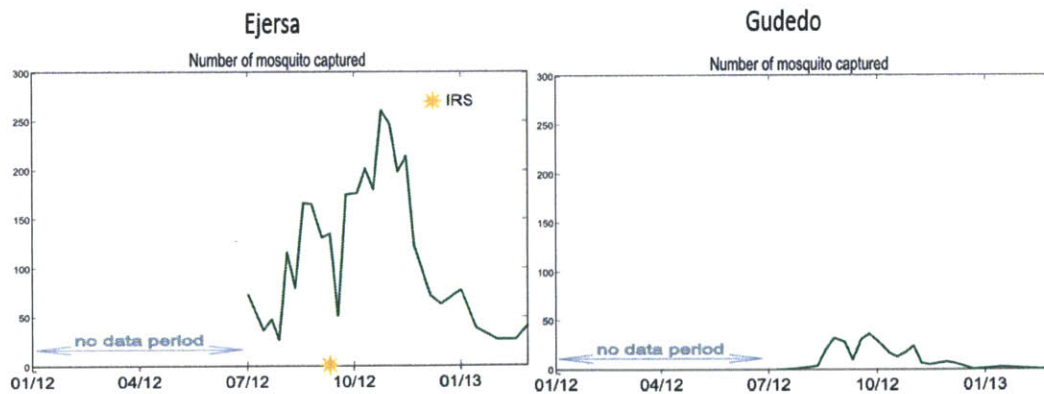


**Figure 4-21 Observed adult *anopheline* population in Ejersa and Guedo**

Numbers of adult *anopheline* mosquitoes captured by six light traps are presented. In Ejersa (left), observed *anopheline* population peaked in Oct. when approximately 250 *Anopheles* mosquitoes were captured at one night. In Sep., IRS was conducted in Ejersa. In Guedo (right), observed *anopheline* population peaked in Sep.; the observed population did not exceed 50 during the study period.



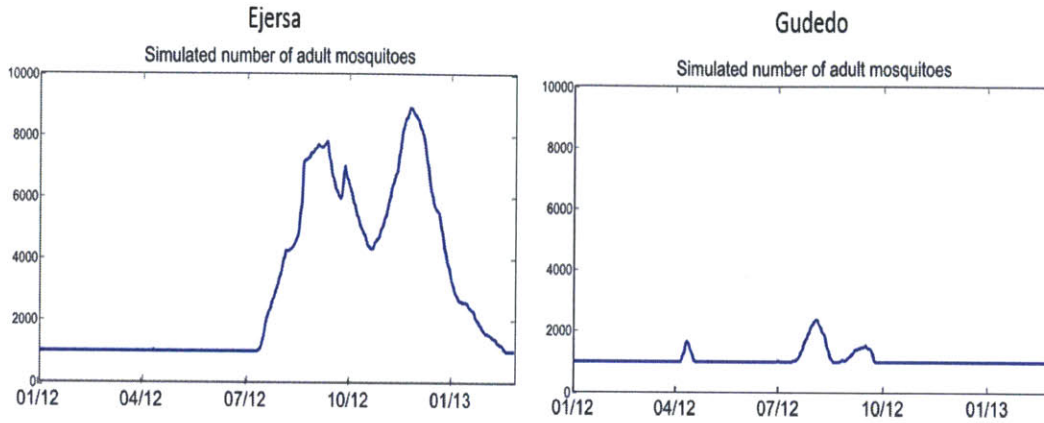


Figure 4-22 Simulated adult *anopheline* population in Ejersa and Gudedo

### 4.3.2 Discussion of Mosquito Dynamics in Ejersa

In Ejersa, mosquitoes were observed in larger numbers and for a longer period than in Gudedo. Larger *Anopheles* population was simulated because rain-fed pools persisted longer and because the reservoir provided permanent breeding sites for mosquitoes. The simulation results demonstrated that the mosquito population was sustained after the rainy season by the creation of shallow shoreline breeding sites, when the increased reservoir water level inundated a relatively flat area.

During the rainy season, rain-fed pools simulated in the Ejersa model persisted longer than that in the Gudedo model, although the precipitation forcing was comparable. As a result, a larger number of mosquitoes were simulated in Ejersa. This difference in pool persistence may be attributed to a combination of topography, soil type, vegetation type, and shallow GWT due to the proximity to the reservoir. In the south of the simulation domain in Ejersa, where most of the rain-fed pools were simulated, the GWT is expected to be shallow because of its low elevation. In addition, the reservoir itself served as a source of *Anopheles* mosquito supply. The reservoir breeding sites during the rainy season were, however, not productive enough to contribute significantly to mosquito population dynamics because of the narrow shoreline breeding zone and the large distance from the shoreline to human houses.

HYDREMATS simulated the mosquito breeding season for a longer period than observed after the main rainy season. The sustained mosquito population in the post-rainy season is due to the creation of shallow shoreline breeding area inundated by increased reservoir water level (Fig. 4-5, Fig. 4-12). The newly created inundation area, not only expands favorable breeding sites for mosquitoes, but also is more accessible for mosquitoes because advancement of shoreline nears human settlement. The discrepancy between the simulation and the observation could be

partially because the effect of reservoir water fluctuation was neglected. When the reservoir water level decreases rapidly, some larvae become stranded and deposited on land. Some of them die from desiccation or encounter predators such as ants.

Vasconcelos and Novo (2003) found in southeast Para in Brazil that a rapid reduction in water level is associated with a decrease in malaria transmission. They argued that this is because the fast drop in water level eliminates the macrophyte stands, increasing the organic loads in water by plant decomposition, resulting in conditions unfavorable to the main vector in the study site. Previous studies at the Koka Reservoir also found associations between the reservoir water fluctuation and malaria incidence or mosquito population (Lautze *et al.*, 2008; Lautze 2008b; Teklu *et al.*, 2010). Regression analyses in the studies revealed that water dropdown rates are negatively correlated with malaria incidence and the number of positive breeding sites. A linear association between the increasing water level and malaria cases was not found (Lautze 2008b). Absolute reservoir water level had no correlation with the number of positive breeding sites (Teklu *et al.*, 2010). These studies provides useful implications; however, they are based on simple correlation analyses, possibly neglecting other important physical or environmental factors, or being confounded by more important factors. In addition, these correlation analyses have limitations in extrapolating results. While regression analyses may draw a relationship between variables in an observed range, the same relationship does not necessarily hold outside the range or for different environment. Thus, drawing general conclusions on the impact of water fluctuation on mosquito population dynamics may not be appropriate.

An opposite impact from water drawdown was found by Darrow (1949) on stranding larvae. Darrow conducted field experiments at the Wilson Reservoir in the US on the movement of *An. quadrimaculatus* larvae against water recession at a vegetated shoreline. The results indicated a higher drawdown rate of water results in stranding fewer larvae.

Limited literature makes it difficult to correctly evaluate the mortality rates associated with change in reservoir water level. The impact of water fluctuation on larvae is expected to depend on location-specific environmental factors such as micro-topography and vegetation as well as fluctuation speed. Quantifying the effect of reservoir water fluctuation on larvae mortality will be conducted in a future study. The findings will also be incorporated into HYDREMATS to improve the simulation capability.

Vegetation at the shoreline is another important factor for the productivity of larvae. Vegetation types depend on what fraction of the year the land is flooded by the reservoir water. Fig. 4-23 shows shoreline vegetation at the beginning of August, when the reservoir water level is in the middle of its range. This area is submerged under the reservoir for approximately half a year. As a result, water-tolerant short grass dominates. On the other hand, shoreline vegetation at high reservoir water level is leafy (Fig. 4-24) because it is submerged for a shorter period. The

picture in Fig. 4-24 was taken in the middle of September. Although the data are limited, our observation suggests that the larvae productivity is high when reservoir water levels are high, around October (Fig. 2-8). This observation implies that shoreline with leafy vegetation is preferable for the *Anopheles* species present around the Koka Reservoir. Vegetation at a shoreline may work to provide a shelter from predators, to minimize wave effect, and to accumulate nutrients. In HYDREMATS, such a vegetation-dependent productivity was not considered. The effect of vegetation-dependent productivity may account for the gap between observed and simulated mosquito population in October in Ejersa. In the simulation, although the increasing water level expanded the total reservoir area, the area with shallow water decreased (Fig. 4-12 blue line). Accordingly, the shoreline breeding sites recognized in HYDREMATS decreased, leading to smaller oviposition and emergence of mosquitoes. However, although the area of shoreline breeding site decreased, the productivity may have increased due to the existence of herbaceous vegetation at the shoreline. If the increase in productivity had compensated the decrease in area of breeding site, the simulation result would have more closely resembled the observations.



**Figure 4-23 Shoreline vegetation at middle reservoir level**





Figure 4-24 Shoreline vegetation at high reservoir level

#### 4.3.3 Discussion of Mosquito Dynamics in Guedo

HYDREMATS simulated smaller *Anopheles* population in Guedo, whose dynamics follows precipitation patterns. The simulated *Anopheles* population grew in April and July-September responding to the secondary and the main rainy season, respectively. Observational data, however, show increased *Anopheles* population through August to November. Although the simulated adult *Anopheles* population failed to match the observed adult mosquito population, it mirrors observed number of larvae.

The *Anopheles* mosquitoes observed in Guedo from August to November were not accurately simulated in HYDREMATS. The poor simulation of mosquito population dynamics arose from the intrinsic limitation of HYDREMATS' capability and the inadequate input data. Possible reasons for differences between the observed and simulated mosquito population are discussed below.

Altered topography due to a highway construction in Guedo created pools for mosquito oviposition, which were not simulated in the Guedo model. The construction started in early 2012, and the altered topography was not reflected in the DEM, on which the model largely relies. Thus, the hydrology model output may have missed some surface puddles, which could have been used as mosquito breeding sites in the simulation. Although few larvae were

observed in these pools during field surveys, some of those pools likely provide mosquitoes with breeding habitats. In addition, some relatively long lived man-made pools were observed in the field survey. These man-made pools were also not simulated in HYDREMATS.

Water in trenches may have also been used as mosquito breeding habitats. In the hydrology model, the mass balance of water was applied over the simulation domain, but the inflow to and outflow from the trenches were omitted due to the lack of quantitative information. In surface runoff calculations, a periodic boundary condition was applied to the boundaries at the north and the south so that the surface runoff leaving from the south enters to the domain again from the north. However, this consideration may not be sufficient because of the larger amount of water that is expected to accumulate and flow into the trenches from above the simulation domain. Although the speed of the running water at trenches during and soon after rainfall events are observed to be too high for the trenches to be a favorable mosquito breeding habitat, the trenches may serve as mosquito breeding pools at other times, especially if stagnant water pools are created besides water channels in the river bed.

Migration of mosquitoes from outside the simulation domain is another possible explanation for the observed mosquito dynamics. In particular, the migration of mosquitoes may account for the mosquitoes observed after the rainy season, when no pools were simulated. The simulation was conducted over the 2km by 2km simulation domain around Jogo-Guedo *kebele*. This is based on the assumption that the average flight range of *Anopheles* mosquitoes is within 2 km. This assumption was applied to Niger, where HYDREMATS was originally developed, based on Gillies (1961). The author estimated the average flight range of adult *An. gambiae* females as between 1 and 1.5 km in his field observation in Tanzania. However, there is little agreement on the mosquito flight range. Kaufmann (2004) studied the flight potential of *An. gambiae* and *An. atroparvus* in a lab environment using flightmills and found that mosquitoes can fly up to a direct-distance of 12km in a day if blood-fed. Because the mosquito flight path is not straight, their flying distance in natural conditions is much smaller than the values reported by Kaufman. However, this study suggests the possibility that some of the mosquitoes observed in Guedo were born and flew from outside the simulation domain. Expanding the simulation domain could reduce this simulation error. However, it requires a higher computational cost as well as more observation points to cover the area. If the migration of mosquitoes is the major source of the model discrepancy, the agreement between the number of simulated adult mosquitoes and observed larvae proves the accuracy of the simulation of the *Anopheles* population dynamics influenced by hydrology within the simulation domain.

The failure of the simulation is also attributed to the limitation of the model capability and the availability of accurate input data. In simulating surface puddles in the hydrology model, HYDREMATS requires the information on local topography, vegetation and soil type. Those

data are available globally without conducting field surveys. However, the spatial resolution of these data may not be sufficient to explain the entire hydrological system at the soil surface at a scale of 10m or smaller, which is often the size of mosquito breeding pools. As the model explicitly simulates the creation of surface water bodies using deterministic formulas, sub-grid scale heterogeneity is not considered. Although the basis of the hydrology model (i.e., IBIS) in HYDREMATS is a comprehensive model, the model appropriateness is scale-dependent and is limited in the expression of mosquito micro-habitats to some extent. More accurate representation of surface pools will result in better simulation results of mosquito population dynamics.



## Chapter 5: Conclusion and Future Work

Despite the similarity in climate, Ejersa and Gudedo, located approximately 15 km away from each other at the center of Ethiopia, presented different *Anopheles* mosquito population dynamics. Ejersa, located adjacent to the reservoir, experienced enhanced and prolonged mosquito season. Simulation of hydrology in Ejersa revealed that rain-fed pools are sustained longer than in Gudedo and that expanded reservoir area after the main rainy season caused population growth, which explains the reason for enhanced and prolonged mosquito season, respectively. In contrast, Gudedo is located approximately 12 km away from the reservoir, too far away for mosquito population dynamics to be affected by the reservoir. By incorporating how the hydrology is influenced by the reservoir system, HYDREMATS was able to simulate the differences in entomology between Ejersa and Gudedo.

The application of HYDREMATS to the two field sites around the Koka Reservoir demonstrated both the model's capability and its limitations. In the Ejersa model, HYDREMATS was modified to include a reservoir representation in the hydrological system. The Ejersa model was able to simulate the enhanced and prolonged mosquito breeding season, which were not explained by precipitation patterns alone. However, the Ejersa model overestimated the mosquito season in the post-rainy season. The impact of water recession at the reservoir on larval mortality and the vegetation-dependent productivity of breeding pools were neglected in HYDREMATS in this study, and they could partially account for the discrepancy between the simulation and the observation. These factors will be investigated further in the future.

The mosquito dynamics simulated in the Gudedo model correlated well with rainfall and were comparable with observed larvae population. The original HYDREMATS developed by Bomblies *et al.* (2008) was used in the Gudedo model. The Gudedo model, however, failed to simulate the observed population dynamics of *Anopheles* mosquitoes. This failure is partially attributed to the migration of mosquitoes from outside the simulation domain. The limited accuracy of inputs such as the DEM, soil type and vegetation type are also possible explanations. In particular, HYDREMATS is largely reliant on the quality of the DEM. The 30-meter-resolution ASTER DEM was applied in the Gudedo model. The sub-grid scale variability in the topography in Gudedo is expected to have resulted in decreased accuracy in the surface pool simulation.

In this study, HYDREMATS was applied to and calibrated for the two study sites for a period of 14 months. For the purpose of model calibration and validation, the scarcity of observation was evident. Data collection has been continued for both hydrological variables and entomological variables, and those data will be used in a future study to improve the model. Especially, a larger quantity of more accurate data on soil moisture and groundwater table

should be obtained to calibrate the hydrology component of the model. The model capability will be tested when data become available for multiple years, to see if the inter-annual variability of mosquito population is correctly simulated. Incorporating the effect of water level fluctuation and shoreline vegetation at a reservoir in HYDREMATS is another task for the future research.

## References

Abebe, M. (2001) Sedimentation in the Koka Reservoir, Ethiopia; Hydropower in the New Millennium: Proceedings of the 4th International, Swet & Zeitlinger Publisher, Neitherlands.

Alertnet (2013) Ethiopia plans to power East Africa with hydro, <http://www.trust.org/alertnet/news/ethiopia-seeks-to-power-east-africa-with-hydro> (accessed on Mar. 28, 2013).

Amerasinghe, F.P. (1987) Changes in irrigation techniques as a means to control disease vector production, Joint WHO/FAO/UNEP Panel of Experts on Environment.

Animut, A., Balkew, M., Gebre-Michael, T., Lindtjørn, B. (2013) Blood meal sources and entomological inoculation rates of anophelines along a highland altitudinal transect in south-central Ethiopia, *Malaria Journal*, 12(1):76.

Aynew, T., Demlie, M., Wohnlich, S. (2008) Hydrogeological framework and occurrence of groundwater in the Ethiopian aquifers, *Journal of African Earth Sciences*, 52(3):97-113.

Bombliès, A., Duchemin, J., Eltahir, E.A. (2008) Hydrology of malaria: model development and application to a Sahelian village, *Water Resources Research*, 44(12).

Bombliès, A. (2008) The hydrology of malaria: field observations and mechanistic model of the malaria transmission response to environmental and climatic variability, Ph.D. thesis, Massachusetts Institute of Technology.

Bombliès, A., and Eltahir, E.A.B. (2009) Assessment of the impact of climate shifts on malaria transmission in the Sahel, *EcoHealth*, 6(3): 426-437.

Campbell Scientific, Inc. (2012) CS616 and CS625 water content reflectometers, Instruction manual 2002-2012, revision: 3/12.

Charlwood, J.D. and Braganca, M. (2012) The effect of rainstorms on adult *Anopheles funestus* behavior and survival, *Journal of vector ecology*, 37(1):252-256.

Chekol, D.A., Tischbein, B., Eggers, H., Vlek, P. (2007) Application of SWAT for assessment of spatial distribution of water resources and analyzing impact of different land

management practices on soil erosion in Upper Awash River Basin watershed, Catchment and lake research, 110-117.

Clennon, J.A., Kamanga, A., Musapa, M., Shiff, C., Glass, G.E. (2010) Identifying malaria vector breeding habitats with remote sensing data and terrain-based landscape indices in Zambia, *International journal of health geographics*, 9(1):58.

Darrow, E.M. (1949) Factors in the elimination of the immature stages of *Anopheles quadrimaculatus*, *American Journal of Hygiene*, 50(2):207-235.

Davis, R. G., Kamanga, A., Castillo-Salgado, C., Chime, N., Mharakurwa, S., Shiff, C. (2011) Early detection of malaria foci for targeted interventions in endemic southern Zambia, *Malaria Journal*, 10(1):260.

Depinay, J.M.O., Mbogo, C.M., Killeen, G., Knols, B., Beier, J., Carlson, J., Dushoff, J., Billingsley, P., Mwambi, H., Githure, J., Toure, A.M., McKenzie, F.E. (2004) A simulation model of African *Anopheles* ecology and population dynamics for the analysis of malaria transmission, *Malaria Journal*, 3:29.

Endo, N. (2013) Field survey conducted around the Koka Reservoir since August 2013.

Erlanger, T.E., Keiser, J., Castro, M.C.D, Bos, R., Singer, B.H., Tanner, M., Utzinger A.J. (2005) Effect of water resource development and management on lymphatic filariasis, and estimates of populations at risk, *American Journal of Tropical Medicine and Hygiene*, 7A3(3): 523–533.

Ermert, V., Fink, A.H., Jones, A.E., Morse, A.P. (2011) Development of a new version of the Liverpool Malaria Model. I. Refining the parameter settings and mathematical formulation of basic processes based on a literature review, *Malaria Journal*, 10(1):35.

EEPCo (Ethiopian Electric Power Corporation) (2013), <http://www.eepco.gov.et> (accessed on Mar. 25, 2013).

Ethiopia MoH (Federal Democratic Republic of Ethiopia Ministry of Health) (2006) National five year strategic plan for malaria prevention and control in Ethiopia 2006-2010, information was also obtained from <http://www.moh.gov.et/English/Information/Pages/MalariaPreventionControlProgram.aspx>.

Fontenille, D., L. Lochouarn, N. Diagne, C. Sokhna, J. J. Lemasson, M. Diatta, L. Konate, F. Faye, C. Rogier, and J. F. Trape. (1997) High annual and seasonal variations in malaria , transmission by Anophelines and vector species composition in Dielmo, a holoendemic area in Senegal, *American Journal of Tropical Medicine and Hygiene*, 56:247–253.

Forey, A.J., Prentice, I.C., Ramankutty, N., Levis, S., Pollard., D., Sitch, S., Hazeltine, A. (1996) An integrated biosphere model of land surface processes, terrestrial carbon balance, and vegetation dynamics, *Global biochemical cycles*, 10(4):603-628.

Furi, W., Razack, M., Haile, T., Abiye, T.A., Legesse, D. (2011) The hydrogeology of Adama-Wonji basin and assessment of groundwater level changes in Wonji wetland, Main Ethiopian Rift: results from 2D tomography and electrical sounding methods, *Environmental Earth Sciences*, 62(6): 1323-1335.

Gallup, J. L. and Sachs, J. D. (2001) The economic burden of malaria, *The American Journal of Tropical Medicine and Hygiene*, 46:85-96.

Gianotti, R.L., Bomblies, A., Eltahir, E.A.B. (2009) Hydrologic modeling to screen potential environmental management methods for malaria vector control in Niger, *Water Resources Research*, 45(8).

Gillies, M.T. (1961) Studies on the dispersion and survival of *Anopheles gambiae* giles in East Africa, by means of marking and release experiments, *Bulletin of Entomological Research*, 52: 99-127.

Gillies, M.T., and de Meillon, B. (1968) The Anophelinae of Africa south of the Sahara (Ethiopian zoogeographical region), *The South African Institute for Medical Research*, 54:1-343.

Jobin, W. (1999) *Dams and Diseases: ecological design and health impacts of large dams, canals and irrigation systems*, E & FN Spon.

Jobin, W. (2011) *Health and environmental impacts of dams: how to tell a good dam from a bad dam*, Boston Harbor Publisher.

Johnson, A.L. (1967) Specific yield -- compilation of specific yields for various material, U.S. Geological Survey Water-Supply Paper 1662-D.

Keiser J, Utzinger J, Singer BH (2002) The potential of intermittent irrigation for increasing rice yields, lowering water, *Journal of the American Mosquito Control Association*, 18(4):329-340.

Keiser, J., Singer, B.H., Utzinger, J. (2005) Reducing the burden of malaria in different eco-epidemiological settings with environmental management: a systematic review, *The LANSSET Infectious Diseases*, 5(11): 695–708.

Kibret, S., McCartney, M., Lautze, J., Jayasinghe, G. (2009) Malaria transmission in the vicinity of impounded water: Evidence from the Koka Reservoir, Ethiopia, *IWMI Research Report* 132.

Kibret, S., Lautze, J., Boelee, E., McCartney, M. (2012) How does an Ethiopian dam increase malaria? Entomological determinants around the Koka reservoir, *Tropical Medicine and International Health*, 17 (11): 1320-1328.

Kiszewski A., Johns B., Schapira A., Delacollette C., Crowell V., Tan-Torres T., Ameneshewa B., Teklehaimanot A., and Nafu-Traoré F. (2007) Estimated global resources needed to attain international malaria control goals, *Bulletin of World Health Organ* vol.85 n.8 Geneva Aug. 2007, ISSN 0042-9686.

Koenraadt, C.J.M., Paaijmans, K.P., Githeko, A.K., Knols, B.G.J., Takken, W. (2003) Egg hatching, larval movement and Larval survival of the malaria vector *Anopheles gambiae* in desiccating habitats, *Malaria Journal*, 2:20.

Konradsen, F., Matsuno, Y., Amerasinghe, F.P., Amerasinghe, P.H., van der Hoek, W. (1998) *Anopheles culicifacies* breeding in Sri Lanka and options for control through water management, *Acta Tropica*, 71(2):131-138.

Lal, W. (1998) Performance comparison of overland flow algorithms, *Journal of Hydraulic Engineering*, 124:342-349.

Lautze, J., Kirshen, P., McCartney, M., Kibret, S., Griffiths, J. (2008) Dam Operations and Malaria Transmission in Ethiopia: Evidence from Koka, *World Environmental and Water Resources Congress* 1-10.

Lutze, J. (2008b) Incorporating malaria control into reservoir management: a case study from



Ethiopia, Ph.D. thesis, Tufts University.

Manga, L., Toto, L.C., Le Goff, G., Brunhes, J. (1997) The bionomics of *Anopheles funestus* and its role in malaria transmission in a forested area of southern Cameroon, *Transactions of the Royal Society of Tropical Medicine and Hygiene*, 91(4): 387-388.

Martens, W.J., Niessen, L.W., Rotmans, J., Jetten, T.H., McMichael, A.J. (1995) Potential impact of global climate change on malaria risk, *Environmental health perspectives*, 103(5):458-465.

Martens, P. (1998) *Health and climate change: modeling the impacts of global warming and ozone depletion*, Earthscan UK.

Martens, P., Kovats, R. S., Nijhof, S., Vries, P. De., Livermore, M. T. J., Bradley, D. J. Cox, J., McMichael, A. J. (1999) Climate change and future populations at risk of malaria, *Global environmental change*, 9:89-107.

Parham, P.E., Pople, D., Christiansen-Jucht C., Lindsay, S., Hinsley, W., Michael, E. (2012) Modeling the role of environmental variables on the population dynamics of the malaria vector *Anopheles gambiae sensu stricto*, *Malaria Journal*, 11:271.

Patz, J.A., Campbell-Lendrum, D., Holloway, T., Foley, J.A. (2005) Impact of regional climate change on human health, *Nature*, 438:311-317.

Personal correspondence with EEPCo, Ethiopia, 2012.

Personal correspondence with local administrator, Dungugi-Bekele *kebele*, Ethiopia, 2012.

Personal correspondence with local person, Gudedo, Ethiopia, 2012.

Personal correspondence with regional clinic, Mojo, Ethiopia, 2012.

Personal correspondence with regional clinic, Mojo, Ethiopia, 2013.

Pollard, D., Thompson, S.L. (1995) Use of a land-surface-transfer scheme (LSX) in a global climate model: the response to doubling stomatal resistance, *Global planetary change*, 10:129-161.

Qunhua, L., Xin, K., Changzhi, C., Shengzheng, F., Yan, L., Rongzhi, H., Zhihus, Z., Gibson,

G., Wenmin, K. (2004) New irrigation methods sustain malaria control in Sichuan Province, China, *Acta Tropica*, 89:241-247.

Reis J., Culver T.B., McCartney M., Lautze J., Kibret S. (2011) Water resources implications of integrating malaria control into the operation of an Ethiopian dam, *Water Resources Research*, 47 (9).

Remson, I., Hornberger, G.M., Molz, F.J. (1971) *Numerical methods in subsurface hydrology, with an introduction to the finite element method*, New York, Wiley-Interscience.

Sachs, J. and Malaney, P. (2002), The economic and social burden of malaria, *Nature*, 415(6872):680-5.

Sow, S., de Vlas, S. J., Engels, D., Gryseels, B (2002) Water-related disease patterns before and after the construction of the Diama dam in northern Senegal, *Annals of Tropical Medicine and Parasitology*, 96(6): 575-586(12).

Steinmann, P., Keiser, J., Bos, R., Tanner, M., Utzinger, J. (2006) Schistosomiasis and water resources development: systematic review, meta-analysis, and estimates of people at risk, *The Lancet Infectious Diseases*, 6(7): 411–425.

Takken, W and Knols, B. (1999) Odor-mediated behavior of afrotropical malaria mosquitoes, *Annual Review of Entomology*, 44:113-157.

Teklu, B.M., Teki, e H., McCartney, M., Kibret, S. (2010) The effect of physical water quality and water level changes on the occurrence and density of *Anopheles* mosquito larvae around the shoreline of the Koka reservoir, central Ethiopia, *Hydrology and Earth System Science Discussion*, 7:6025-6055.

Tennessee Valley Authority (1947) *Malaria Control on Impounded Water*, U.S. Public Health Service, Tennessee Valley Authority.

UN Secretary-General, SG/SM/14974 (2013) With \$3 billion annual shortfall in controlling malaria, Secretary-General says replenishing Global Fund should be priority to prevent resurgence, 2013 <http://www.un.org/News/Press/docs/2013/sgsm14974.doc.htm> (accessed on July2, 2013).

Vasconcelos, C.H. and Novo, E (2003) Influence of precipitation, deforestation and Tucurui

reservoir operation on malaria incidence rate in southeast Para, Brazil, Geoscience and Remote Sensing Symposium, IEEE International, 7: 4567-4569.

Welderufael, W.A., Roux, P.A.L., Hensley, M. (2008) Quantifying rainfall–runoff relationships on the Dera Calcic Fluvic Regosol ecotope in Ethiopia, Agricultural water management, 95(11):1223-1232.

The World Commission on Dams (2000) Dams and development: A new framework for decision-making, Earthscan Publications Ltd.

World Health Organization (1982) Manual on environmental management for mosquito control, with special emphasis on malaria vectors.

World Health Organization (2011), Refined/updated GMAP objectives, targets, milestones and priorities beyond 2011, WHO offset publication No.66.

World Health Organization (2012), World Malaria Report 2012.

Yamana, T. and Eltahir, E.A.B. (2010) Early warnings of the potential for malaria transmission in rural Africa using the hydrology, entomology and malaria transmission simulator (HYDREMATS), Malaria Journal 9:323.

Yamana, T. (2011) Assessing the Impacts of Climate Change on Malaria Transmission in West Africa, Session 7-1, presented at the 2011 Water & Health Conf. U of N. Carolina, Chapel Hill, NC, Oct. 2-7.

Yamana, T. and Eltahir, E.A.B. (2013) Projected impacts of climate change on environmental suitability for malaria transmission in West Africa, Environmental health perspective, 121(10):117901186.

Ye-Ebiyo, Y., Pollack, R.J., Kiszewski, A., Spielman, A. (2003) Enhancement of development of larval *Anopheles arabiensis* by proximity to flowering maize (*Zea mays*) in turbid water and when crowded, American Journal of Tropical Medicine and Hygiene, 68(6): 748-752.

Yewhalaw, D., Legesse, W., Bortel, W.V., GebreSelassie, S., Kloos, H., Duchateau, L., Speybroeck, N. (2009) Malaria and water resource development: the case of Gilgel-Gibe hydroelectric dam in Ethiopia, Malaria Journal, 8:21 doi:10.1186/1475-2875-8-21.

Yewhalaw D., Getachew Y., Tushune K., W/Michael K., Kassahun W., Duchateau L., Speybroeck N. (2013) The effect of dams and seasons on malaria incidence and anopheles abundance in Ethiopia, *BMC Infectious Diseases*, 13:161.

Zeilhofer, P., dos Santos, E. S., Ribeiro, A. L. M., Miyazaki, R. D., dos Santos, M. A. (2007) Habitat suitability mapping of *Anopheles darlingi* in the surroundings of the Manso hydropower plant reservoir, Mato Grosso, Central Brazil, *International journal of health geographics*, 6:7.